



National Aeronautics and Space Administration  
*Summer High School Apprenticeship Research Program (SHARP)*

Validation of the NASCART-GT Flow Solver via Data  
Comparison

Jude Allred  
David Calloway

Georgia Institute of Technology



June-July 2003

Dr. Stephen Ruffin

## Table of Contents

I.	Abstract.....	3
II.	Introduction.....	4
III.	Problem Definition.....	5-9
	<i>Flight Regimes</i> .....	5
	<i>Geometries</i> .....	6
	<i>NASCART-GT, Computational Grid, and Computer Aided Design</i> .....	7
	<i>Objectives</i> .....	9
IV.	Method of Solution.....	9
	<i>Background Reading</i> .....	9
	<i>NACA 0012</i> .....	10
	<i>Buzz</i> .....	12
	<i>DLR-F4</i> .....	15
V.	Results and Discussion.....	20-28
	<i>NACA 0012</i> .....	20
	<i>Buzz</i> .....	23
	<i>DLR-F4</i> .....	25
VI.	Conclusions and Further Research.....	28
VII.	Works Cited.....	29
VIII.	Bibliography.....	29
IX.	Appendix A Charts and Graphs.....	31-57
X.	Appendix B NACA 0012.....	58-64
XI.	Appendix C DLR-F4.....	65
XII.	Appendix D Buzz.....	66
XIII.	Appendix E Test Case Data Base.....	68-76

## Abstract

Within the research field of computational fluid dynamics, engineers may employ a computer program known as NASCART-GT which has been developed here at Georgia Tech by Dr. Stephen Ruffin. NASCART-GT generates a Cartesian grid around a specified geometry and at every intersecting grid point a calculation is performed. Said calculations are used to find drag, density, Mach number, pressure and various effects of the flow. A specific procedure is followed in order to perform these calculations. The first order is to input the geometry. Geometry data is basically a set of coordinates into an unformatted data file such as Notepad; and then flow, numerical scheme, and grid variables were imputed into another like file. Some of the flow variables used are Mach number, pitch or angle of attack, yaw, temperature, et. al. Post execution of the program, visualization software such as Fieldview is used to analyze a visual representation of the flow. If the visual results are accurate then all of the NASCART output files are catalogued. In addition to flow simulations, there have been several logos created for the NASCART-GT program, as well as a database of various flow cases for the purpose of validating the NASCART-GT software. In conducting the research, one must learn to utilize several computer programs intrinsic to the fast growing field of computational fluid dynamics. The research stated herein would not have been possible without the assistance of Dr. Stephen Ruffin and the help of Dr. Ruffin's graduate students J.D. and Jin.

## Introduction

The practice of computational fluid dynamics (CFD) is employed by a variety of different industries. CFD has many applications in industrial, automotive, civil, naval, and aerospace engineering. In the industrial aspect, CFD is used to determine flow parameters in cast iron molding and the manufacturing turbine engines. In the automotive section it may be utilized in order to determine flow around and through vehicle bodies and engines. In the civil sector, CFD may be employed in the rheology<sup>1</sup> of rivers, lakes, plumbing, etc. Naval CFD includes the calculation of flow around submarine and torpedo bodies. Within the field of aerospace, CFD may produce data pertaining to fluid flow around airfoils and full wing/body geometries. This research paper covers running validation test cases using 3D and 2D geometries such as the DLR-F4 fixed-wing geometry and NACA 0012 airfoil in a CFD program code entitled Numerical Aerodynamic Simulation via CARTesian<sup>2</sup> Grid Techniques (NASCART-GT). It was required to design several logos for the NASCART code. In order to proceed with the research, it was necessary to make use of several programs such as Intelligent Light's Fieldview 8<sup>3</sup> for Windows, Catia V5, and NASCART-GT itself. The research has also called upon relatively simple functions located within Microsoft Excel and Microsoft Word.

---

<sup>1</sup> a branch of physics dealing with the way matter flows and changes shape

<sup>2</sup> a grid that becomes more refined at cells closer to the geometry body

<sup>3</sup> visualization software that enables the user to supplement NASCART-GT's numerical data output with a visual scalar representation

## Problem Definition

### *Flight Regimes:*

Testing the airfoil consisted of running numerous test cases for a sweep of various flight conditions such as Mach Number ( $M_\infty$ ) and angle of attacks ( $\alpha$ ). Mach numbers ranged from  $0.2 \leq M_\infty \leq 50$ . Angle of attacks ranged from  $0 \leq \alpha \leq 130$ . Mach number is the speed of an object relative to the speed of sound. The speed of sound is a variable relative to articles such as flow density, pressure, and temperature. There are three Mach number ranges. *See figure 1-1.*

Range	$M_\infty$ Min.	$M_\infty$ Max.
Subsonic	0	0.8
Transonic	0.8	1.2
Supersonic	1.2	5
Hypersonic	5	-

(Fig. 1-1) Mach Number Ranges

Angle of attack or pitch is the degree difference measure of the airfoil in relation to the freestream flow<sup>1</sup>. The aforementioned variables were key to accurate validation. One must first comprehend flow properties associated compressible and incompressible flows. Compressible flow is a freestream flow that is traveling at supersonic and hypersonic levels; since the flow is traveling at such a high speed it becomes more dense than normal therefore becoming compressed. Incompressible flow is in the transonic and subsonic ranges. Incompressible flow is where the flow is not traveling fast enough to become compressed. The difference between compressible and incompressible flow can best be demonstrated through the use of color maps depicting  $M_\infty$ . *See appendix figures 1-1 and 1-2.*

---

<sup>1</sup> freestream flow refers to conditions that are  $\infty$  in front of the airfoil

### *Geometries:*

The geometries that one inputs into NASCART-GT are inserted via numerical input or by importation from a computer aided design (CAD) program such as Catia. The primary geometry used for the validation of NASCART-GT is designated NACA 0012. NACA stands for the National Advisory Committee for Aeronautics; this organization was the precursor to NASA. The numerical identification shows that the airfoil has a symmetrical aspect ratio<sup>1</sup> as expressed by the first two digits (00) and that the airfoil has a thickness of twelve percent as illustrated by the trailing digits (12). The NACA 0012 is a baseline airfoil that is widely used in the aerospace community hence why it was chosen to be the main test geometry for NASCART. *See Figure 1-2.*

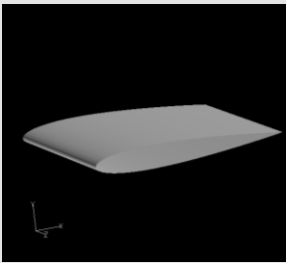


(Fig. 1-2) NACA 0012

NASCART-GT was built to handle several different types of geometries inclusive of 3D geometries. The SHARP program has tested two different 3d geometries, the first a fixed wing aircraft dubbed the DLR-F4, and the second is a model of Buzz the Georgia Tech Mascot.

---

<sup>1</sup> the ratio of the length of an aircraft's wing to the mean distance between the front and back edge of the wing

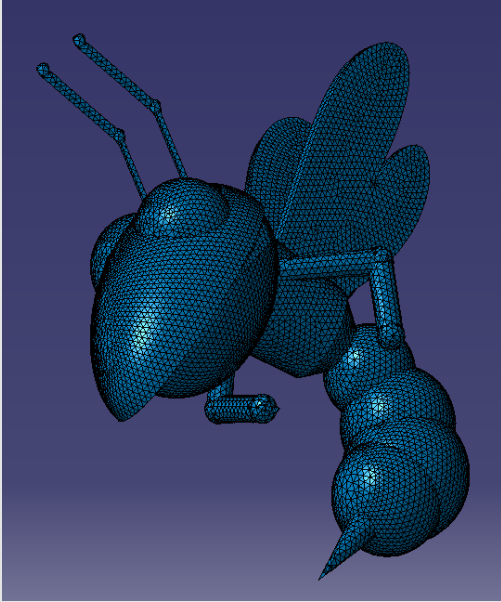


(Fig.1-3) Buzz's Mesh

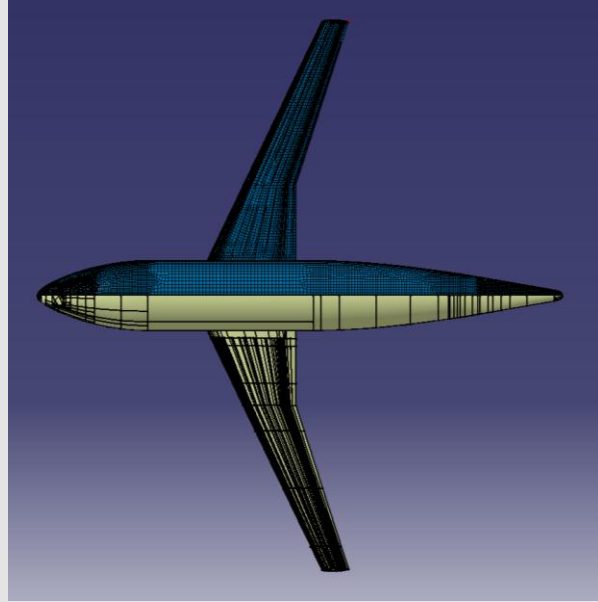


(Fig.1-4) DLR-F4 Fine Mesh

Buzz's mesh contains approximately 43,000 polygons and is not symmetrical. Two versions of the DLR-F4 were created, a fine mesh for computational purposes which contains 38,569 cells, and a coarse mesh of approximately 4,350 cells for troubleshooting purposes. Both DLR-F4 geometries are symmetrical on the  $y = 0$  plane, effectively doubling their polygon count.

*NASCART-GT, Computational Grid, and Computer Aided Design:*

A solution adaptive, Cartesian-grid based flow solver, NASCART-GT generates an orthogonal, Cartesian grid around complex single or multiple geometries in an automated fashion. A variety of input formats are available including simple x,y,z coordinates of surface nodes, Catia™V5 files, and PLOT3D™ surface files. Structured-grid based CFD programs often require significant man-hours, substantial human interaction and an expertise in grid generation. NASCART-GT's automated grid

generation and flow solver minimizes these issues while conducting high-fidelity flow analysis. After NASCART-GT generates the 3-D or 2-D computational grid, either inviscid or viscous, ideal-gas flow is computed for any Mach number range. NASCART-GT performs adaptive mesh refinement (i.e. solution adaptation) in high flow gradient regions to yield high accuracy and efficiency. NASCART-GT's governing equations are the Euler Equations, Euler + Integral Boundary Layer Equations, and the Navier-Stokes Equation. Roe's Approximate Riemann solver may be used for 1<sup>st</sup>, 2<sup>nd</sup>, or 3<sup>rd</sup> order accurate Inviscid Fluxes. Navier Stokes viscous fluxes either fully laminar or fully turbulent utilize the Baldwin-Lomax turbulence model. Thwaites' Method for Laminar, Michel's Criterion to identify transition, Head's method for Turbulent, and a shape factor criterion are integrated into NASCART-GT's Integral Boundary Layer Method. NASCART-GT reports all surface flow conditions and the time history of force coefficients and convergence residuals to its respective output files. The grid and solution may be visualized using the VISCART program or by using FIELDVIEW™ (after use of the NASCARTOFV file converter). VISCART and NASCARTOFV are included with the download of the NASCART-GT flow solver.

*Objectives:*

The two main objectives of this research were to improve NASCART-GT by running a number of two and three-dimensional geometries and to prove that NASCART is an accurate software package. In order to accomplish these main objectives there were several smaller objectives to be completed. Firstly, an amount of background reading was required. A data base was created containing various two-dimensional and three-

dimensional test cases from outside sources. The next objective was to run NACA 0012 NASCART-GT test cases and document the results by means of numerical data, graphs, and color maps including variables such as pressure, Mach number, temperature, density, stagnation enthalpy<sup>1</sup> and stagnation pressure. It was also very important to test the grid generation abilities of NASCART-GT, such as its adaptability to complex and high resolution geometries such as mascots. In addition, to validate NASCART's three dimensional aspect, the DLR-F4 geometry was to be computed and the results compared to those of the American Institute of Aeronautics and Astronautics (AIAA) Drag Prediction Workshop.

## Method of Solution

### *Background Reading:*

All of the background reading that was required for this research was taken from listed references. CFD is a very complex field and it takes one years to learn the trade. However, since this research was only over a period of two months a “crash course” method was used.

### *Test Case Catalogue:*

In order to create a test case database online data sources were summarized and data was placed into an Excel spreadsheet. The data catalogue contained information on experimental data, computed results references, flow type, geometry description, boundary layer specifications and other variables. The data base contains twenty-nine separate test

---

<sup>1</sup> a thermodynamic property equal to the sum of the internal energy of a system and the product of its pressure and volume

cases and covers approximately eight pages. This information took approximately three weeks to compile. *See Appendix.*

#### *NACA 0012 Cases:*

The NACA 0012 test cases covered the bulk of the research for this project. Over 100 separate cases were run in NASCART. In order to run a test case in NASCART one must first input geometry data. The primary two ways to input data into the program; one is inputting the data grid point by grid point; the second method is to input the geometry via Catia by generating a surface mesh and exporting it into a .DAT. After inputting the geometry data one must specify variables governing the flow, grid, and the numerical scheme. All of these input variables are contained within a Notepad data file designated INPUT.DAT. This input file is where one inputs flow variables including  $M_\infty$ ,  $\alpha$ , yaw, freestream density, whether it is a viscous<sup>1</sup> or inviscid<sup>2</sup> flow. Some of the grid variables include options that specify whether the geometry is 2D or 3D. Others allow the user to specify the minimum and maximum values of the computational domain. The computational domain is the “box” that is generated around the geometry which contains the grid. A feature that is unique to NASCART is the ability to automatically generate a grid around a given geometry. The process of automatic grid generation makes NASCART run slower than if a grid is input manually due to the fact that the program is constantly refining the grid around the geometry. Some other grid variables include specifying how often the user wants NASCART to write out a solution adaptation and refine the grid. The numerical scheme variables specify when a restart file is to be

---

<sup>1</sup> used to describe a fluid that has a relatively high resistance to flow

<sup>2</sup> having zero or negligible viscosity

written. Depending on the complexity of the case being computed one should set the restart file to be written at the end every 500 iteration set. For each case there are about 25 output files which are all in data file format. One may use Fieldview to generate a visual representation of the geometry and flow. NASCART-GT files are not compatible with Fieldview so the translator “nascartofildview” is readily available. After running the translator, a file designated “Fieldview.uns” is created which can be read into Fieldview as an unstructured data file. Graphical visualizations (graphs) may be generated in Excel. The main variable that has been plotted was pressure distribution ( $C_p$ ).  $C_p$  was plotted by exporting the data file “bodytab.dat” into Excel. Once the data is in an Excel spreadsheet it must be sorted by the value “y.” The data must then be separated by positive and negative “y” values. The data section where the  $C_p$  values are collectively larger is the lower surface of the airfoil “ $C_p\_Lower$ ,” and the data set with the lesser  $C_p$  values is the upper surface “ $C_p\_Upper$ .” Note that if the airfoil is at  $\alpha = 0$  then the  $C_p$  will be equal for both sides of the airfoil since there is no lift being generated. The area of low pressure, as shown in the color floods, on the upper surface of the airfoil represents what is known as “the suction peak.” The suction peak is where the lift along the upper surface of the airfoil is being generated. There is a similar peak on the under side of the airfoil as well; this represents an area of high pressure, these areas of pressure must be present in order for the airfoil to function properly. Color floods were also generated through the use of Fieldview. Floods for density, pressure, temperature, Mach number, stagnation Enthalpy, and stagnation pressure were documented. In addition to graphs and color floods, several video clips were developed to illustrate streamlines and

sweeps of the grid through the airfoil. See Appendix A for graphs and Appendix B for color floods.

*Buzz:*

To the knowledge of the authors, the Georgia Tech mascot Buzz has never before been modeled three-dimensionally and had its fluid dynamics calculated. Though the ultimate goal of incorporating Buzz into NASCART-GT was to create a software logo, his intricacies as a college mascot (antennae and a stinger) provided for testing and further optimization of the NASCART-GT code. The geometry was based upon a picture recovered from The (Unofficial) Buzz Image Page, and a visually approximated reproduction was created using Catia.



(Fig. 2-1) Original Buzz



(Fig.2-2) Catia Buzz

The first step of buzz replication was to create a “spine” of sorts from which to base his body off of. This was done by simply creating a series of points and connecting designated points with lines. Once this base shape was developed, Buzz’s body geometry was able to be

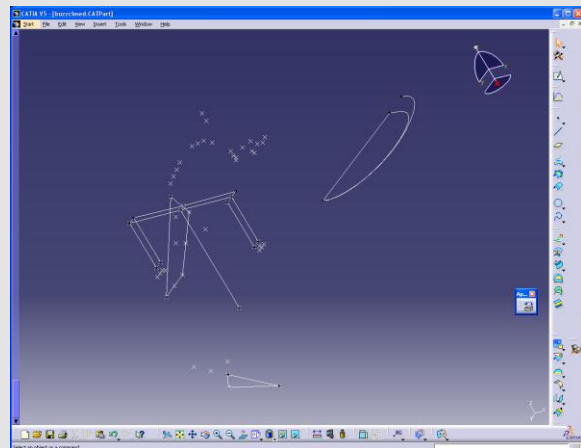


(Fig.2-3) Buzz’s “Spine”

fabricated using simple geometric shapes such as spheres, cones, and cylinders. His dimpled-football-slice head was created using a series of points with a spline lain across

them and put into a 180° rotation. The jaw was then created using this same principle but based upon a spline of smaller scale.

In order to create a sphere, one may access the “Start” pull-down menu located in the upper left corner of the screen and navigate to Shape>Generative Shape Design. Once here, locate the sphere creation tool on the right panel, designate a point and a radius, and a sphere is created.

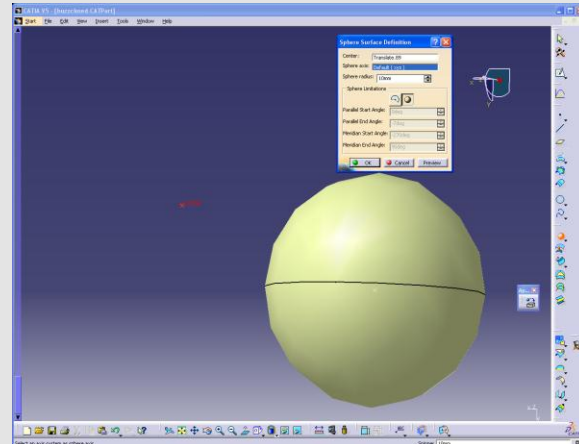


(Fig. 2-4) Sphere Creation

To perform revolutions, one would navigate to the same tool panel as that of the sphere creation tool and locate the revolution tool. A revolution requires a minimum of two base elements, firstly an object to revolve, and second an axis with which to revolve around. Once the revolution is performed, a surface will be created.

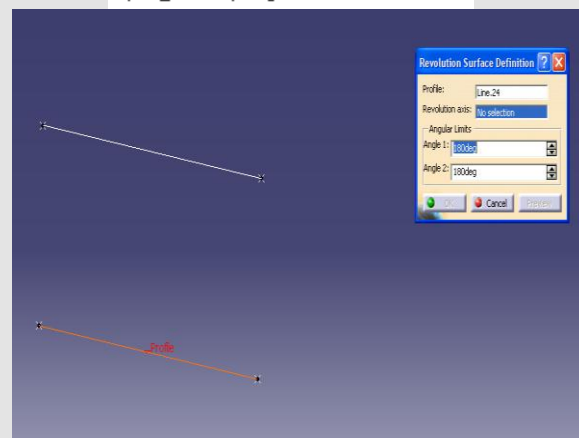


(Fig. 2-5) Revolution Tool

The final and primary tool used in the creation of Buzz was the translation tool. The translation tool, located within the same tool subset, will duplicate an object and allow for the

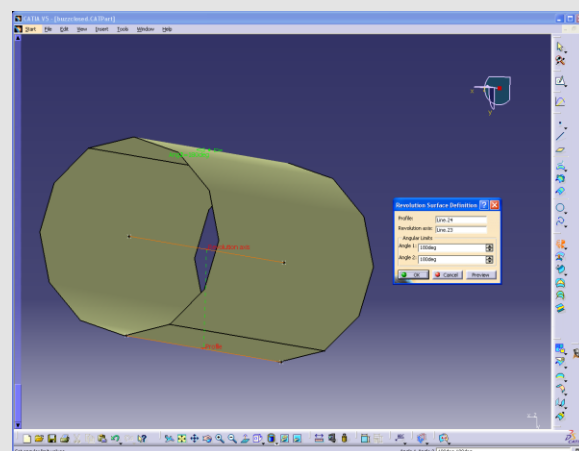


(Fig. 2-6) Revolution

duplication to be translated, or moved, along the X, Y, and/or Z axis. This tool was highly useful as it allowed for a single sphere or other object to be created, duplicated, and altered as opposed to unique objects being entered at every step.

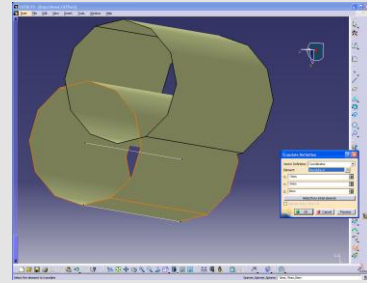


(Fig. 2-7) Translation

Once the buzz geometry was completed, a surface mesh was applied. The mesh tool can be located by navigating within Catia to Start>Analysis and Simulation>Advance Meshing Tools, selecting “Static Mesh”, and then accessing the polygon mesh tool located on the right panel. Because Buzz is not a fixed-wing geometry with statistical value, it was acceptable for him to contain a sloppy geometry. All parts of Buzz were meshed as one piece and this resulted in many intersection polygons. Because

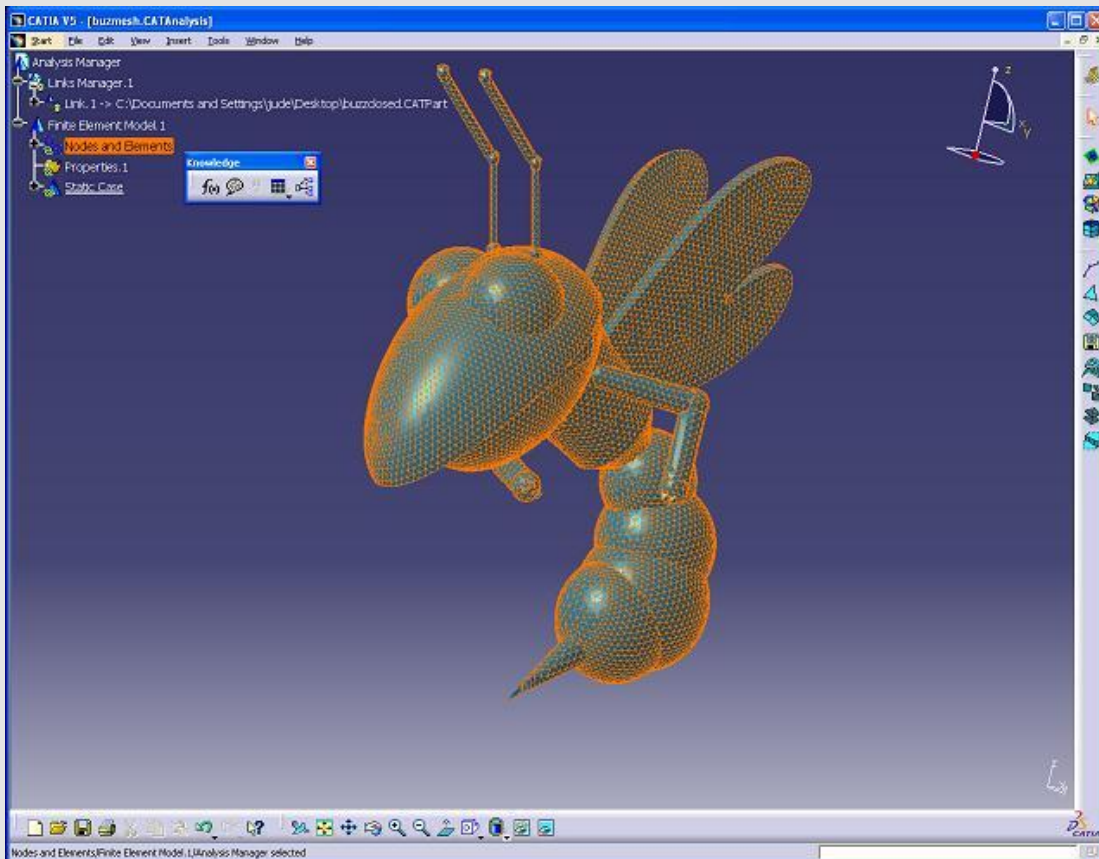


(Fig. 2-8) Buzz's Completed Mesh

there were, however, no holes in the geometry, NASCART-GT accepted this body geometry and performed flow calculations.

*DLR-F4:*

The DLR-F4 Fixed-Wing geometry was obtained via .IGES file from the AIAA's CFD Drag Prediction Workshop. The first task was to import this file into Catia and generate a surface mesh which could then be imported into NASCART-GT. The initial geometry was found to be half of the aircraft, oriented on the  $Y=0$  plane. The geometry was composed of forty surface panels and one face. The wing was not connected to the fuselage, merely protruding through (See Figure 2-11).

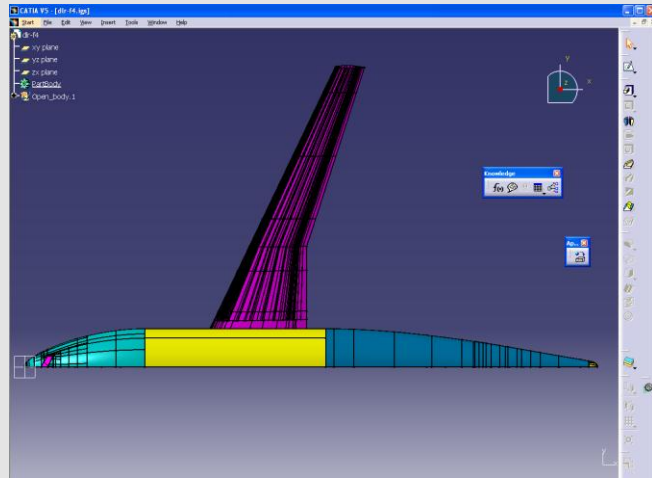


(Fig. 2-9) DLR-F4 Original Geometry Top

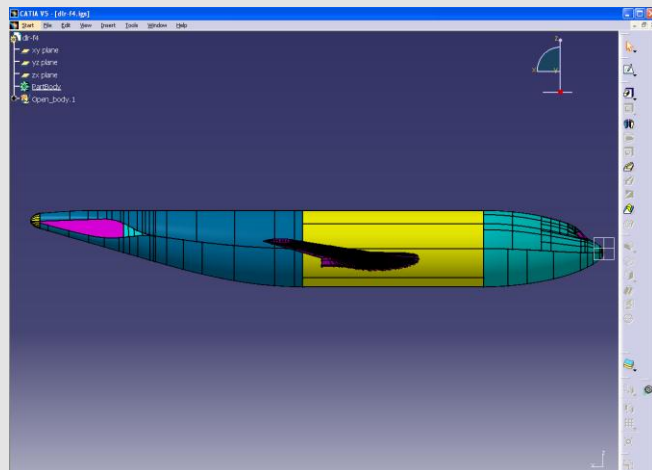


(Fig. 2-10) DLR-F4 Original Geometry Side

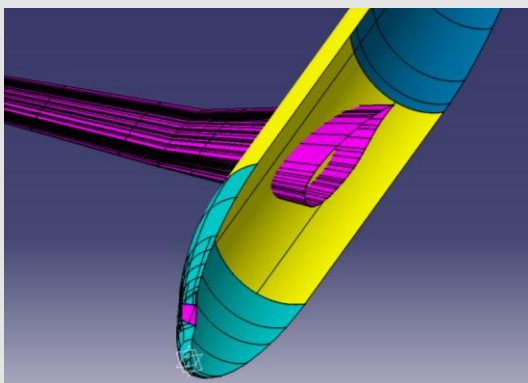


(Fig. 2-11) DLR-F4 Wing Protruding

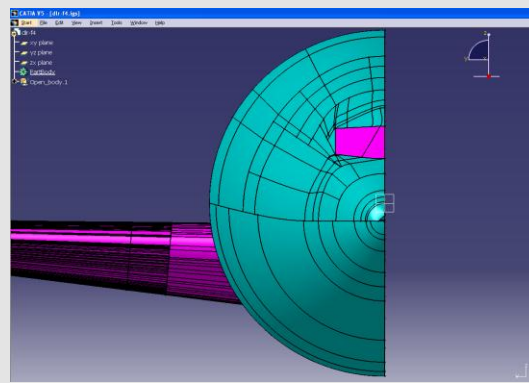


(Fig. 2-12) DLR-F4 Original Geometry Face

Before meshing could begin, several flaws in the geometry needed to be repaired. NASCART-GT isn't capable of computing objects that are infinitely thin, and thus attempting to compute a hollow shell will fail. Holes in a given geometry would produce

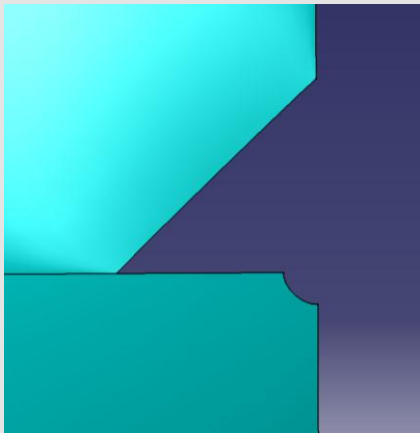


(Fig. 2-13) Nosecone Hole

such an affect, and so gaps must be compensated for.

Discounting the open face on the XZ plane, there were three holes in the geometry. The first located at the

nosecone; an oddly triangular gap requiring delicate patchwork. The

second at the tail cone, a

half circle. And the third, a thin slit along the entire trailing

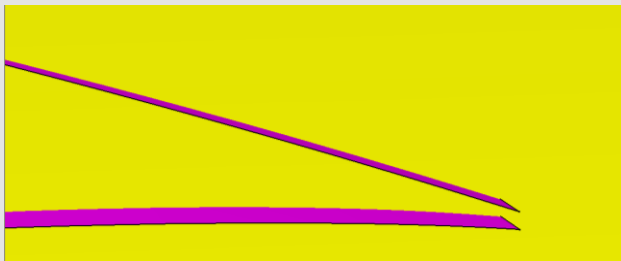


(Fig. 2-15) Wing Slit

edge of the

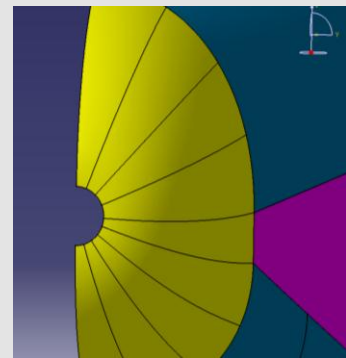


(Fig. 2-14) Tail Cone Hole

wing. In an effort to maintain the accuracy of the model to the greatest extent possible, these holes were fixed

by merging the adjacent polygons to compensate for

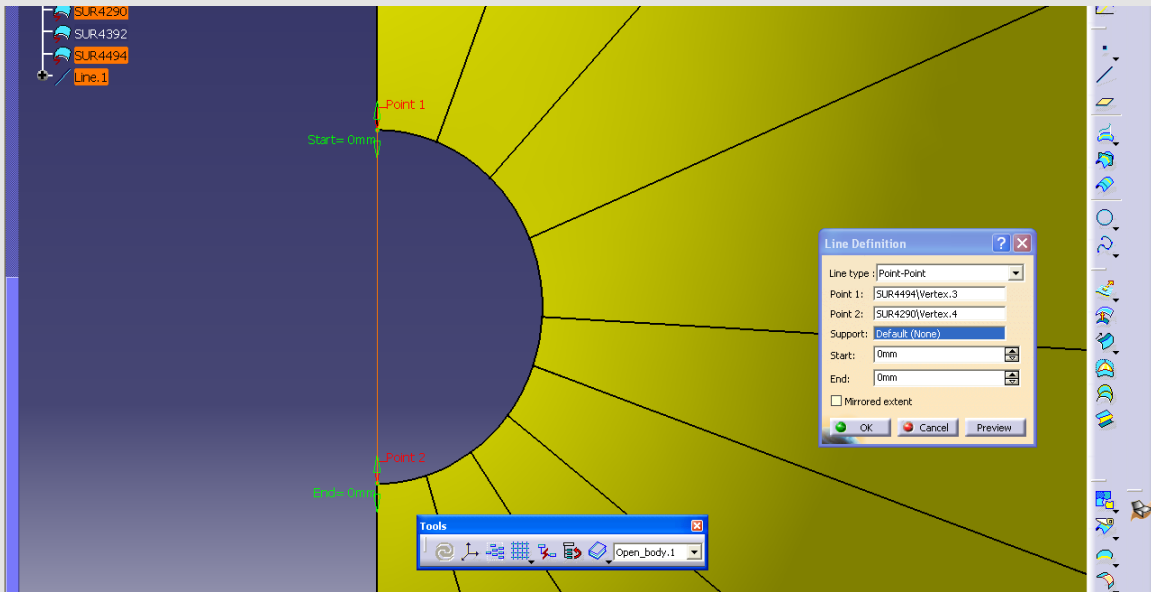
the gap. Lines were created based upon points at the edges of the gap which closed in the

figure. Once the anomaly is contained to a single plane, the fill tool may bridge the gap.

To operate the fill tool, select the appropriate button, and then tag mono-planar lines or

curves until a closed figure is formed. Once the figure is closed, execute the fill and the

gap will be filled. Here is the tail cone problem as an example:



(Fig. 2-16) Fixing a Hole

Two points are tagged for line creation,

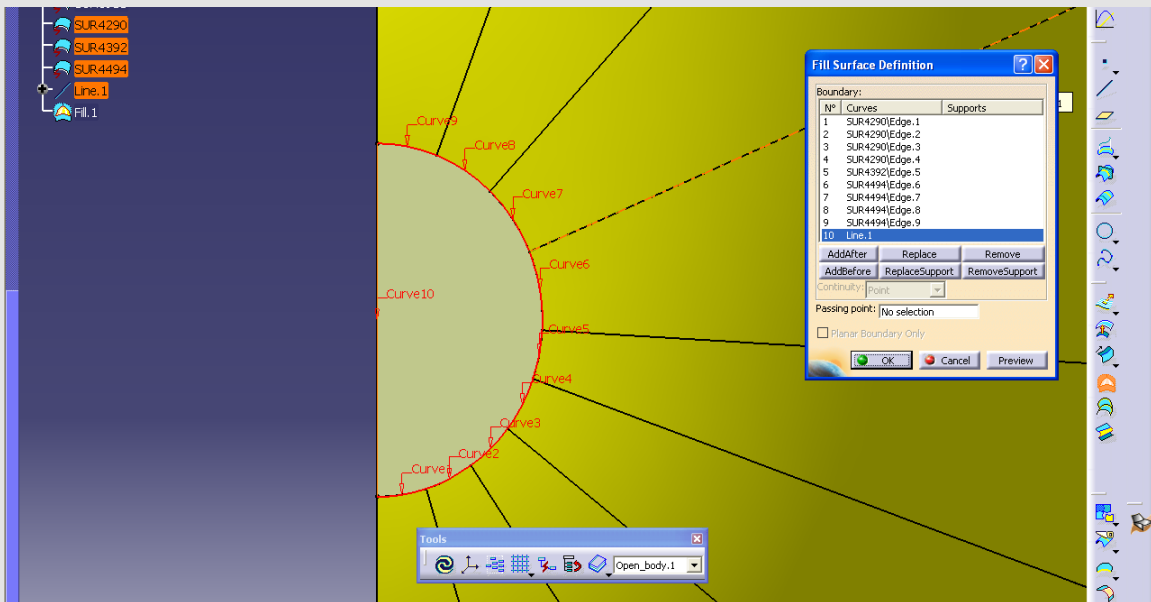


(Fig. 2-17) Mended Tail Cone

and then the new line is employed to complete the figure and execute a fill. It is unknown as to exactly what the geometry should conform to at these locations, and so one can only hope to have followed the original design as closely as possible. With the tail cone mended, the other geometry faults may be repaired using the same methods.

The nosecone issue was significantly more complicated than the tail cone and required several fill operations to be performed.

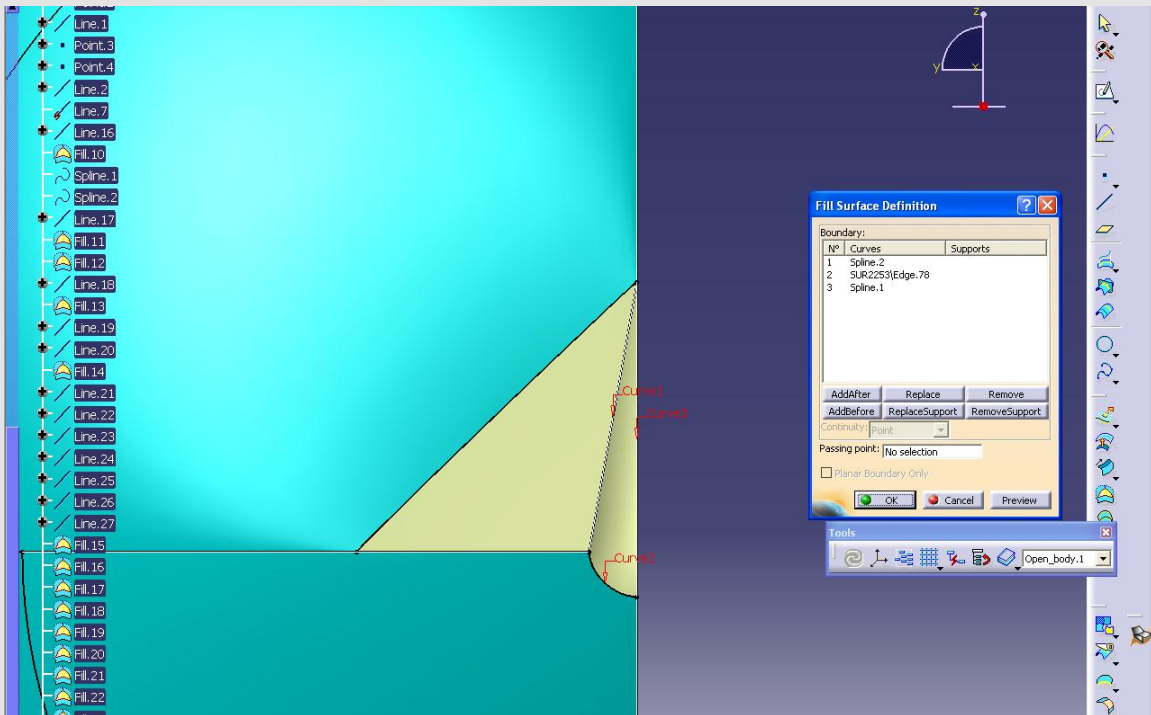


(Fig. 2-18) Mended Nosecone

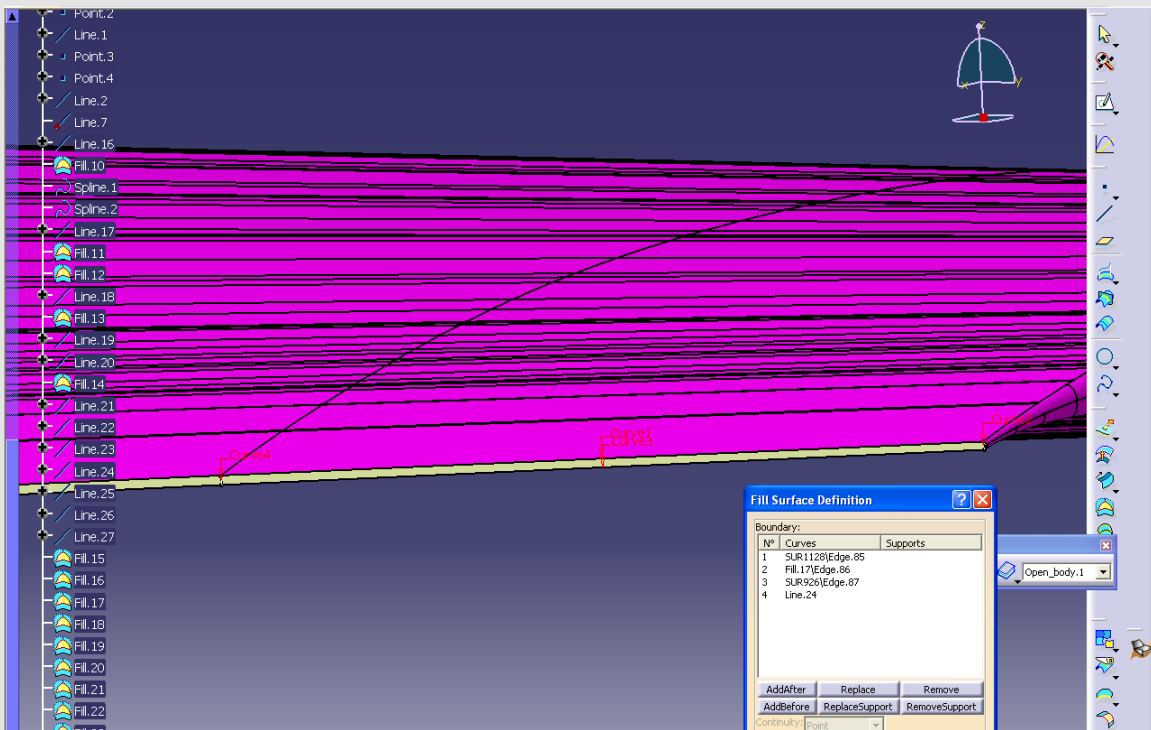


(Fig. 2-19) Mended Wing Slit

With the geometry now mended, a mesh was applied. Each individual geometry panel must be selected for meshing, and numerical logic applies to what order the panels must be selected. It is advisable to apply meshes to the more intricate panels first and generally work towards the larger and more easily adaptable panels. Following this method, a full and flawless surface mesh was generated. The polygon size from the nosecone to the midsection started at 10mm, increasing to 50mm, 100mm, and finally 200mm for the midsection. The tail initially holds polygons measuring 10mm, increasing to 25mm, 50mm, 100mm, and then joining with the midsection. The wingtips and trailing edges hold polygons as small as 5mm, jumping to 50mm for the thicker sections of the wingtip, and then finally 100mm for the main airfoil. It's important for the leading and trailing edges and profiles to have a high polygon count and thusly be smoother and well defined. All other areas, such as the midsection of the fuselage, have relatively little effect on the airflow, and so may be meshed as a coarser level.

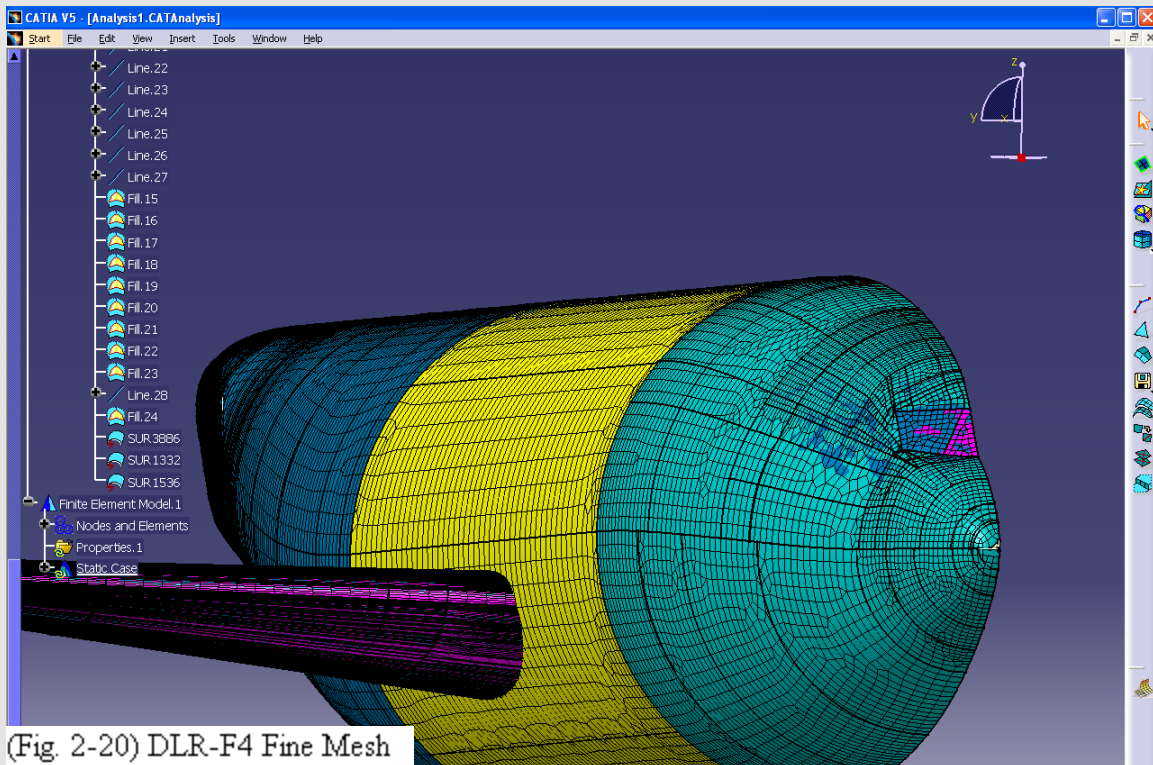


(Fig. 2-20) DLR-F4 Fine Mesh

With the mesh completed, the DLR-F4 geometry was exported to NASCART-GT.

## Results and Discussion

*NACA 0012:*

Computed results for the NACA 0012 test cases are quite extensive. The majority of the results are in the form of a graph or a color map. *See Appendixes A and B.* Data that was gathered through the test cases has been compared to published results from NACA, AGARD and AIAA. Numerical results and reference data were graphed and compared. The results of the comparisons showed that NASCART-GT is an accurate flow solver at  $M_\infty \geq 0.4$ . At  $M_\infty \leq 0.4$  there were oscillations within the flow that were visible in the results. *Figure 4-1 and Figure 4-2.*

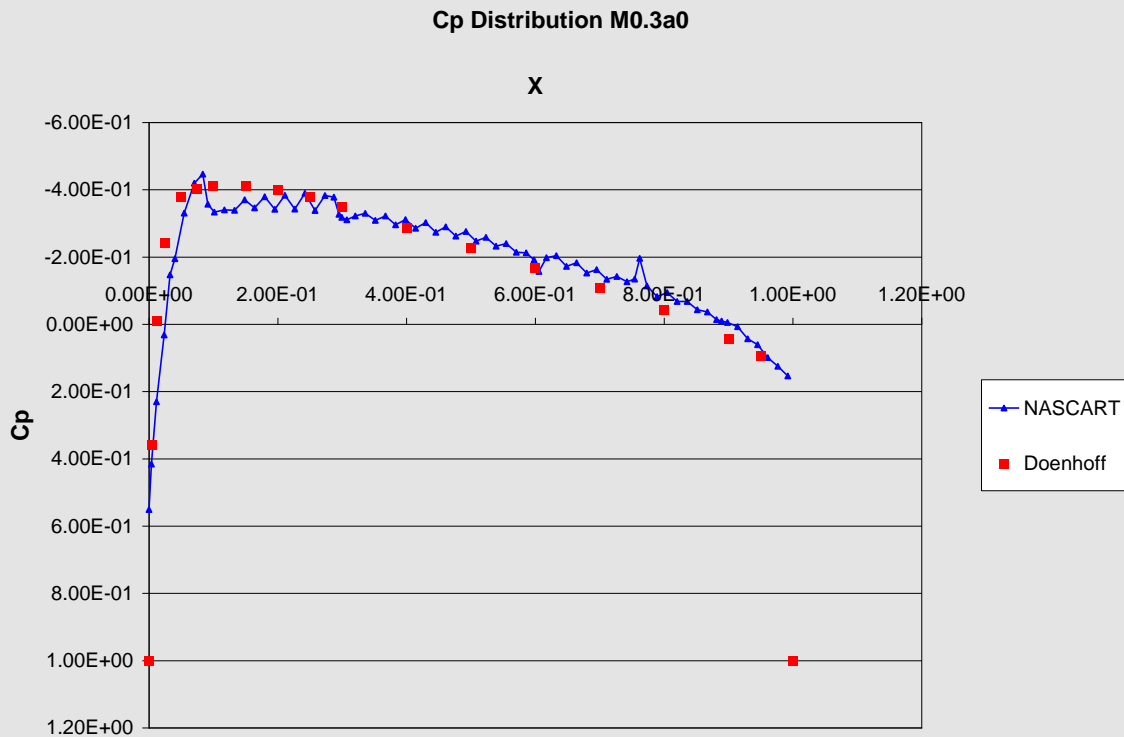


(Fig. 4-1) Pressure Distribution (Cp) Comparison NASCART-GT and Doenhoff  $M_\infty = 0.3$   $\alpha = 0$

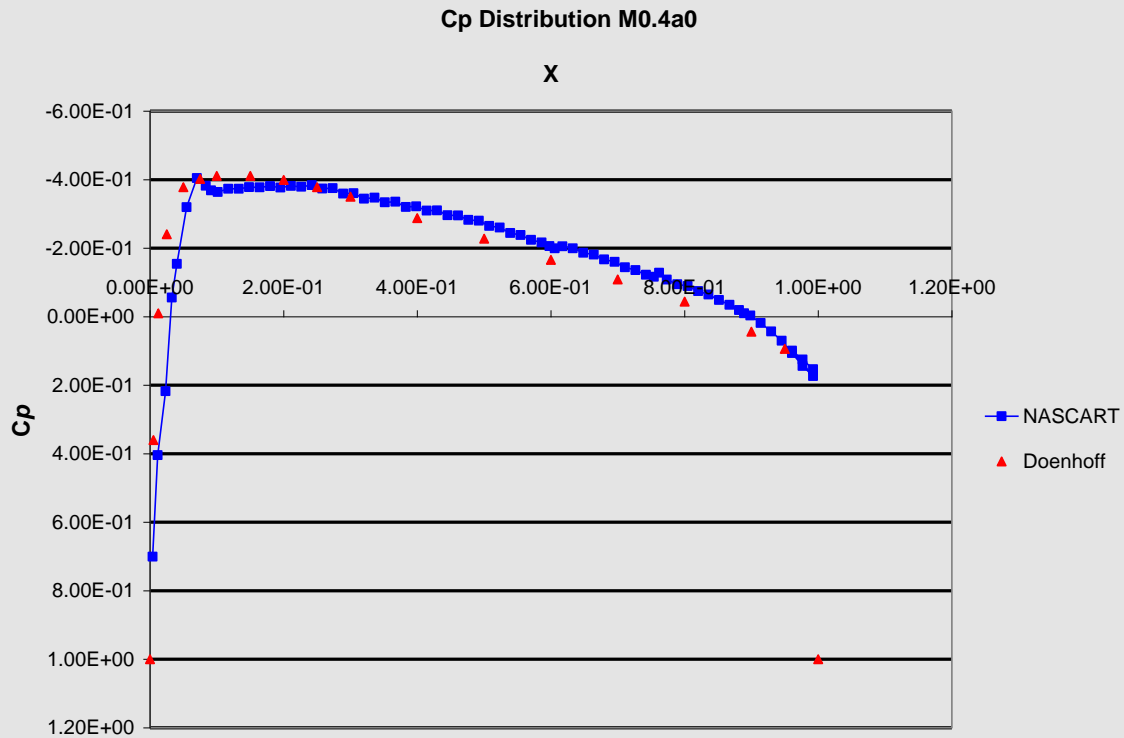


(Fig. 4-2) Pressure Distribution ( $C_p$ ) Comparison NASCART-GT and Doenhoff  
 $M_\infty=0.4 \alpha=0$

Each peak in the NASCART-GT data represents an oscillation near the surface of the airfoil. As one can see the oscillations have dramatically lessened due to the slight increase in  $M_\infty$ . In both cases however the two lines follow the same basic curve which is good, that indicates that NASCART is correctly calculating the  $C_p$  of these cases. The oscillation problem should be easily corrected. NASCART-GT calculates  $C_p$  through the use of surface area; the majority of other flow cases are computed using chord<sup>1</sup>.  $C_p$  can be converted as:

$$C_p = (\text{NASCART } C_p) (\text{Source } C_p) / \text{NASCART Surface Area}$$

<sup>1</sup> the shortest distance between the leading and trailing edges of an airfoil

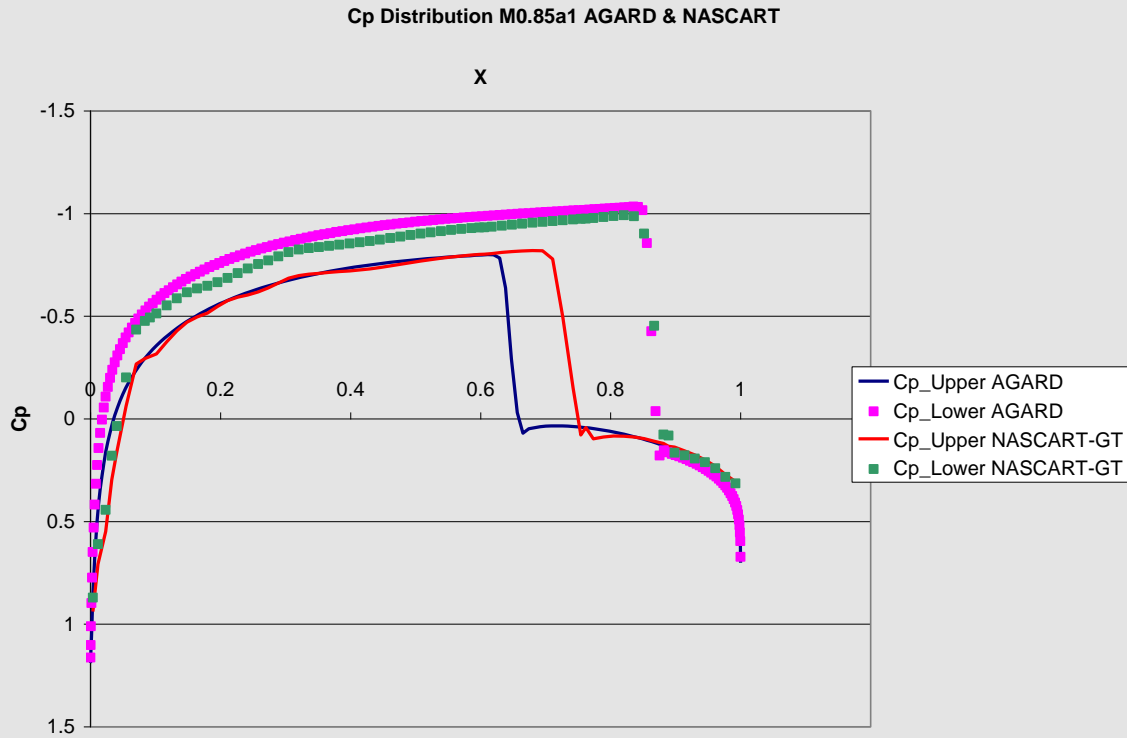


(Fig. 4-3)  $C_p$  Distribution Comparison NASCART-GT and AGARD  $M_\infty=0.85$   $\alpha=1$

The above plot shows the  $C_p$  relationship between NASCART and AGARD. This case was run at  $M_\infty=0.85$  and  $\alpha=1$ . The NASCART data series are below the AGARD series which shows that the NASCART series is generating significantly less lift than the AGARD series. Also the NASCART data drops off earlier than the AGARD data. This could possibly be attributed to difference in chord of these two tested airfoils. Aside from the oscillations in low level incompressible flows the color floods showed accurate results specific to  $M_\infty$  and  $\alpha$ . See Appendix B.

*Buzz:*

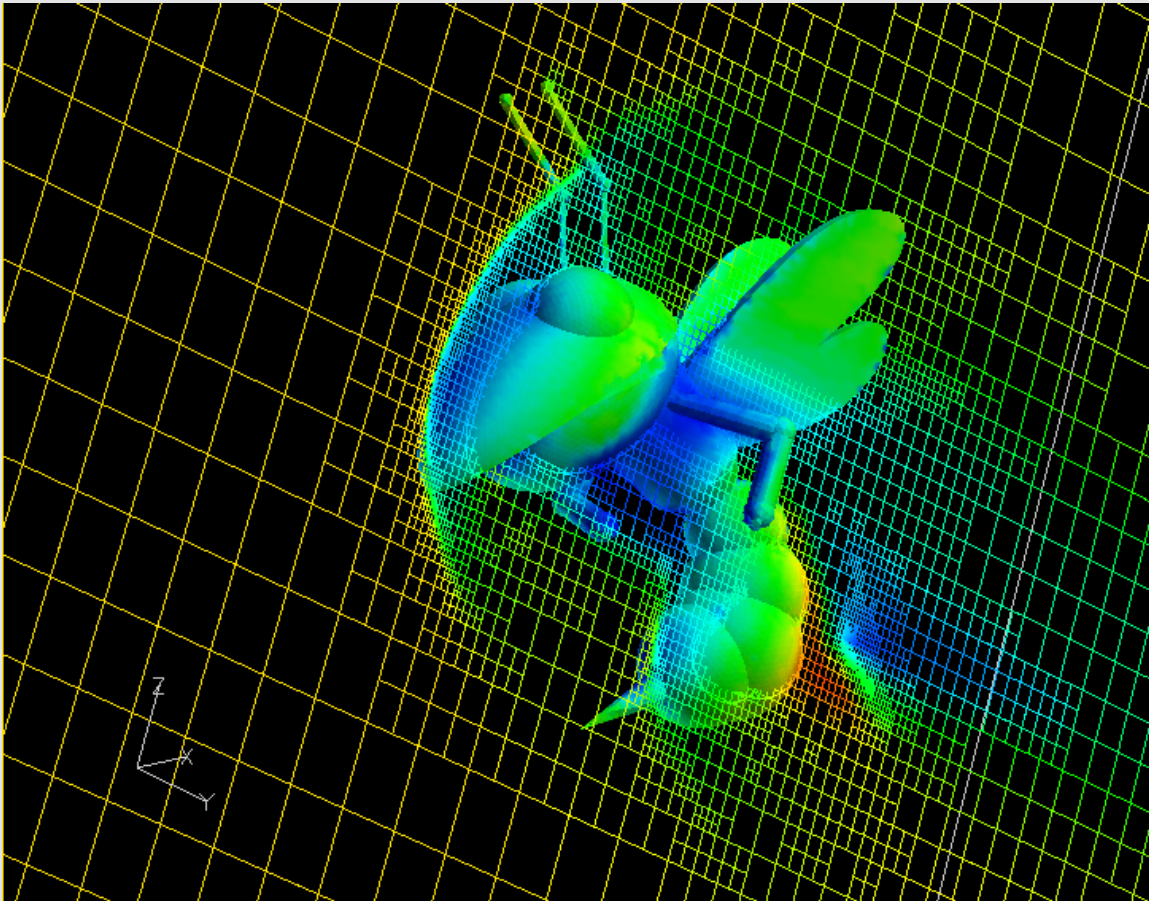


(Fig. 4-4) Buzz

Given that the ultimate goal for the Buzz geometry was to create a visually appealing design, it appears that the method has been a success. The grid generation process for such an interesting geometry proved to be a challenge, however the success of the grid is sort of a marvel. Shown above is Buzz's computational grid colored by Mach number. Buzz is flying at Mach 25. Buzz is generating several shockwaves, as illustrated by arcs in the grid, and is significantly slowing down much of the Mach 25 airflow he is facing, as depicted by his coloring. The grid refinement shown is quite impressive; should NASCART-GT determine that within a given grid cell there is relevant data too intricate to be expressed by the single cell, then the cell is split into fourths and the new cells are reevaluated. The grid lining Buzz's beak is very well

refined, as are portions of his wake. It is logical to conclude that college mascots are poor geometries to fly at Mach 25, however it should be duly noted that – although such geometries lack any relevant data for analysis – they produce pretty colors. Science fails unless it's willing to meet the extremes, from the incessantly complex to the intrinsically goofy.

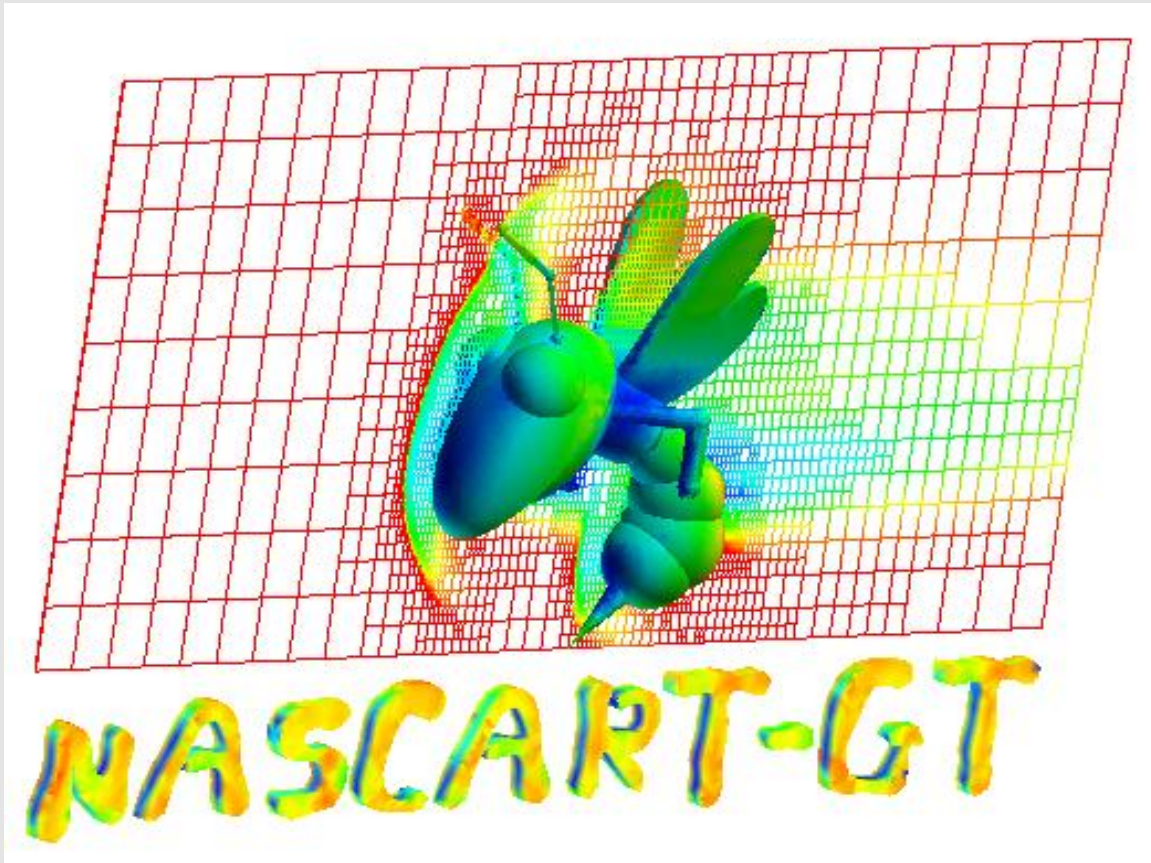


(Fig. 4-5) Buzz Logo

Such goofy ventures do however provide for interesting logo designs.

*DLR-F4:*

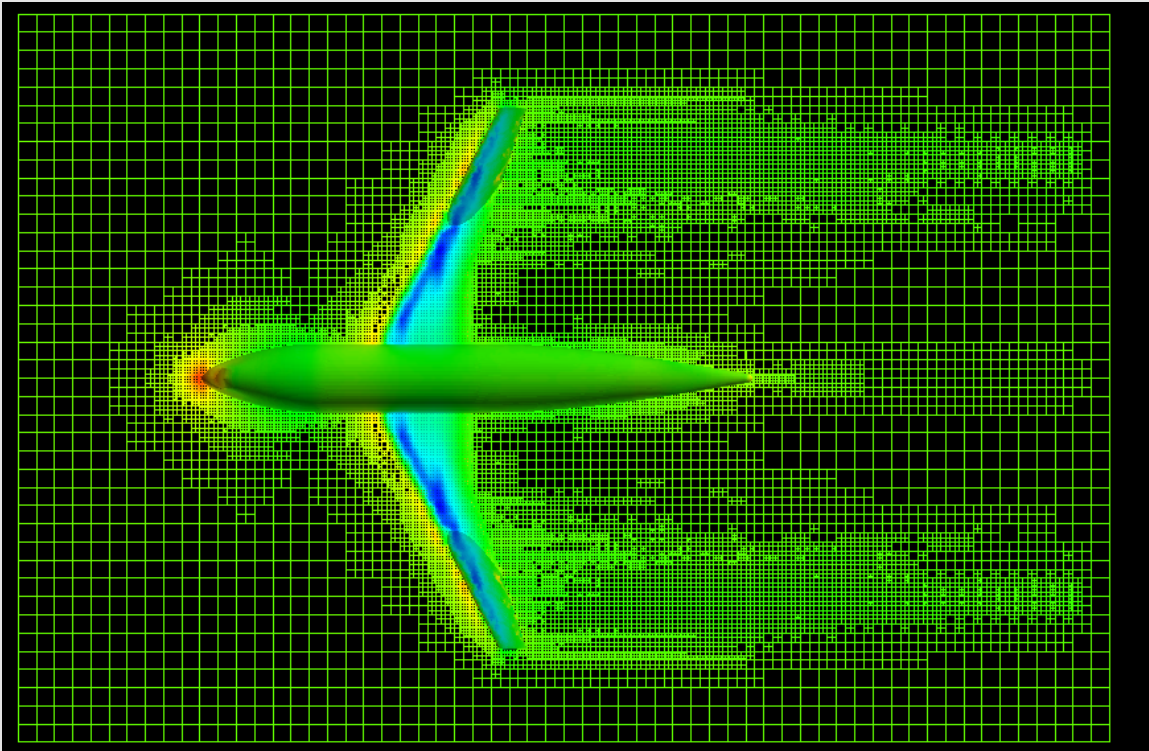


(Fig. 4-6) DLR-F4 Density

The DLR-F4 grid was successfully generated. Due to time constraints, only a rough computation was performed. Because of this restriction, the DLR-F4 generated herein has not been compared with the AGARD case. Shown above is the computational grid of the DLR-F4 traveling at Mach 0.75 with a pitch of 0.0. This grid has a color overlay of pressure ranging from dark blue to red. One may observe from this data the low pressure area along the wings as they generate lift. The highest pressure area is on the nosecone, where the profile drag is highest. It should be noted that the wings of the DLR-F4 are swept back and upwards such that they are not parallel to the grid. As such, a single grid slice is unable to visually interpret the whole of the airfoil. *Figure 4-7* examines the flow of Mach number via a grid slice as it passes through the geometry. Note the grid refinement as the plane passes through the geometry and how the detail is

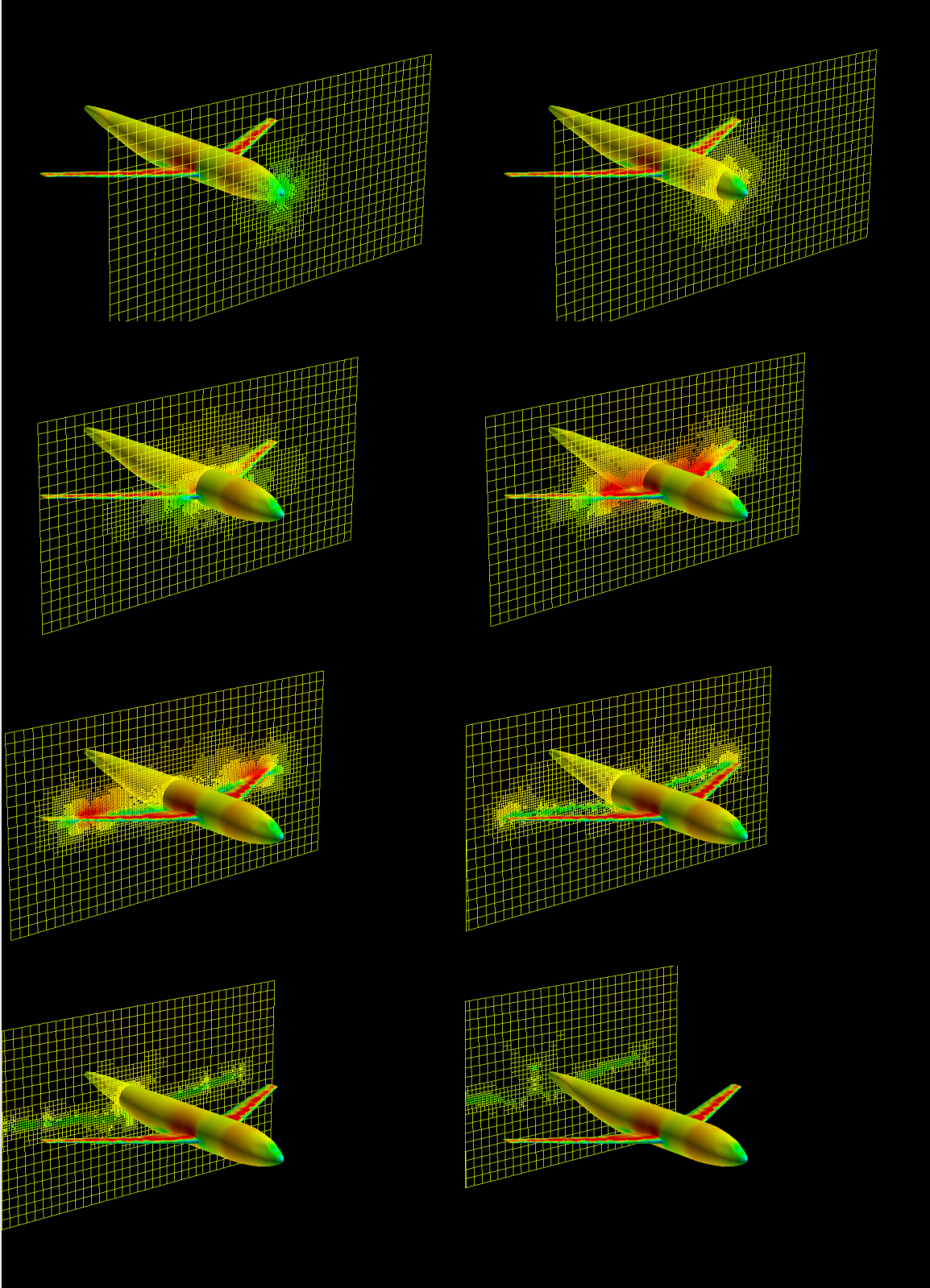


(Fig. 4-7) a scalar grid passing through the DLR-F4 geometry displaying Mach #

greatly increased closer to the surface. There is a surge of low Mach air at the nose and along the frontal profile of the aircraft as the mach speed relative to the aircraft is slowed by the drag. There is a higher mach number along the upper surface of the wings due to the accelerated air. A horizontal wake is visible where the slowed air interacts with the outside flow and regains speed.

## Conclusions and Further Research:

### *Conclusion:*

This research aided Dr. Ruffin and the Aerothermodynamics Research and Technologies Laboratory in the process of creating a solid foundation for validating the NASCART-GT package. An extensive amount of work was done in order to complete this project. Hundreds of man and CPU hours were logged and thousands of files created. Hopefully this research will be used in the future in order help advance the NASCART-GT program at Georgia Tech. The authors are certain that this research will be used to help educate students about the fast growing field of Computational Fluid Dynamics and their experience at Georgia Tech. NASCART-GT's future looks promising according to the research conducted for this project. Overall NASCART was accurate in the areas of pressure distribution, lift, and drag coefficients. Needless to say there are several bugs that need to be corrected, such as the oscillations at low level incompressible flows. During the span of this project several new versions of the NASCART code were published, some of these fixes can be directly attributed to this research. The experiences that the authors have received here are priceless in their minds. The people that they have interacted with will not soon be forgotten. They are extremely grateful towards NASA and Georgia Tech for allowing them to participate in this program. The authors

would like to take this opportunity to thank and acknowledge several people for their guidance and support through-out the course of this project: Ms. Wanda Pierson for her encouragement, support and great sense of humor; Dr. Komerath for allowing the authors to sit in on some of his classes and for his great sense of humor. Finally the authors would like to thank Dr. Stephen Ruffin and his graduate students Jae Doo Lee and Jin Wook Lee of the Aerothermodynamics Research and Technologies Laboratory for their great patience and guidance.

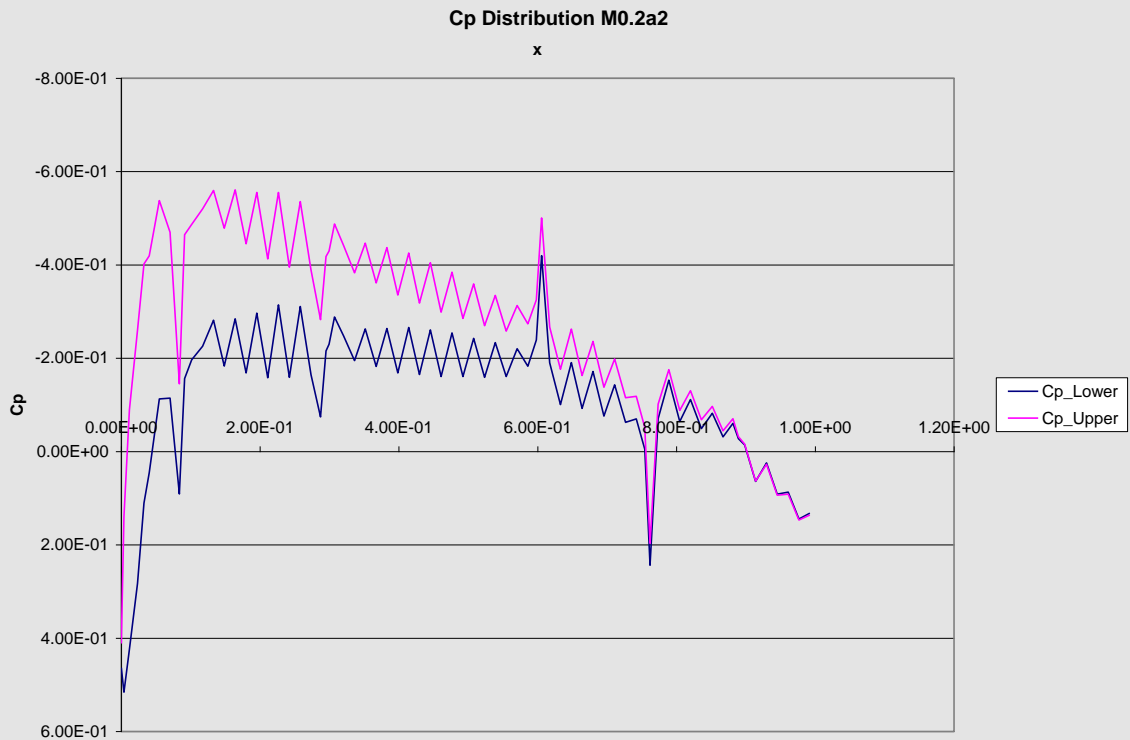
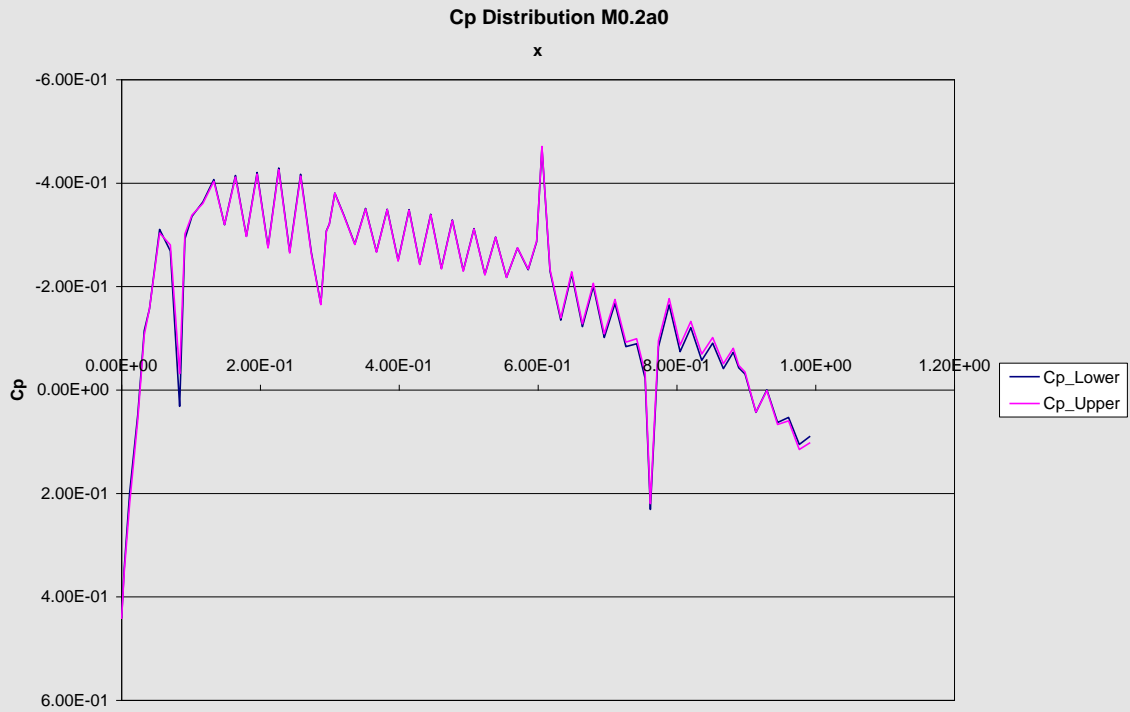
## Bibliography

- "AIAA-85-0435 Finite Volume Solution of the Two-Dimensional Euler Equations on a Regular Triangular Mesh." (1985): 8-10.
- "AIAA-85-0435 Finite Volume Solution of the Two-Dimensional Euler Equations on a Regular Triangular Mesh." American Institute of Aeronautics and Astronautics (1985): 8-10.
- Abbott, Ira H., and Albert E. Von Doenhoff. Theory of Wing Sections Including a Summary of Airfoil Data. New York, NY: Dover Publications, Inc., 1959. 321-462.
- Anderson Jr., John D. Computational Fluid Dynamics the Basics with Applications. New York, NY: McGraw-Hill, Inc., 1995.
- Anderson Jr., John D. Introduction to Flight. New York, NY: McGraw-Hill, Inc., 1989.
- Arrowood, Adam, and Tammy M. Tuley. The (Unofficial) Buzz Image Page. Georgia Institute of Technology. 27 July 2003 <<http://dept.gatech.edu/adam/buzz/>>.
- Bonfiglioli, Aldo.. Compressible, viscous (laminar) flow past a NACA 0012 profile. 19 Oct. 1998. Department of Environmental Physics and Engineering of the University of Basilicata. 20 June 2003 <<http://www.unibas.it/utenti/bonfiglioli/node9.html>>.
- Case Lab Research. 20 Mar. 2001. Oklahoma State University. 13 June 2003 <<http://www.caselab.okstate.edu/research/validation.html>>.
- Chandrasekhara, M. S. "AIAA 96-0073 Reynolds Number Influence on 2-D Compressible Dynamic Stall." American Institute of Aeronautics and Astronautics (1996): 9-14.
- F4 Wing. American Institute of Aeronautics and Astronautics. 29 June 2003 <<http://www.aiaa.org/tc/apa/dragpredworkshop/wing.txt>>.
- Jameson, A., and D. Mavriplis. "AIAA-85-0435 Finite Volume Solution of the Two-Dimensional Euler Equations on a Regular Triangular Mesh." American Institute of Aeronautics and Astronautics (1985): 8-10.
- Lee, Jae Doo, Jin Wook Lee, and Dr. Stephen M. Ruffin. NASCART-GT. 30 June 2003. Georgia Institute of Technology. 27 June 2003 <<http://www.ae.gatech.edu/~sruffin/nascart/>>.

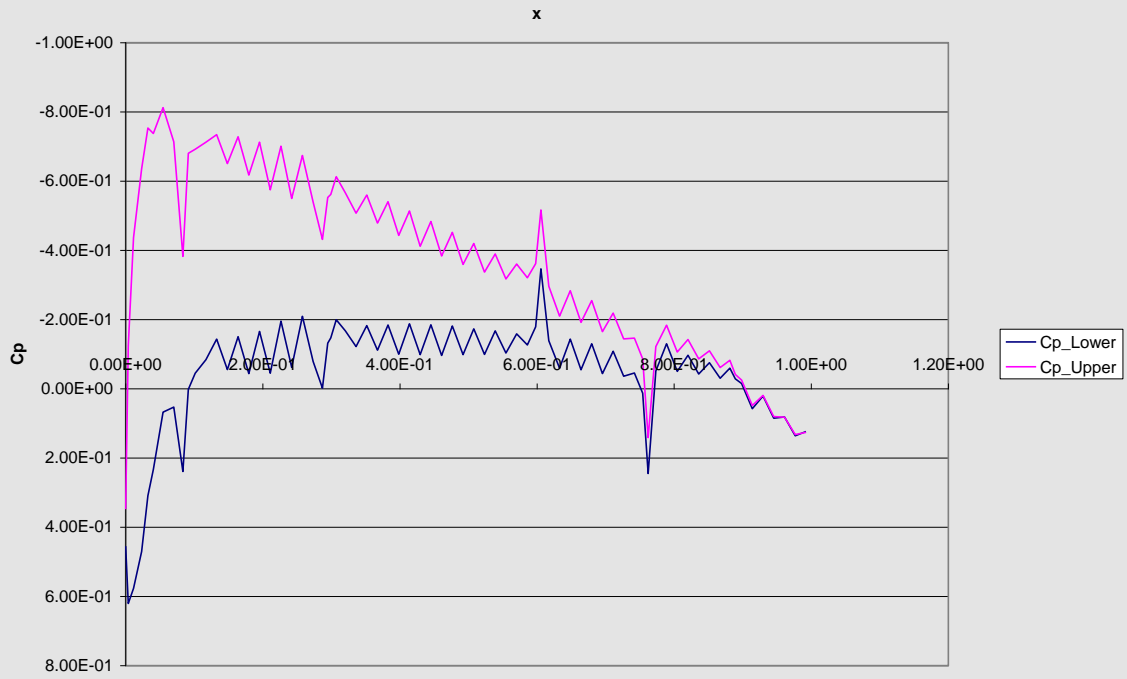
- Leschziner, M. A., and L. Temmerman. European Research Community on Flow, Turbulence and Combustion. 2001. ERCOFTAC. 14 June 2003  
<[http://cfd.me.umist.ac.uk/cgi-bin/cfddb/ezdb.cgi?ercdb+search+retrieve+&&&\\*% % % % dm=Line](http://cfd.me.umist.ac.uk/cgi-bin/cfddb/ezdb.cgi?ercdb+search+retrieve+&&&*% % % % dm=Line)>.
- Marshall, David D. "Extending the Functionalities of Cartesian Grid Solvers: Viscous Effects Modeling and MPI Parallelization." Diss. Georgia Institute of Technology, 2002.
- Menzies, Ryan . NACA 0012 Aerofoil. 7 Apr. 2003. University of Glasgow. 30 June 2003 <<http://www.aero.gla.ac.uk/Research/CFD/projects/cfdval/TN02-016/node15.html>>.
- Menzies, Ryan. Test Case Validation Database. 7 Apr. 2003. University of Glasgow. 25 June 2003 <<http://www.aero.gla.ac.uk/Research/CFD/projects/cfdval/TN02-016/TN02-016.html>>.
- MSN Learning & Research. Encarta. 22 July 2003 <<http://beta.encarta.msn.com/>>.
- NACA 0012 Airfoil- WVU, MAE 115, Fall 1999. 29 June 2003  
<<http://www.access.wvu.edu/class/mae115/exp4/0012.pdf>>.
- NACA 0012 MODIFIED WING. University of Glasgow. 2 July 2003  
<[http://www.aero.gla.ac.uk/Research/CFD/projects/cfdval/resources/DATABASE/NACA\\_WING/NACA\\_0012\\_MODIFIED.htm](http://www.aero.gla.ac.uk/Research/CFD/projects/cfdval/resources/DATABASE/NACA_WING/NACA_0012_MODIFIED.htm)>.
- NAS Division Home Page. 9 July 2003. National Aeronautics and Space Administration. 16 July 2003 <<http://www.nas.nasa.gov/index.html>>.
- NASA Langley Research Center Geometry Laboratory. 17 Sept. 2003. National Aeronautics and Space Administration. 15 June 2003  
<<http://geolab.larc.nasa.gov/cgi-bin/Bene/Gallery/Gallery.pl>>.

## Appendix A: Charts and Graphs

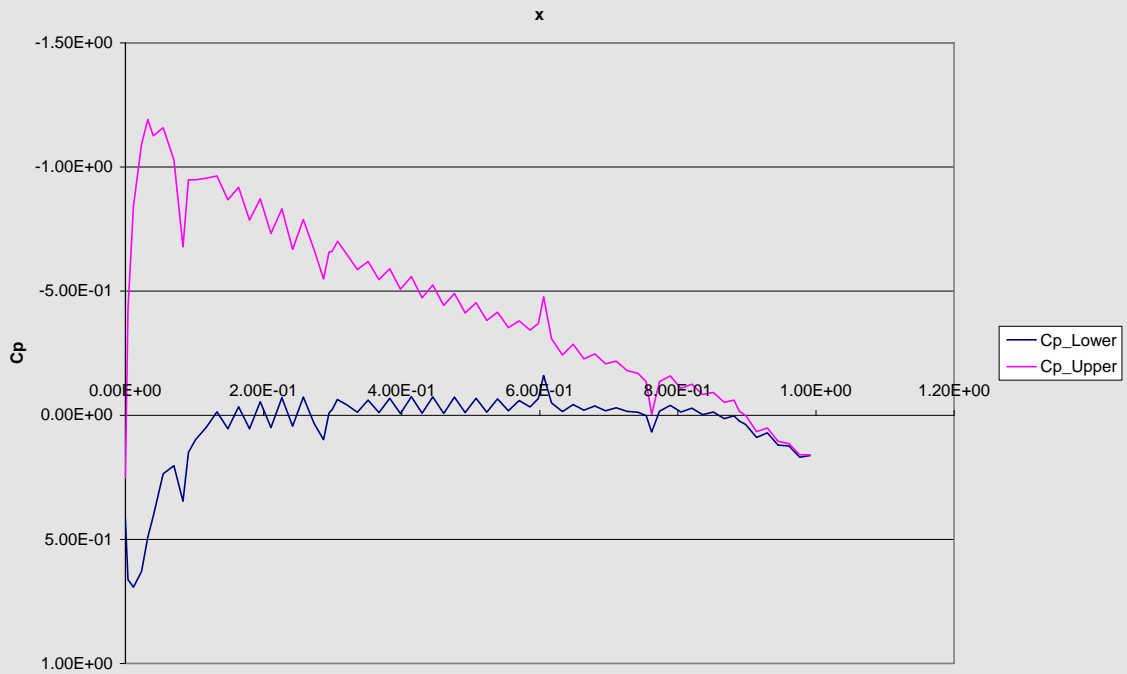
This appendix contains pressure distribution plots for all of the test cases as well as comparison charts and graphs. Please note the oscillation peaks in the low level incompressible flows. Also note that in  $\alpha=0$  the lines are equal.



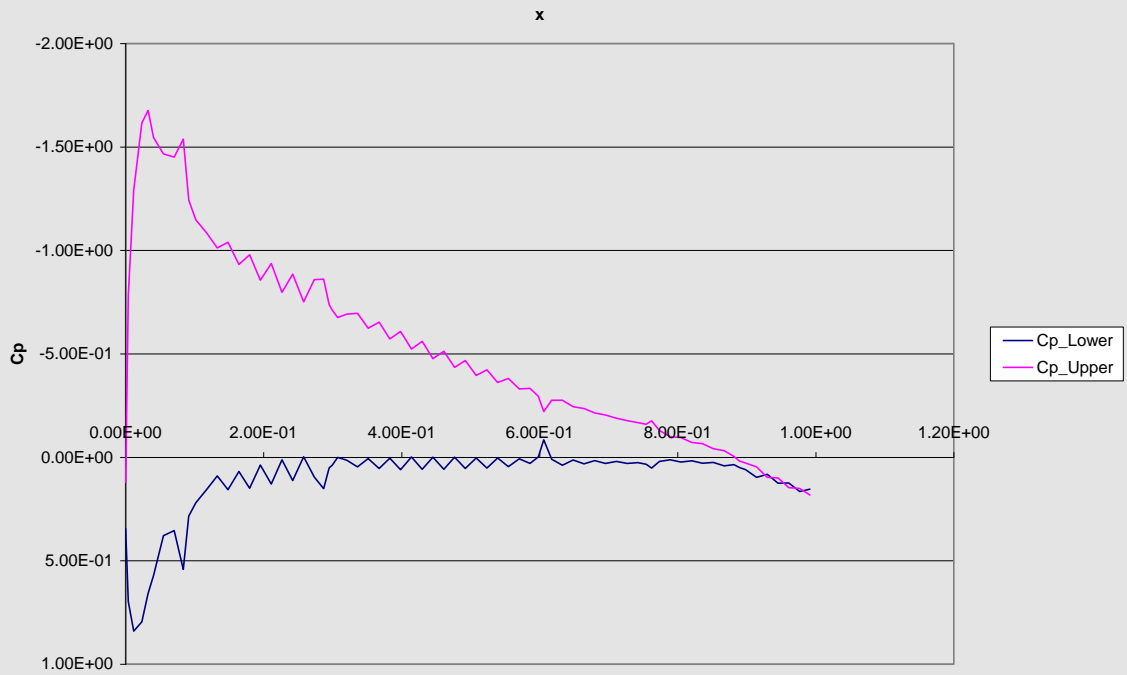
Cp Distribution M0.2a4



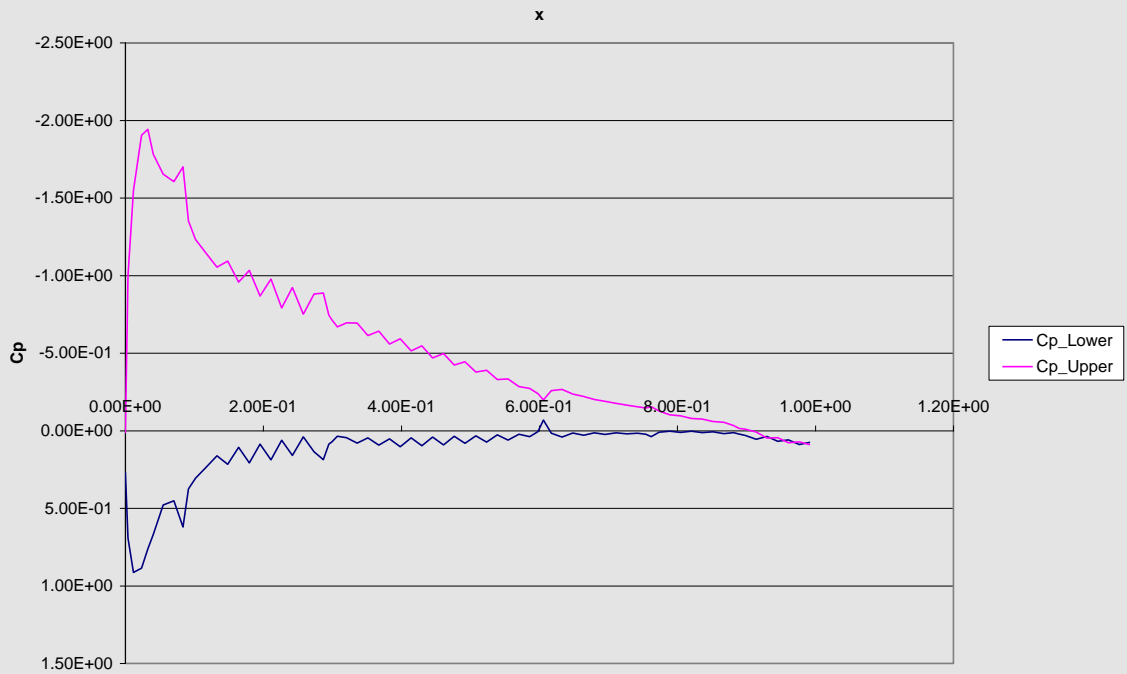
Cp Distribution M0.2a6



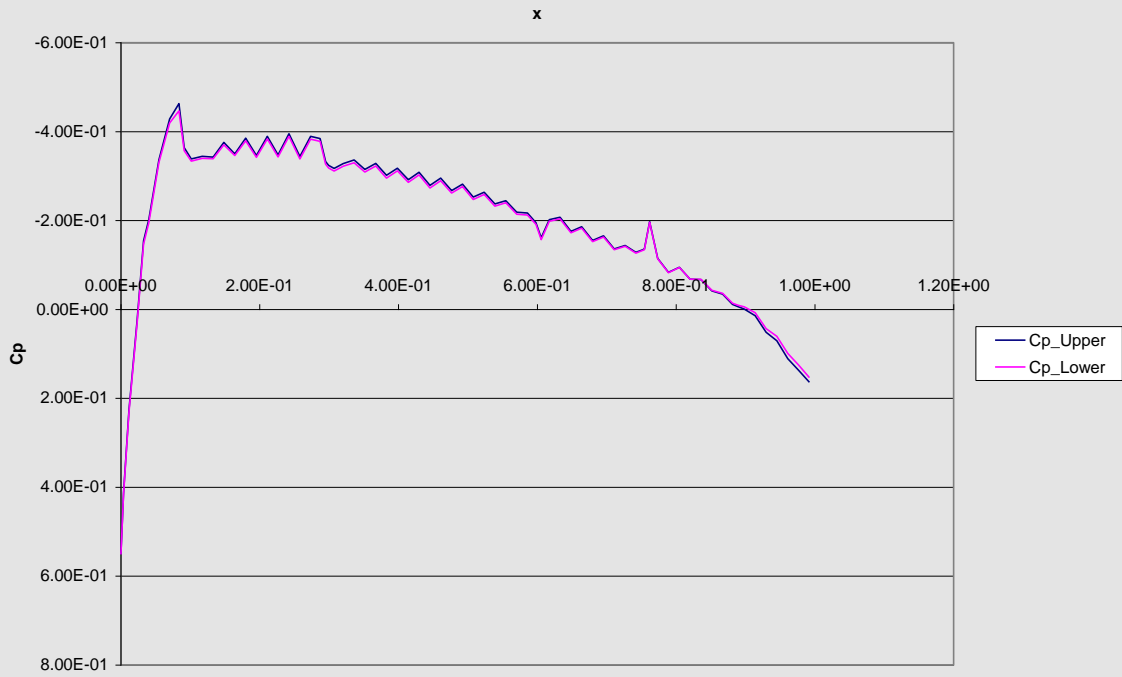
Cp Distribution M0.2a8



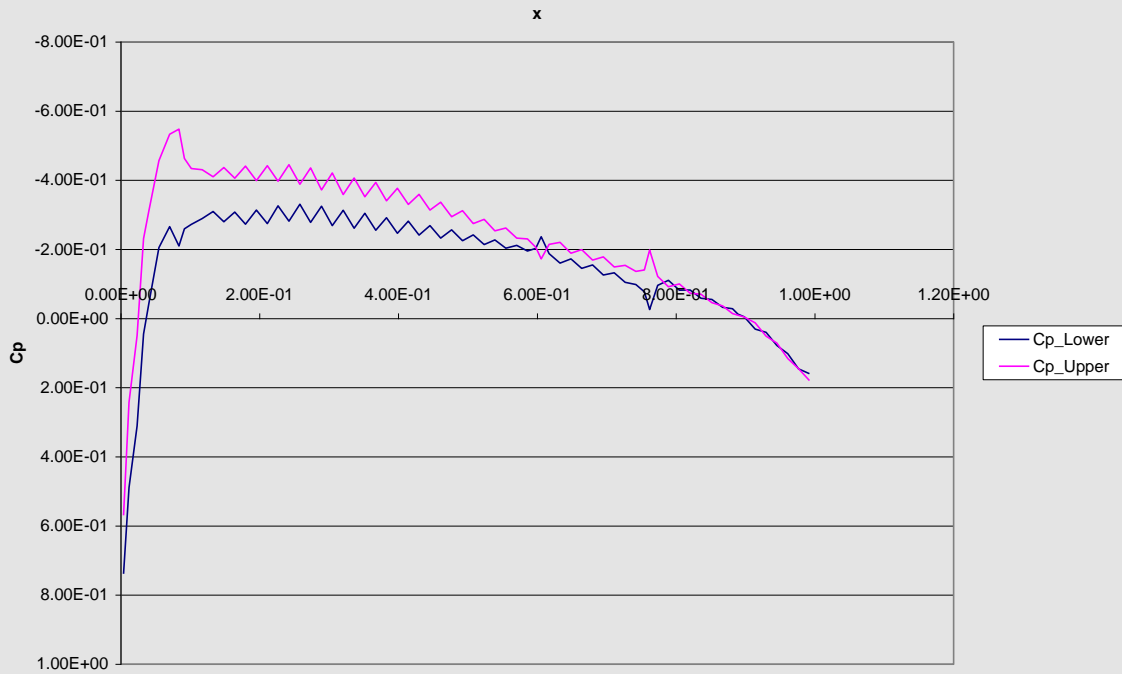
Cp Distribution M0.2a10



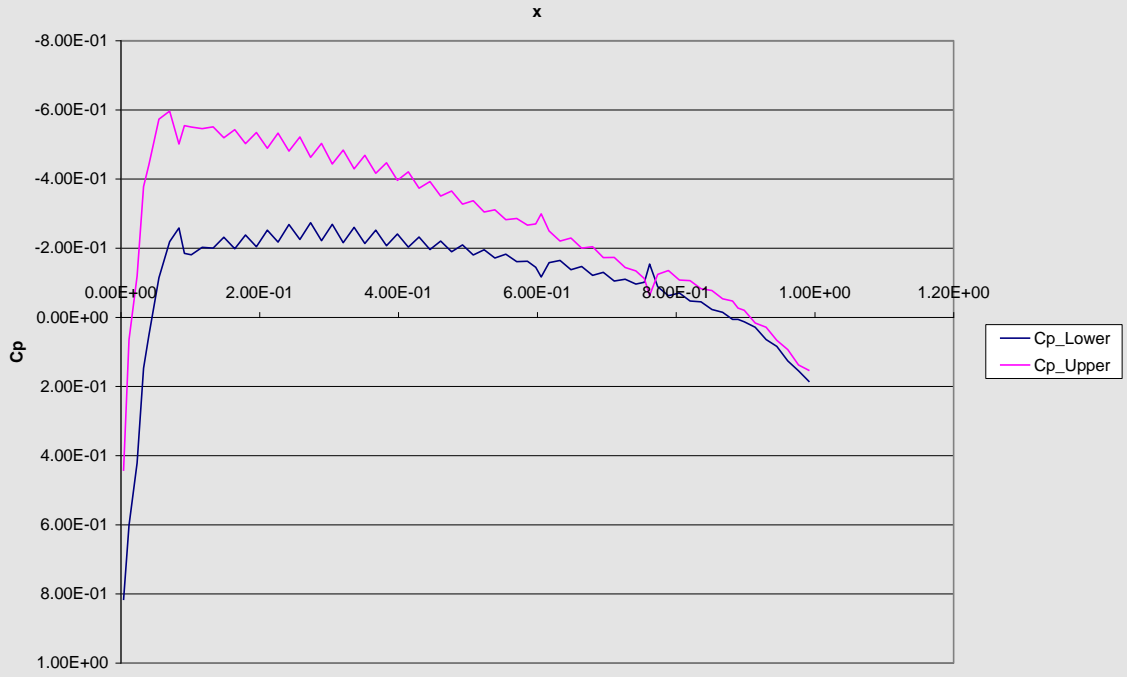
Cp Distribution M0.3a0



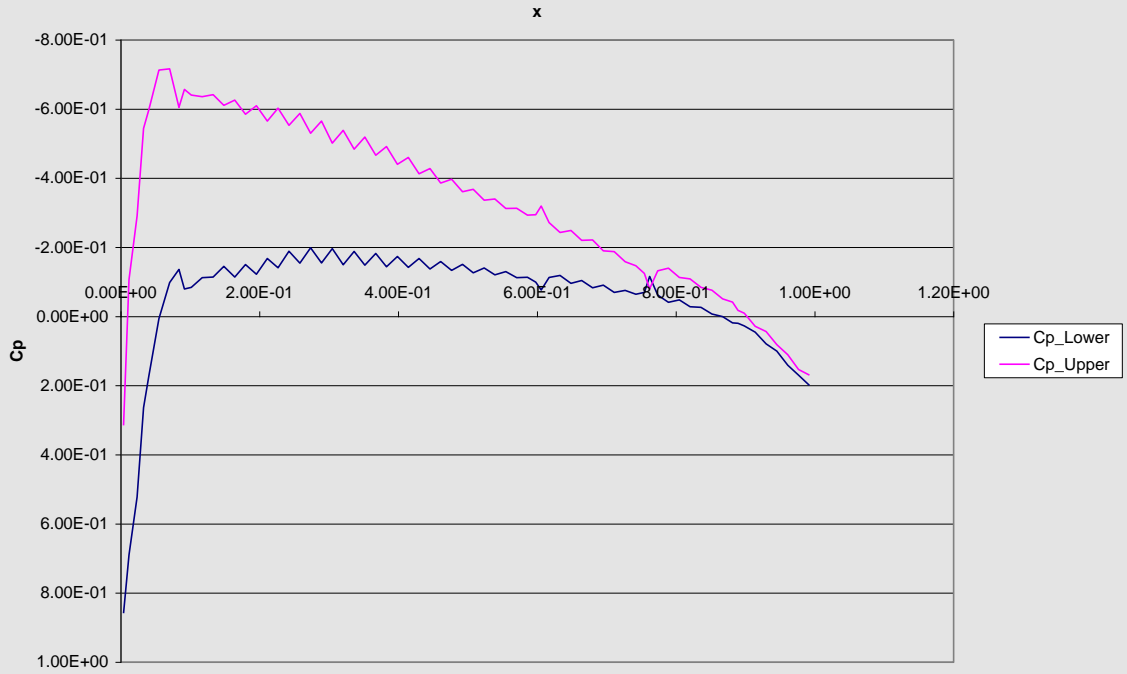
Cp Distribution M0.3a1



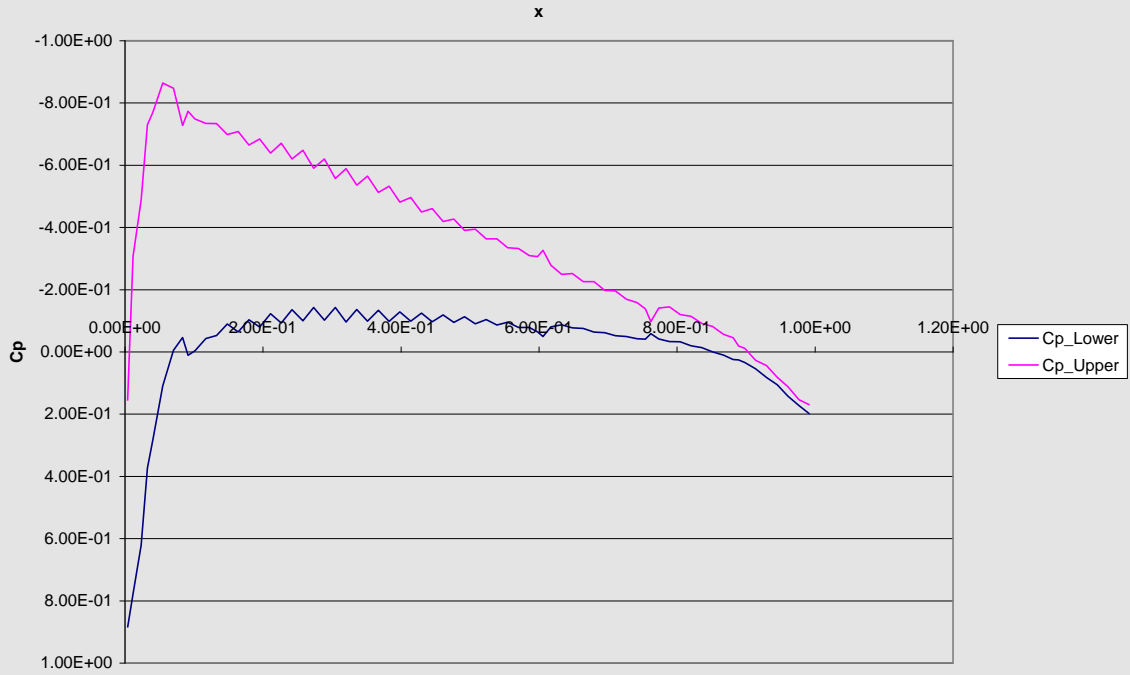
Cp Distribution M0.3a2



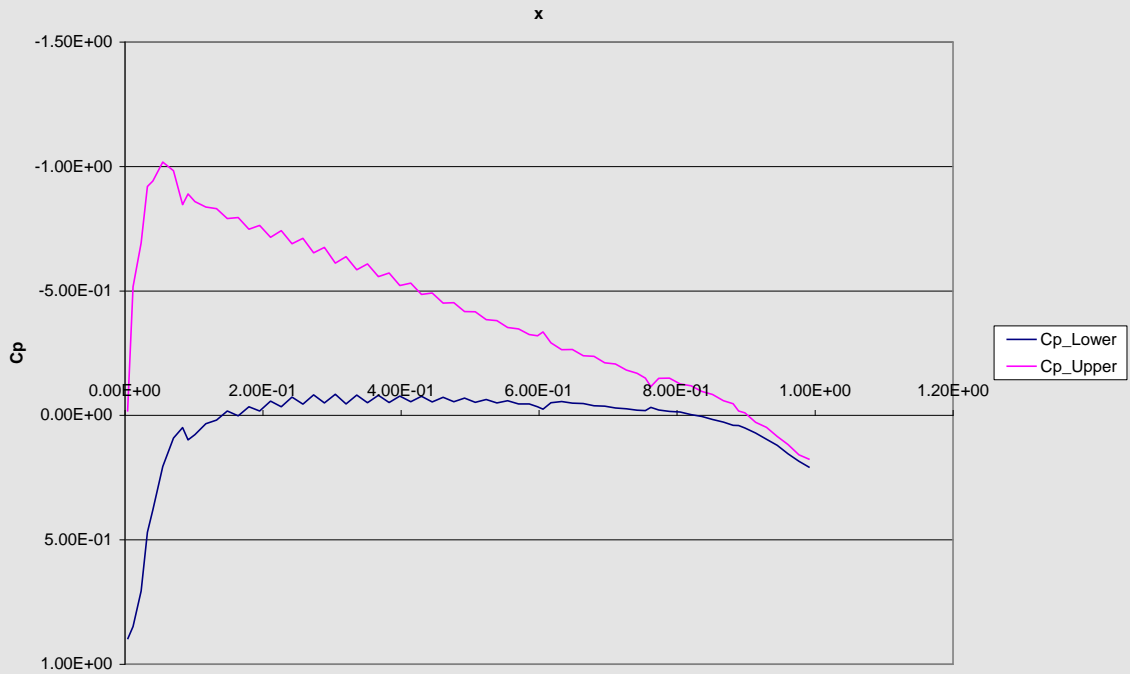
Cp Distribution M0.3a3



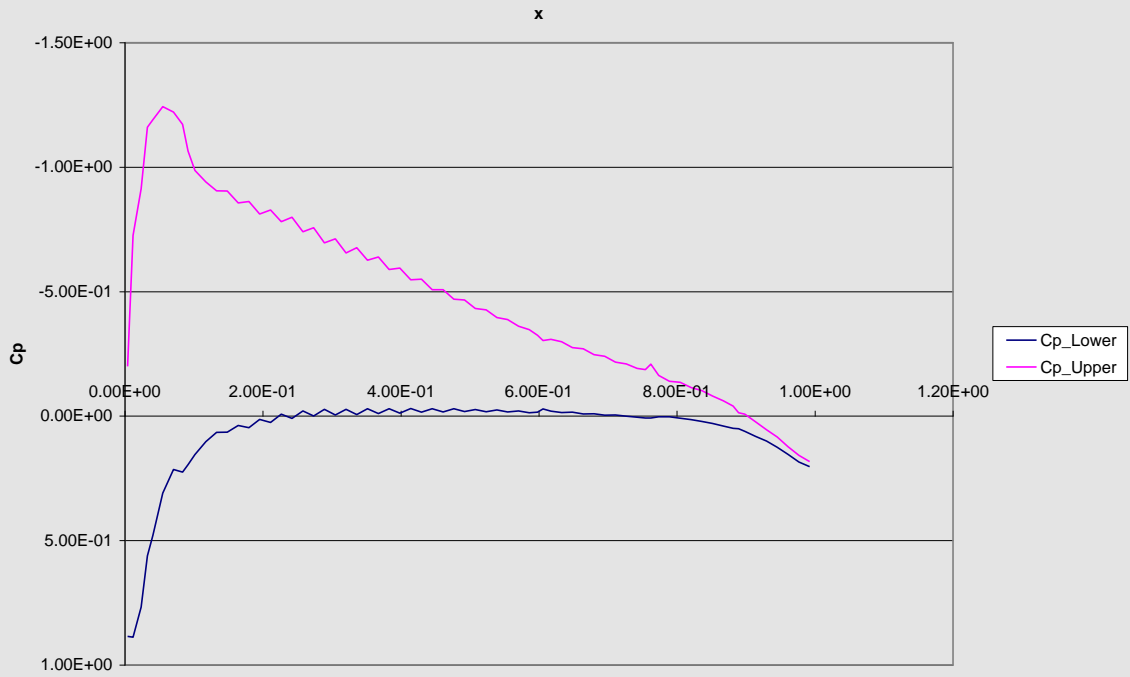
Cp Distribution M0.3a4



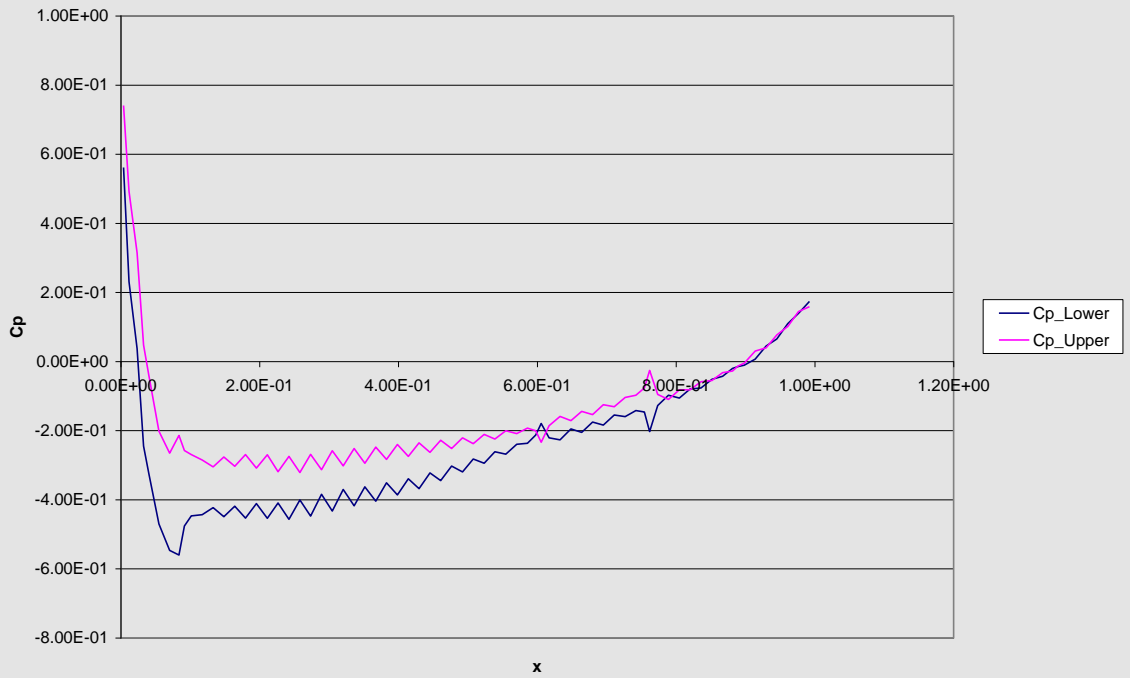
Cp Distribution M0.3a5



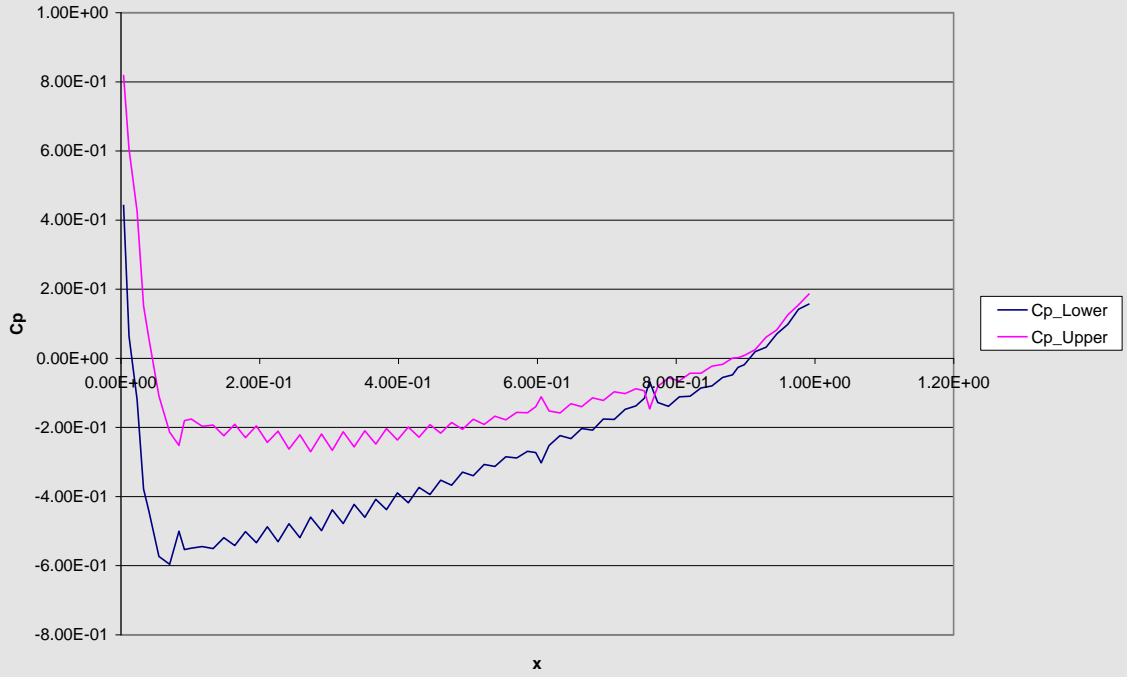
Cp Distribution M0.3a6



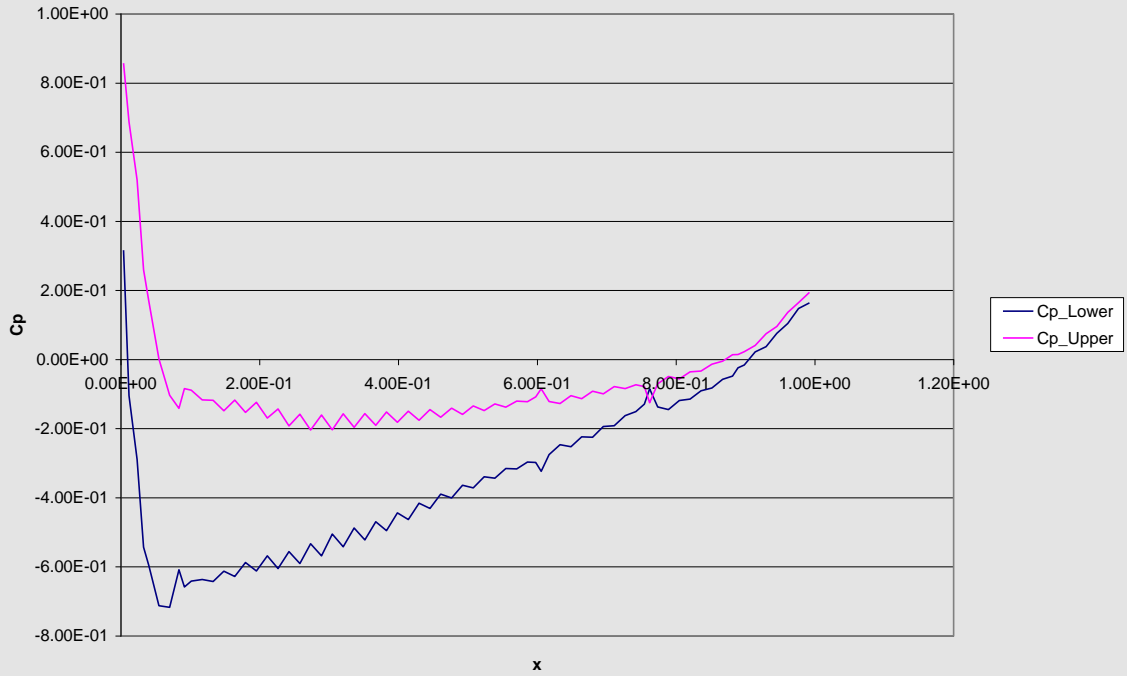
Cp Distribution M0.3a-1



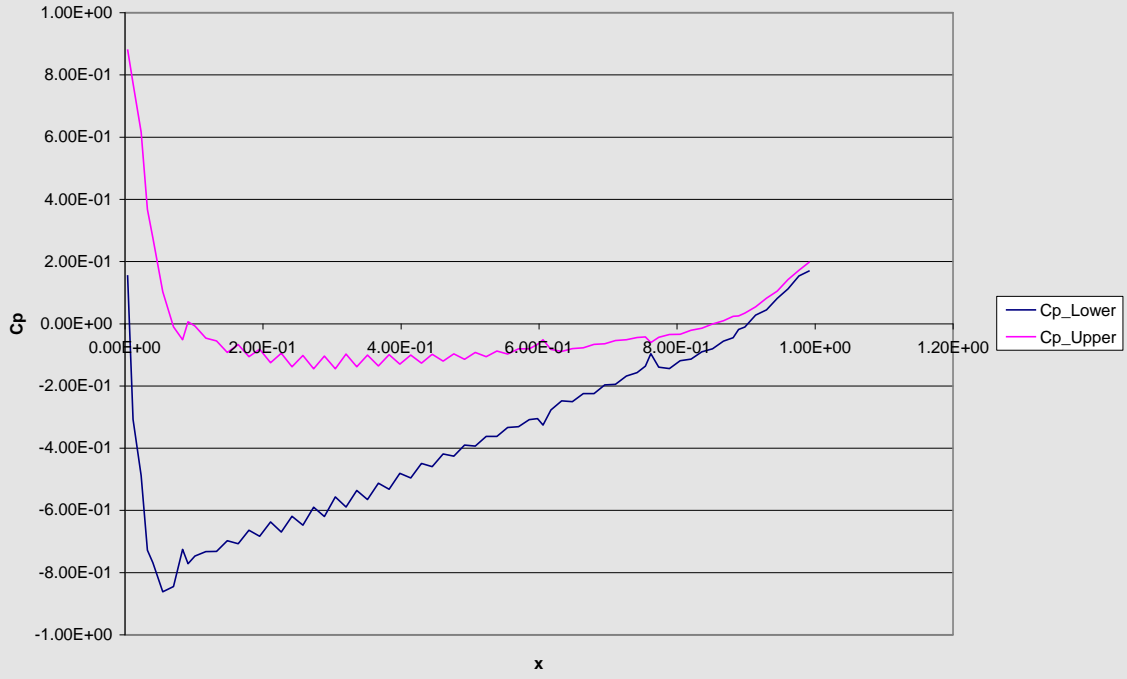
Cp Distribution M0.3a-2



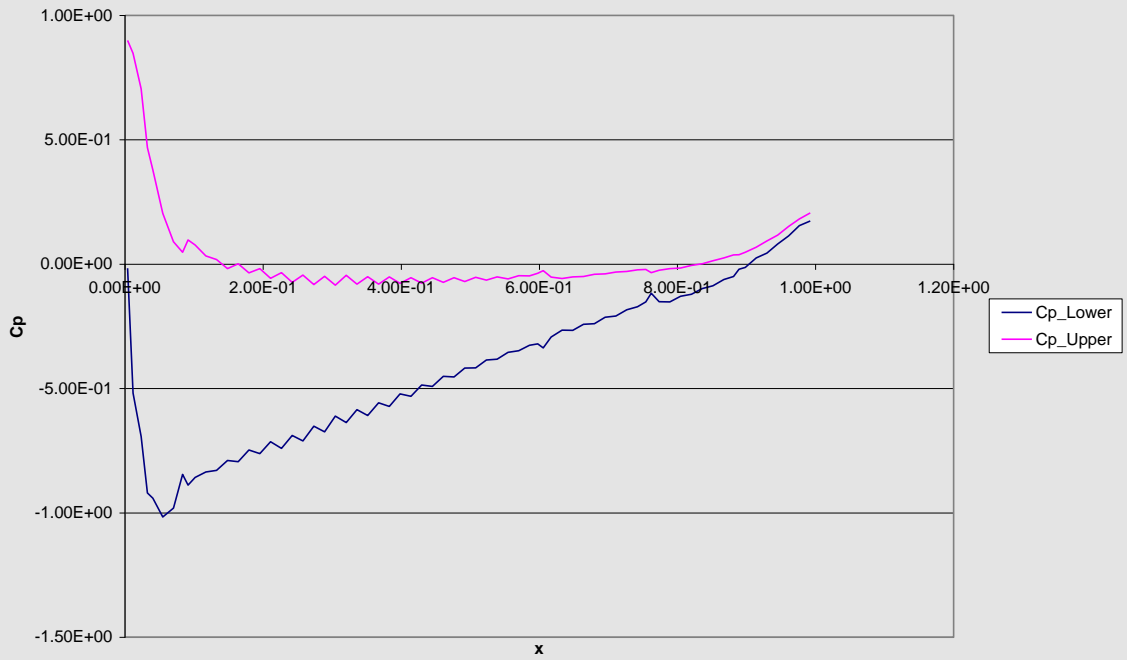
Cp Distribution M0.3a-3



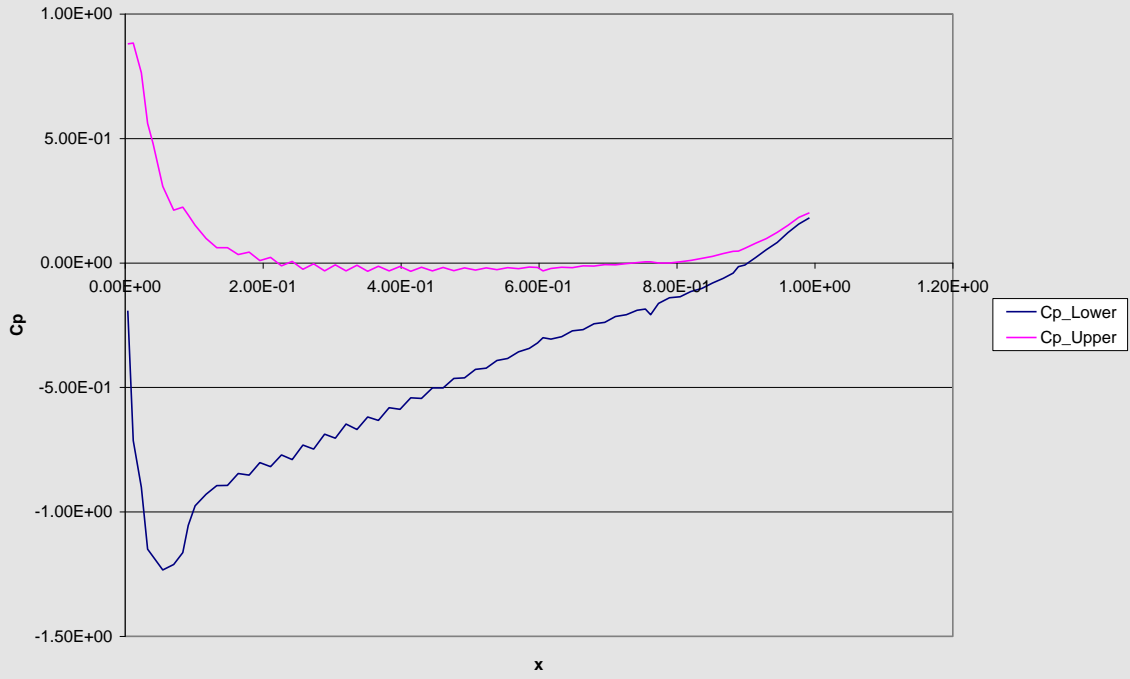
Cp Distribution M0.3a-4



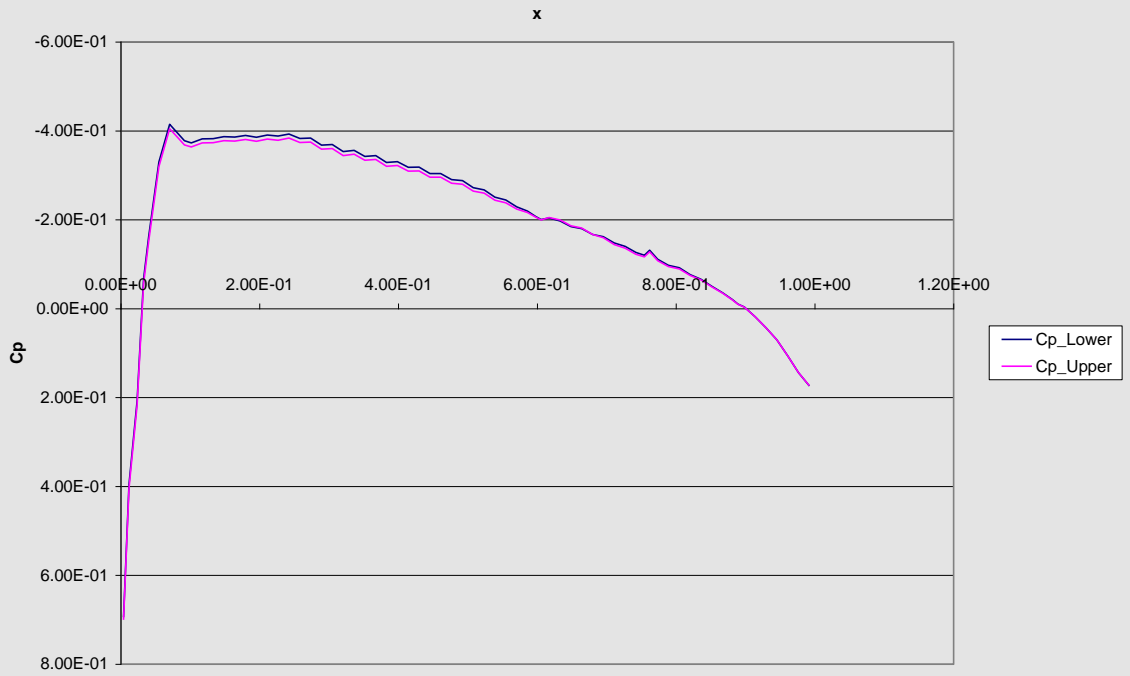
Cp Distribution M0.3a-5



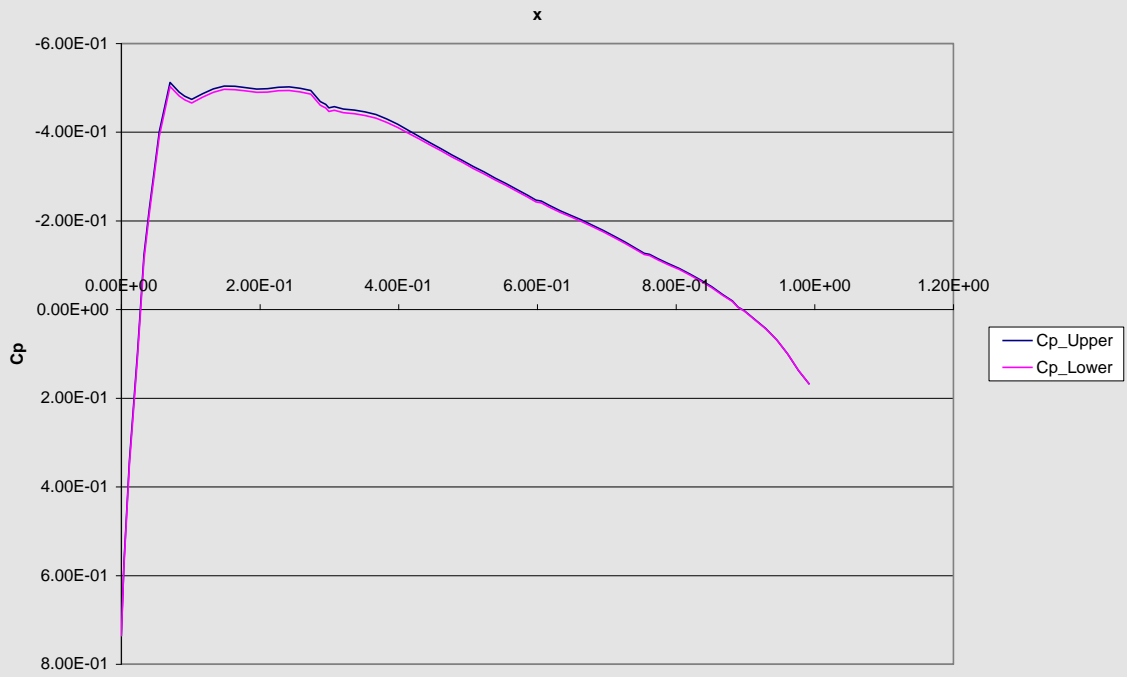
Cp Distribution M0.3a-6



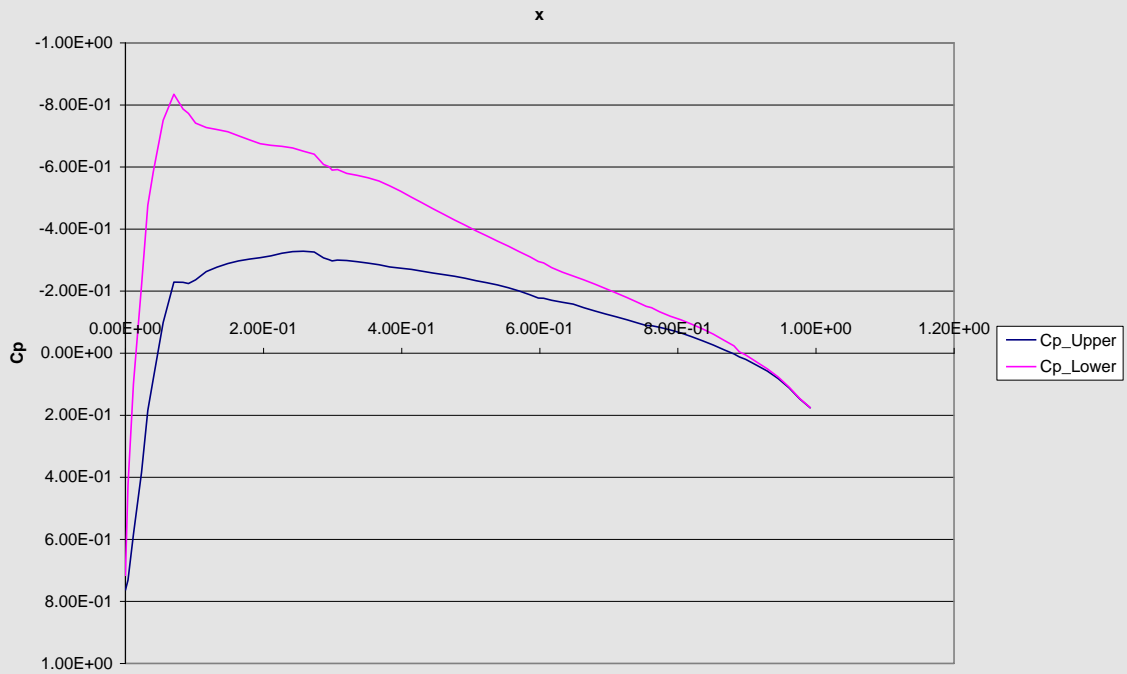
Cp Distribution M0.4a0



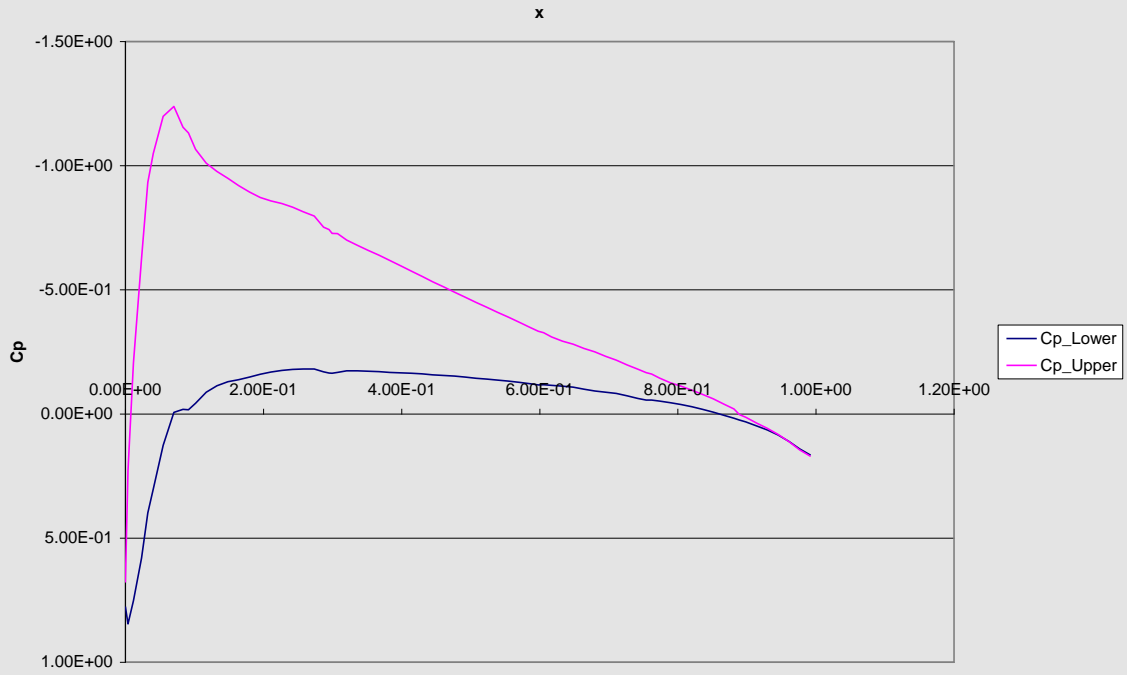
Cp Distribution M0.6a0



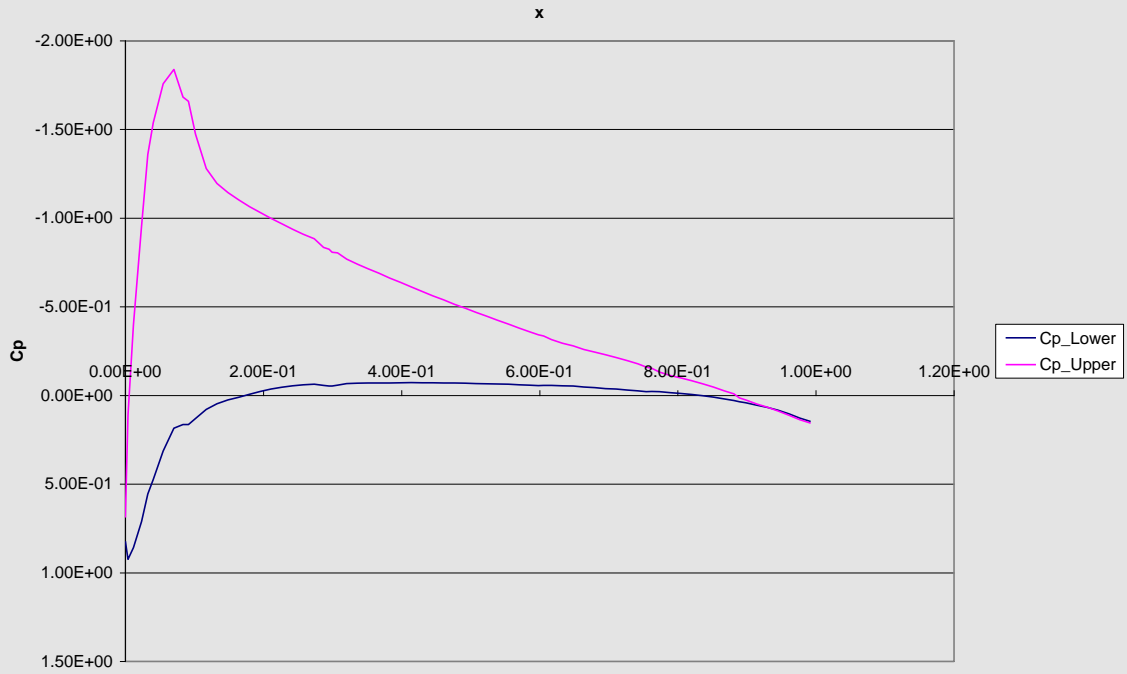
Cp Distribution M0.6a2



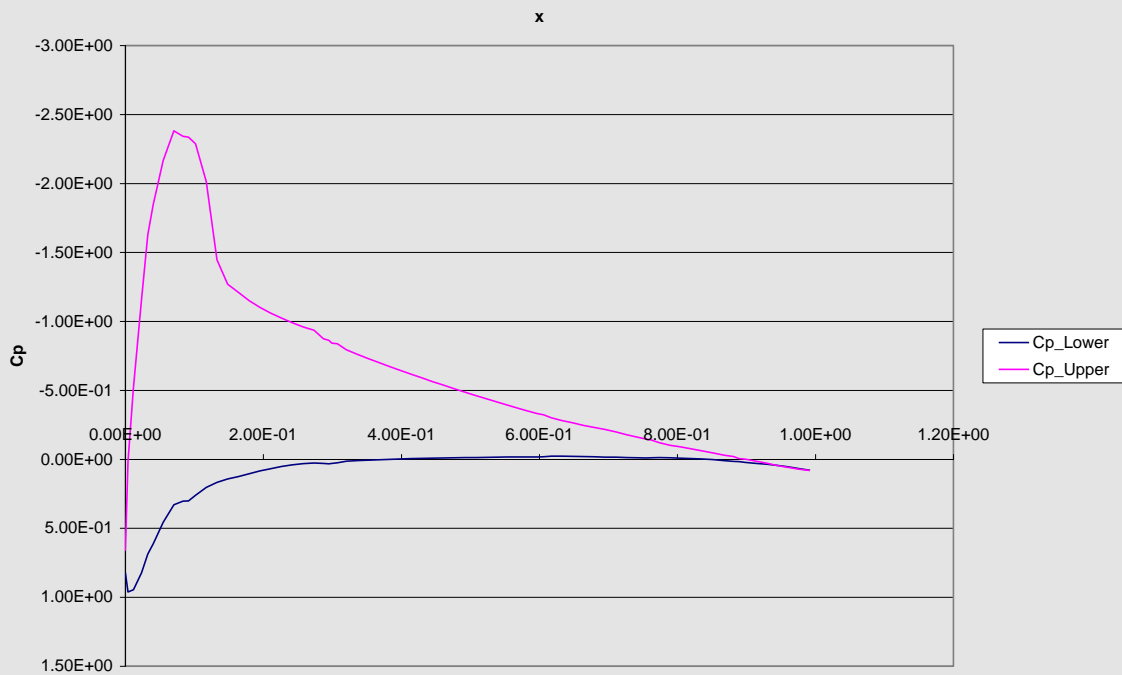
Cp Distribution M0.2a4



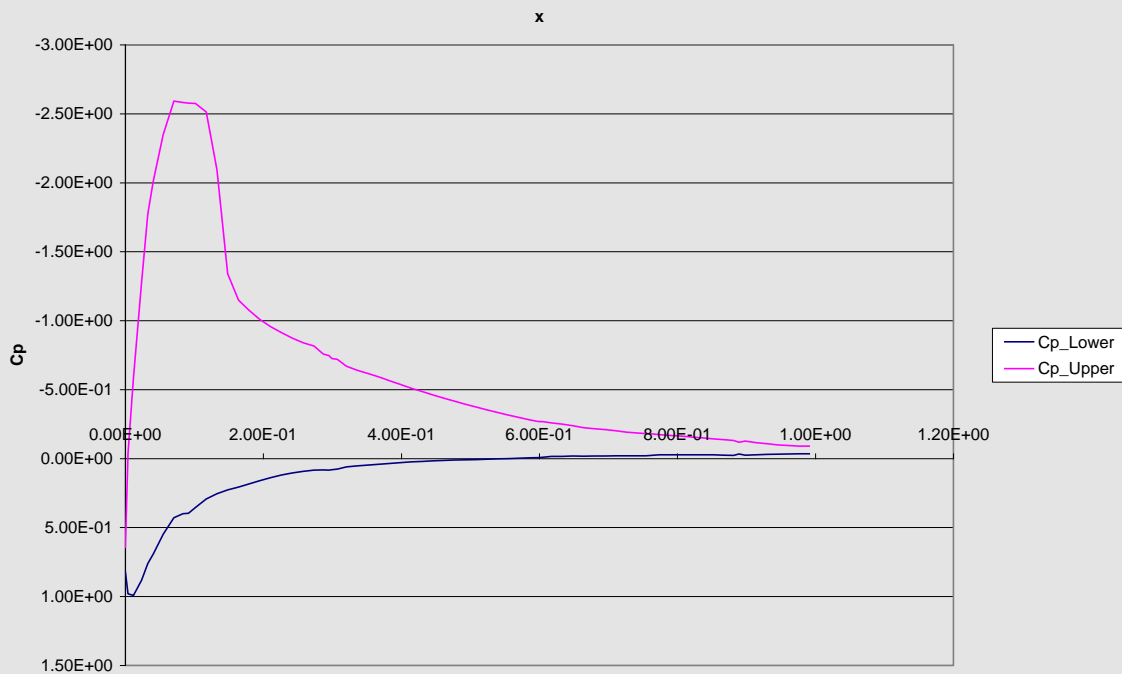
Cp Distribution M0.6a6



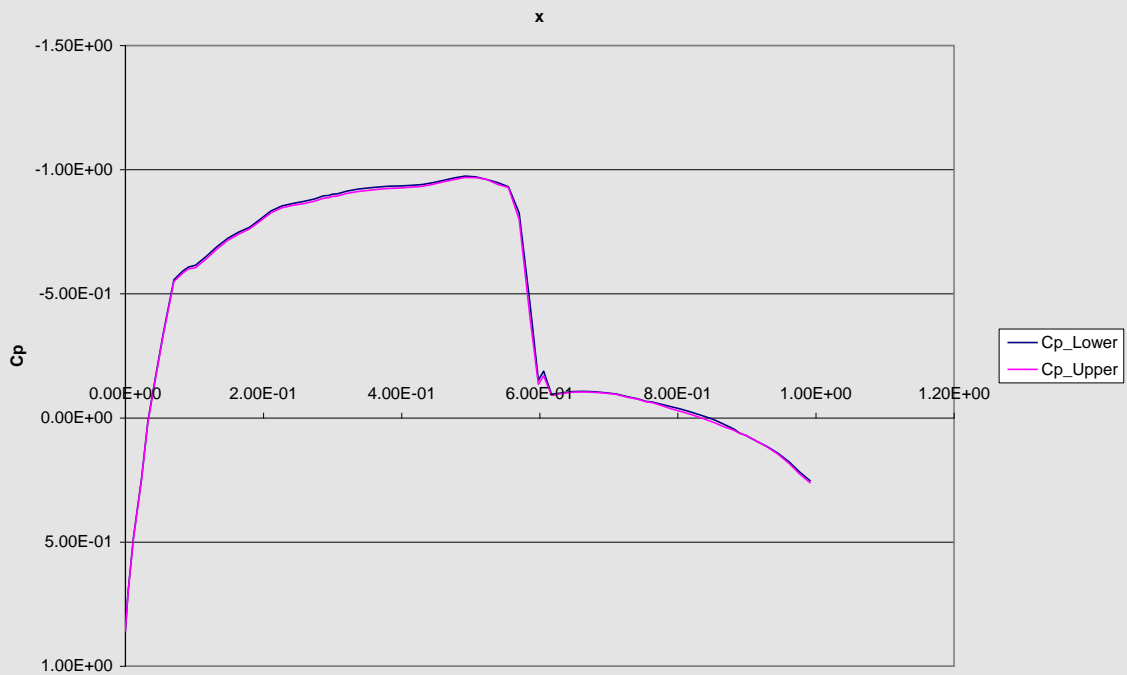
Cp Distribution M0.6a8



Cp Distribution M0.6a10



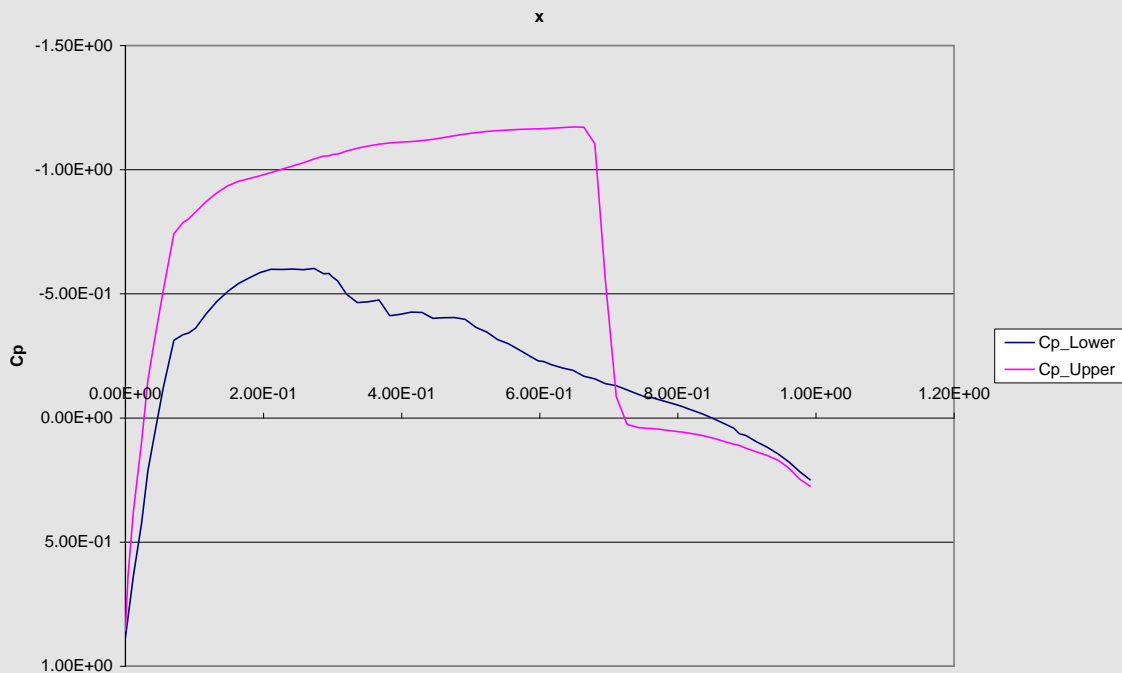
Cp Distribution M0.8a0



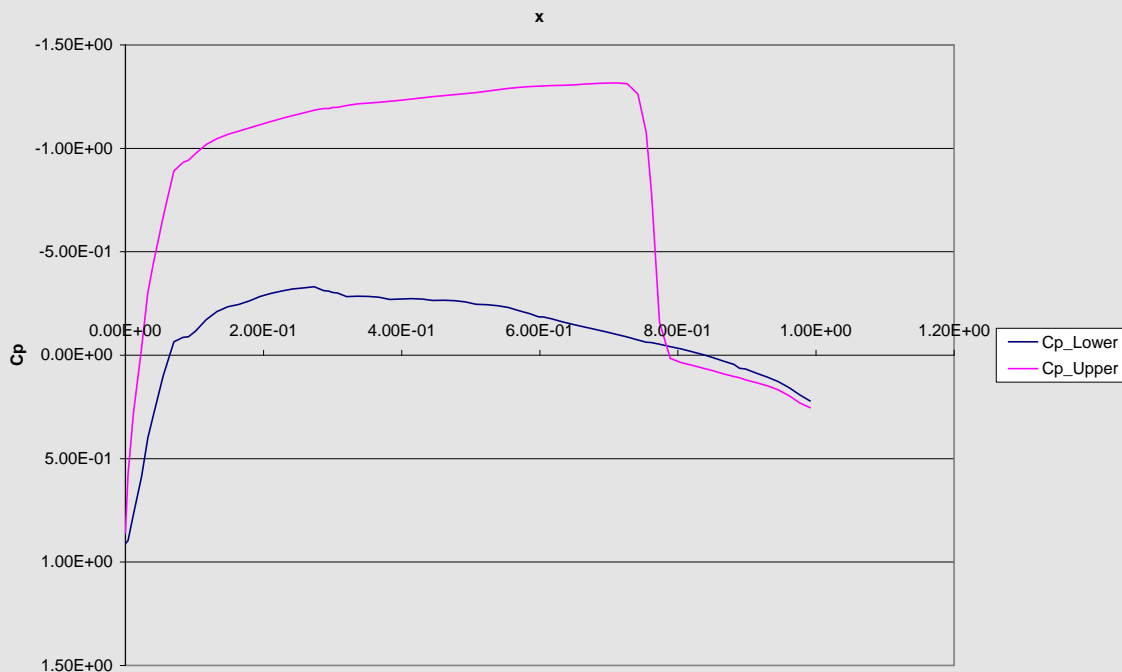
Cp Distribution M0.8a1.25



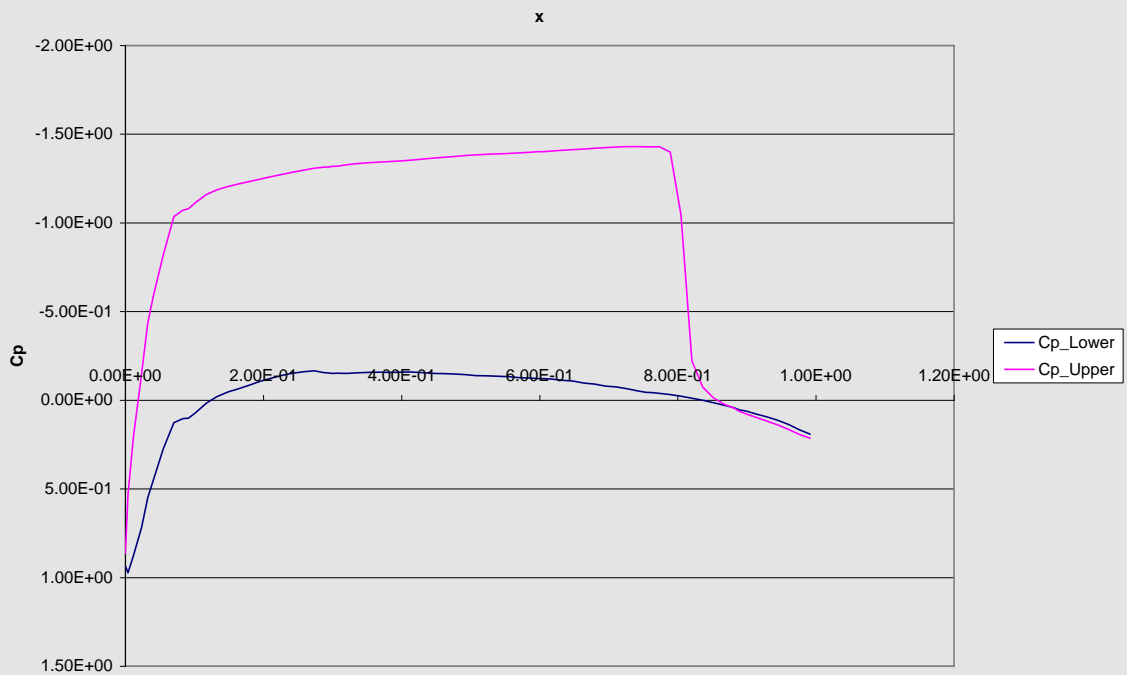
Cp Distribution M0.8a2



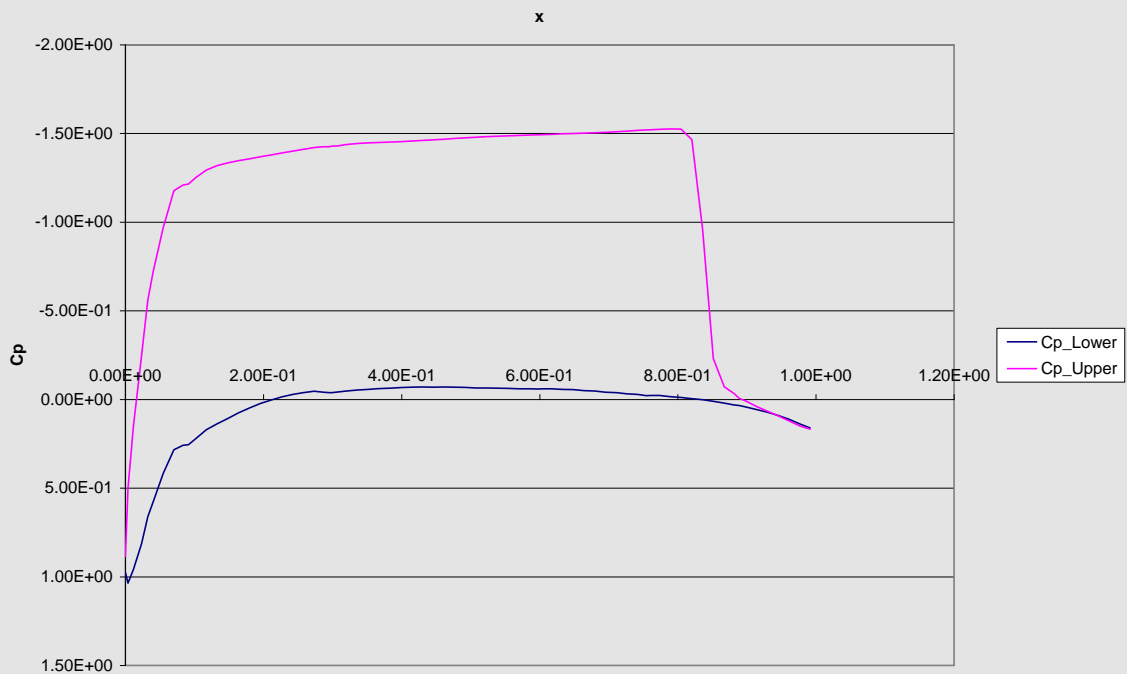
Cp Distribution M0.8a4



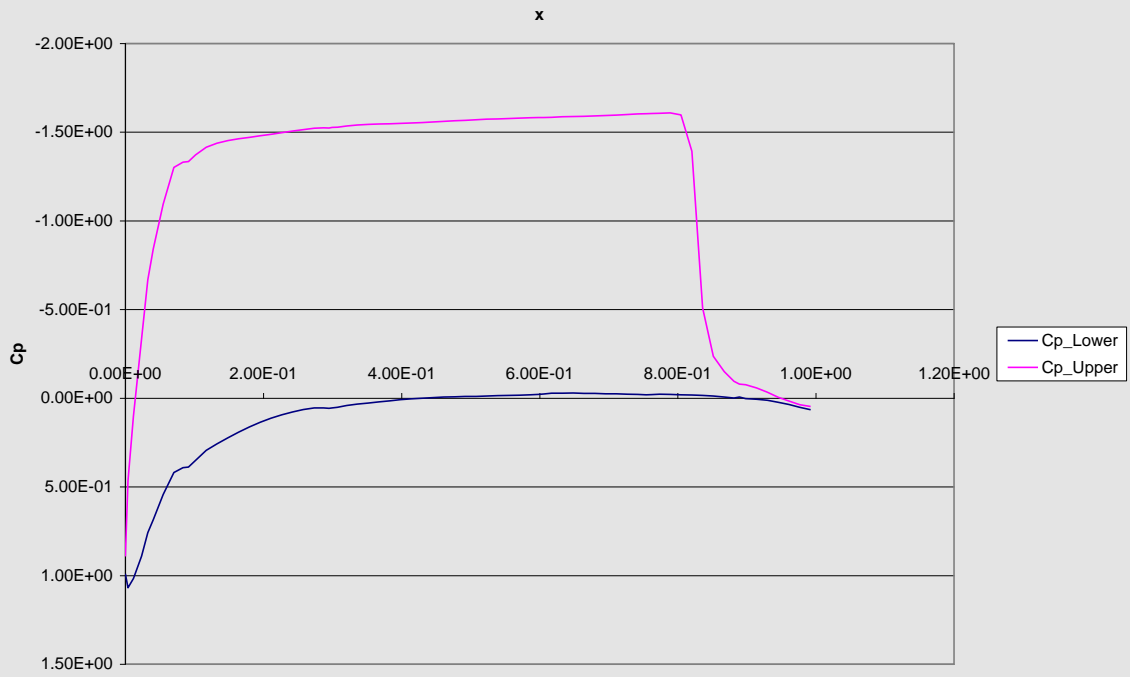
Cp Distribution M0.8a6



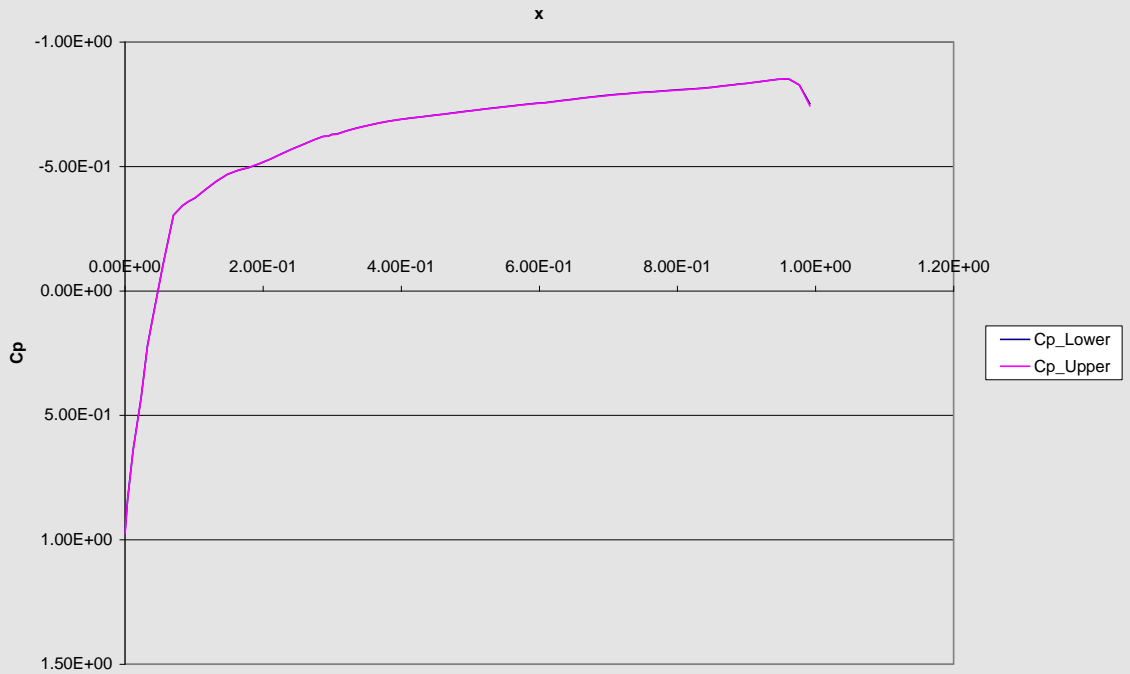
Cp Distribution M0.8a8



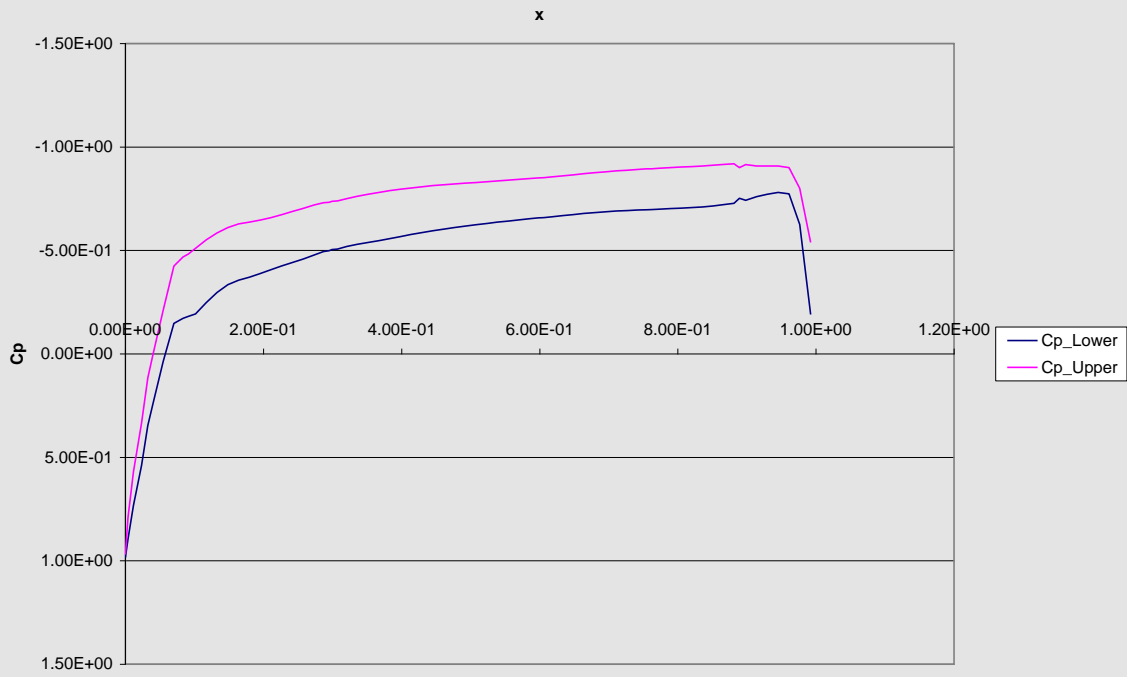
Cp Distribution M0.8a10



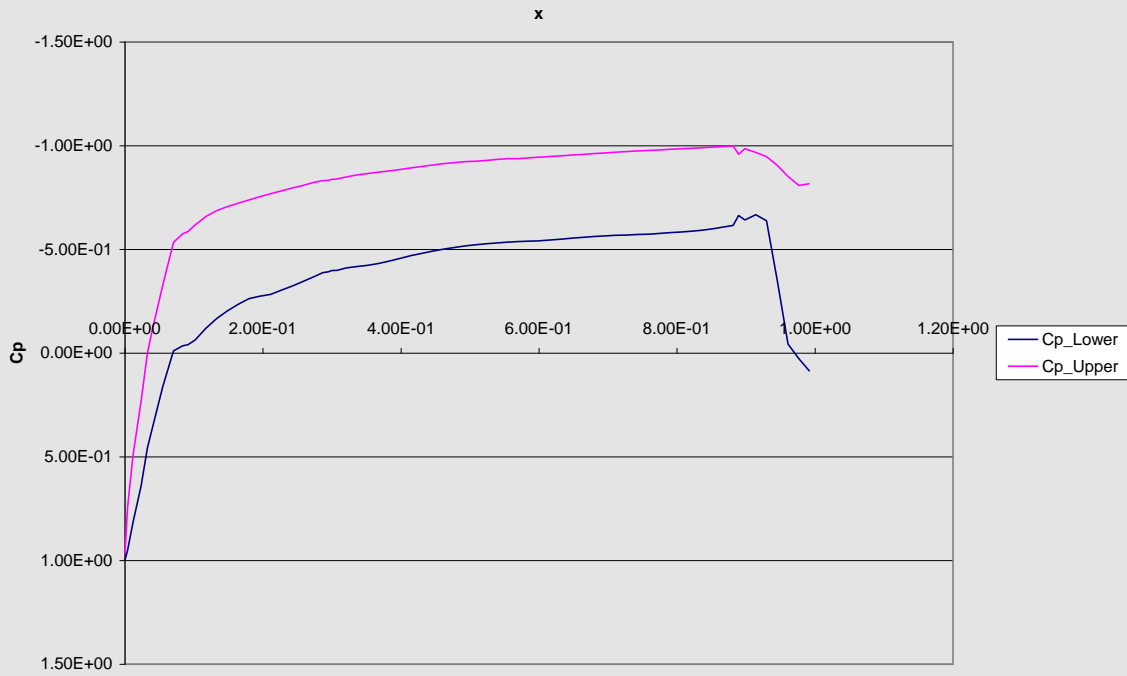
Cp Distibution M0.9a0



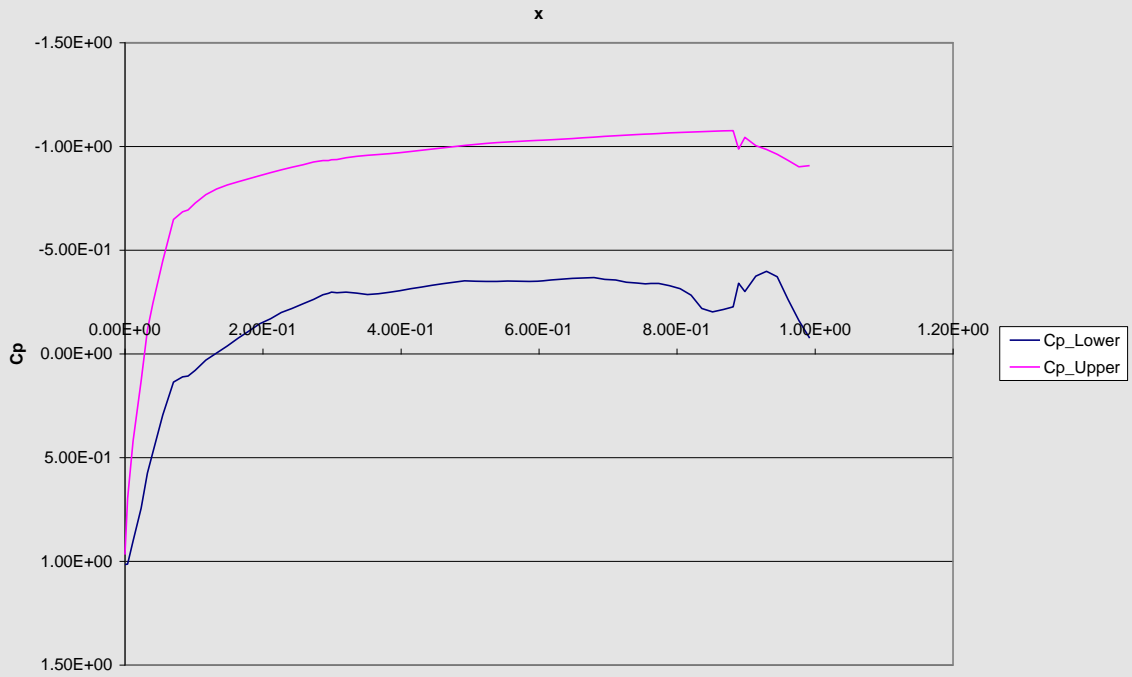
Cp Distribution M0.9a2



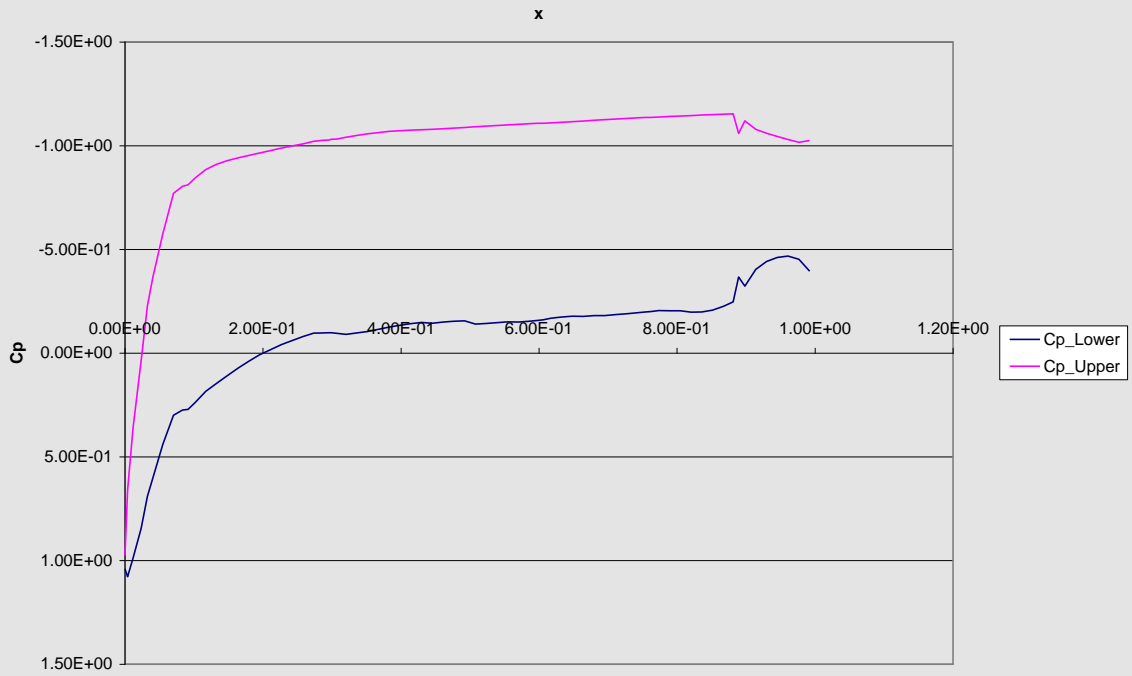
Cp Distribution M0.9a4



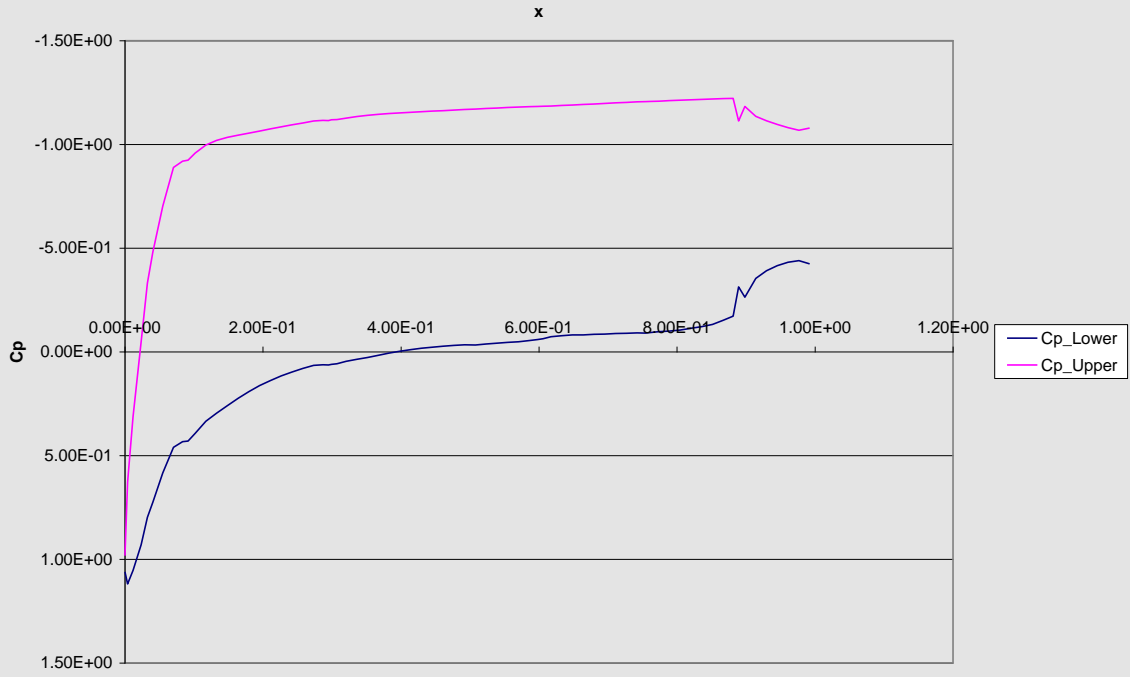
Cp Distribution M0.9a6



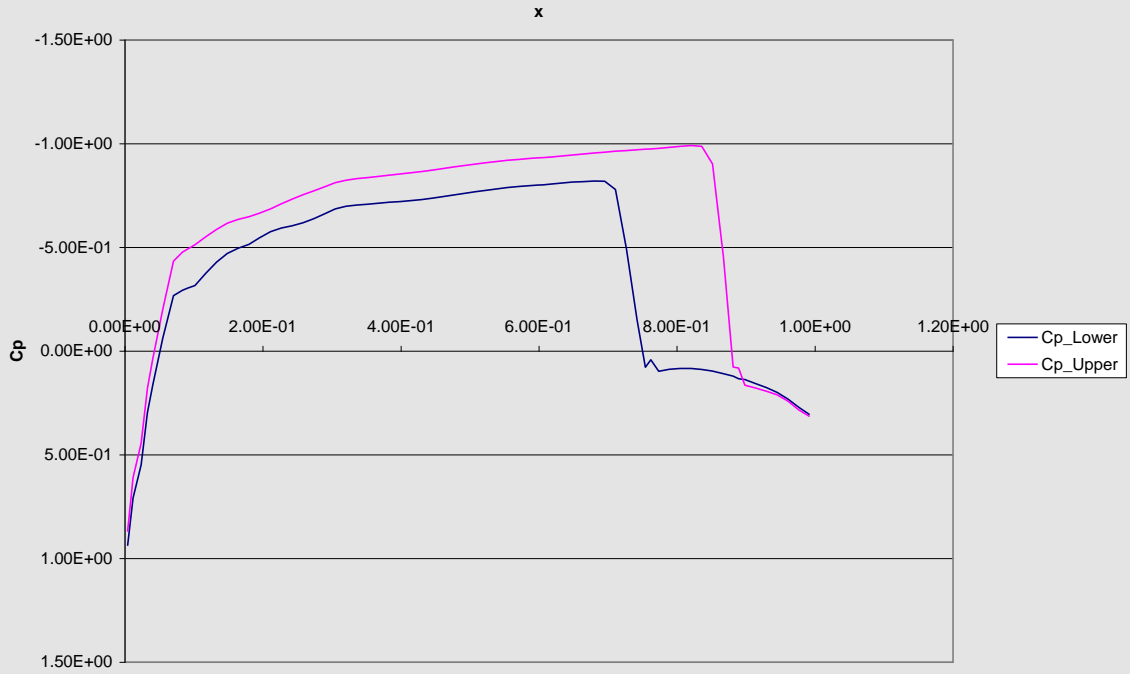
Cp Distribution M0.9a8



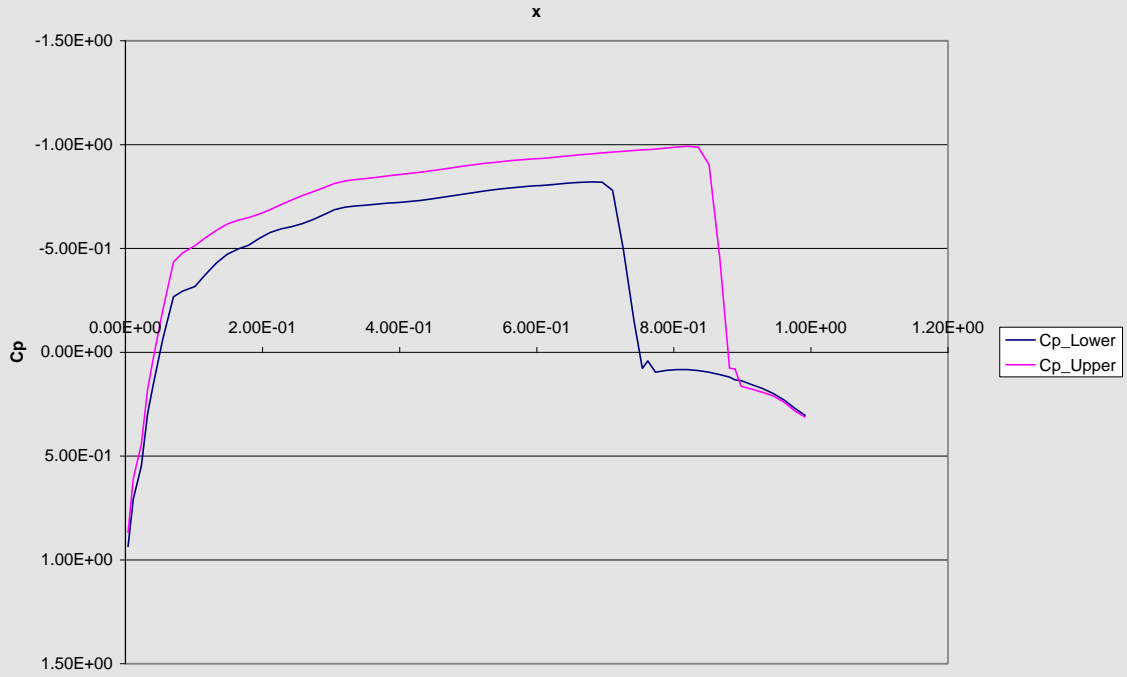
Cp Distribution M0.9a10



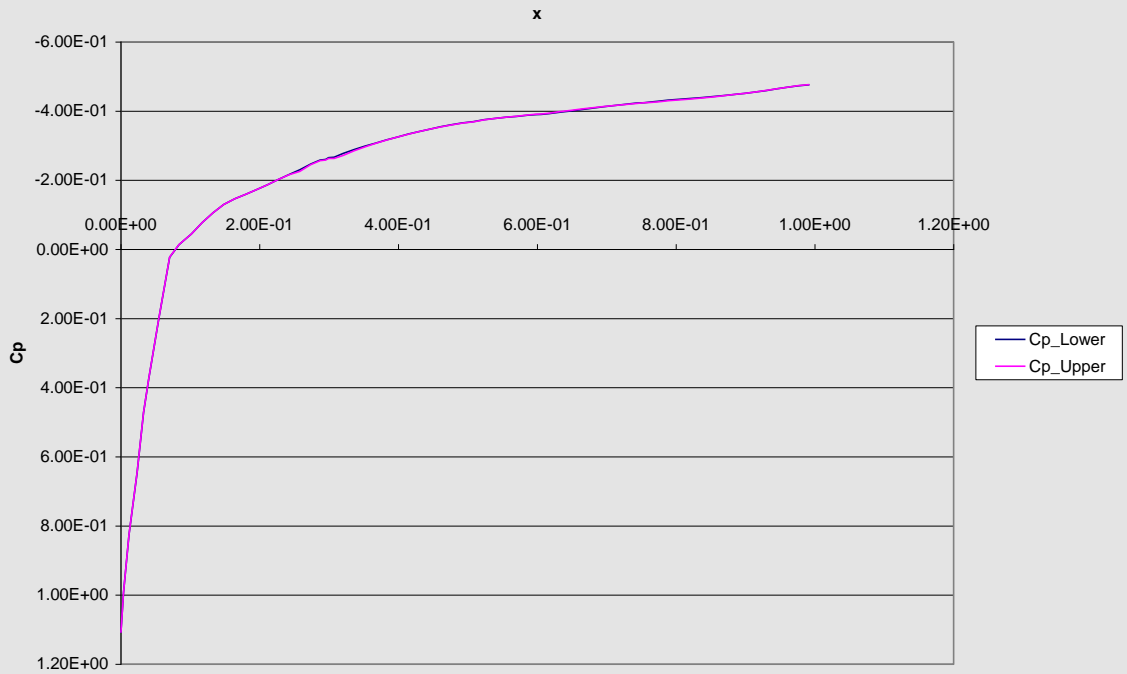
Cp Distribution M0.85a1



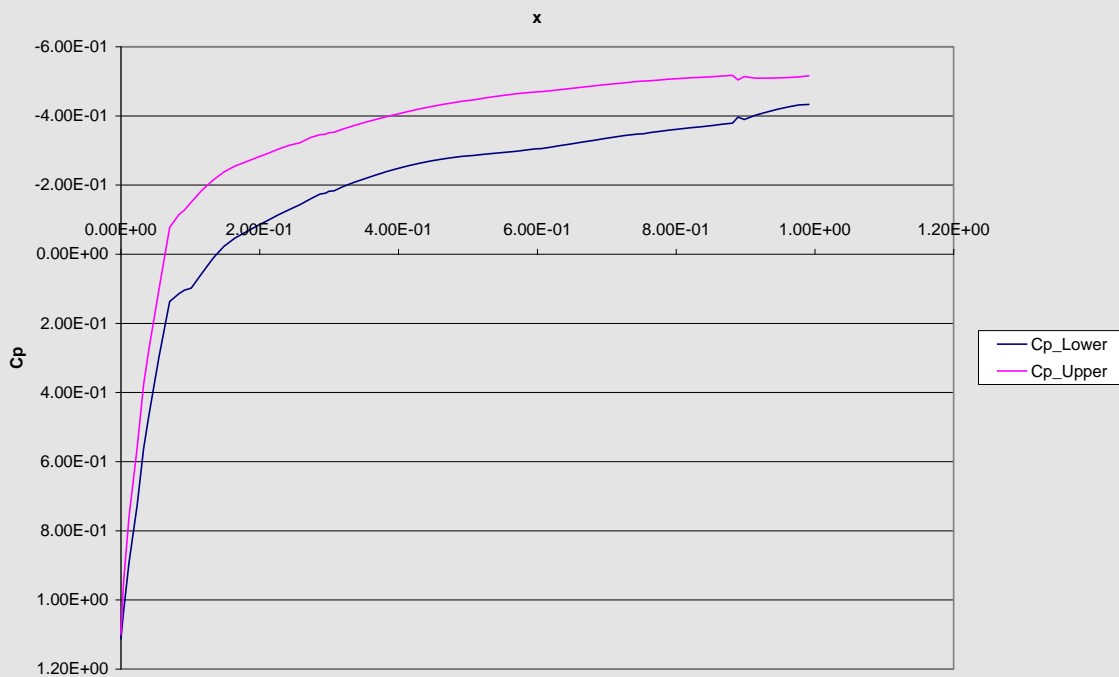
Cp Distribution M0.85a1 nbmin 128



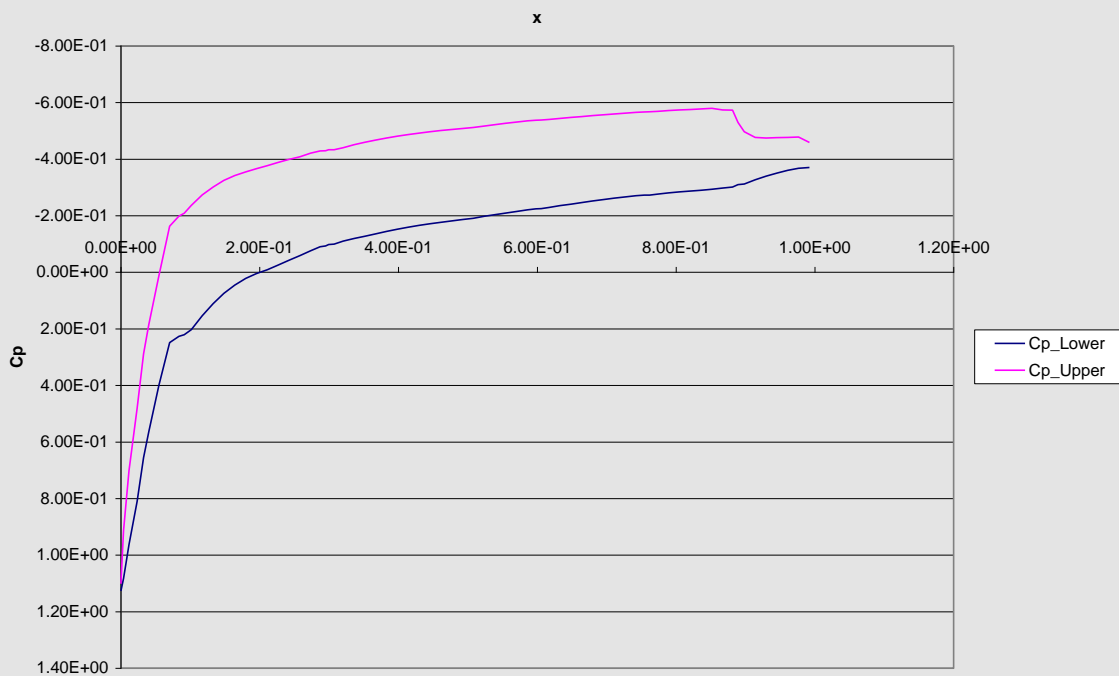
Cp Distribution M1.1a0



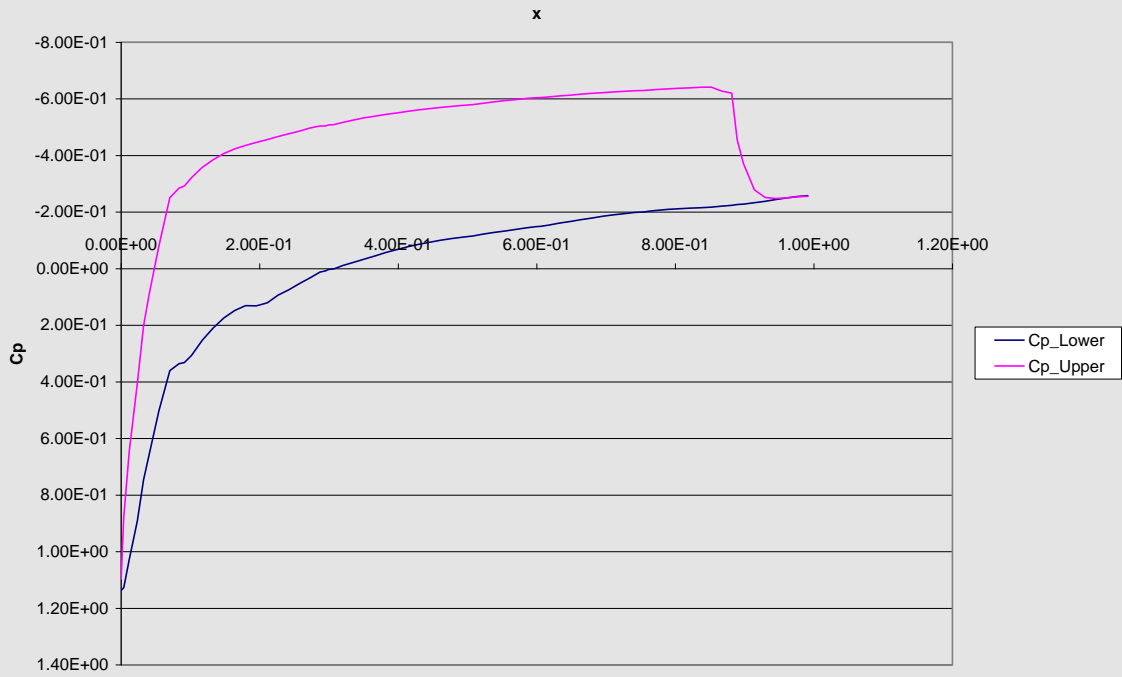
Cp Distribution M1.1a2



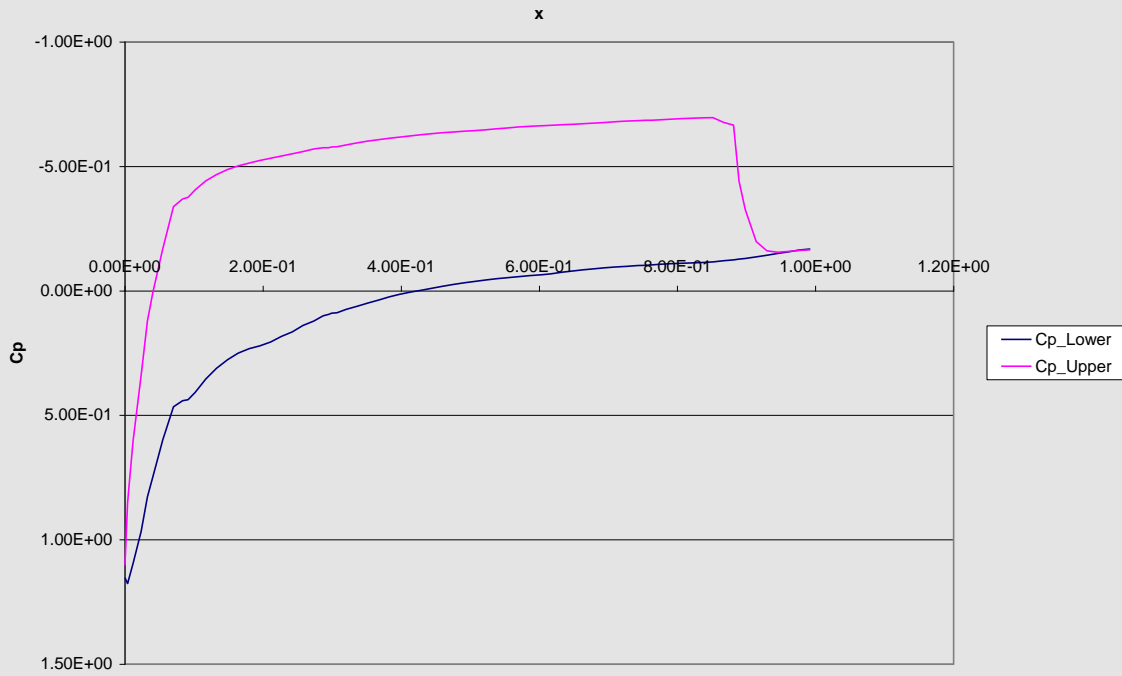
Cp Distribution M1.1a4



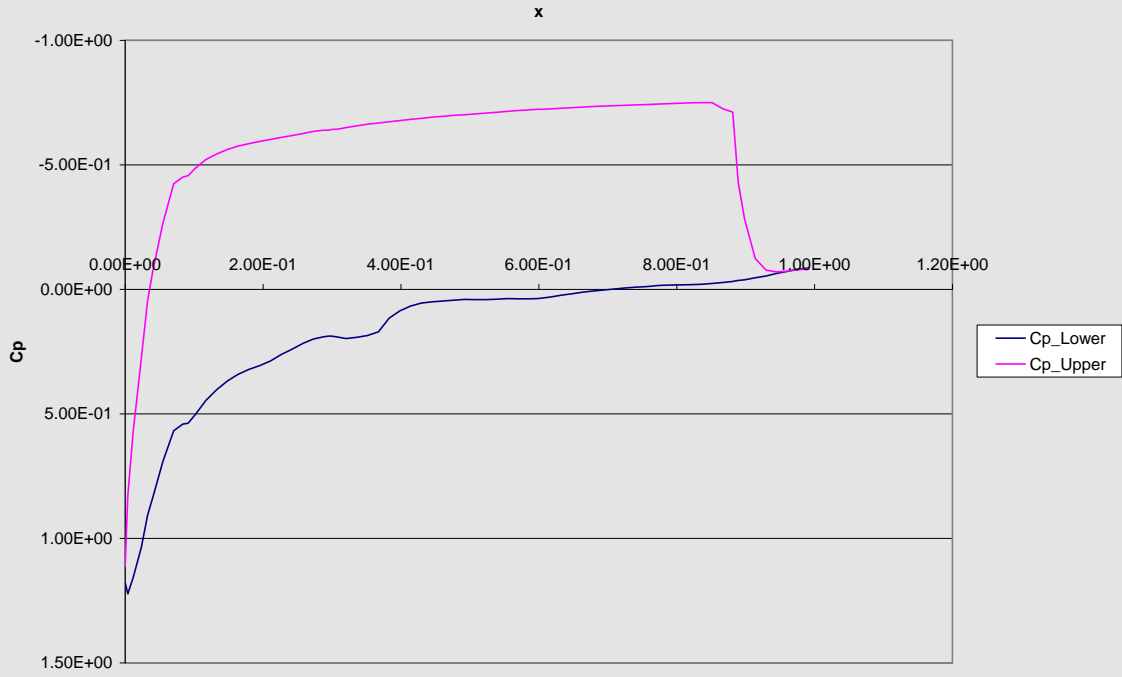
Cp Distribution M1.1a6



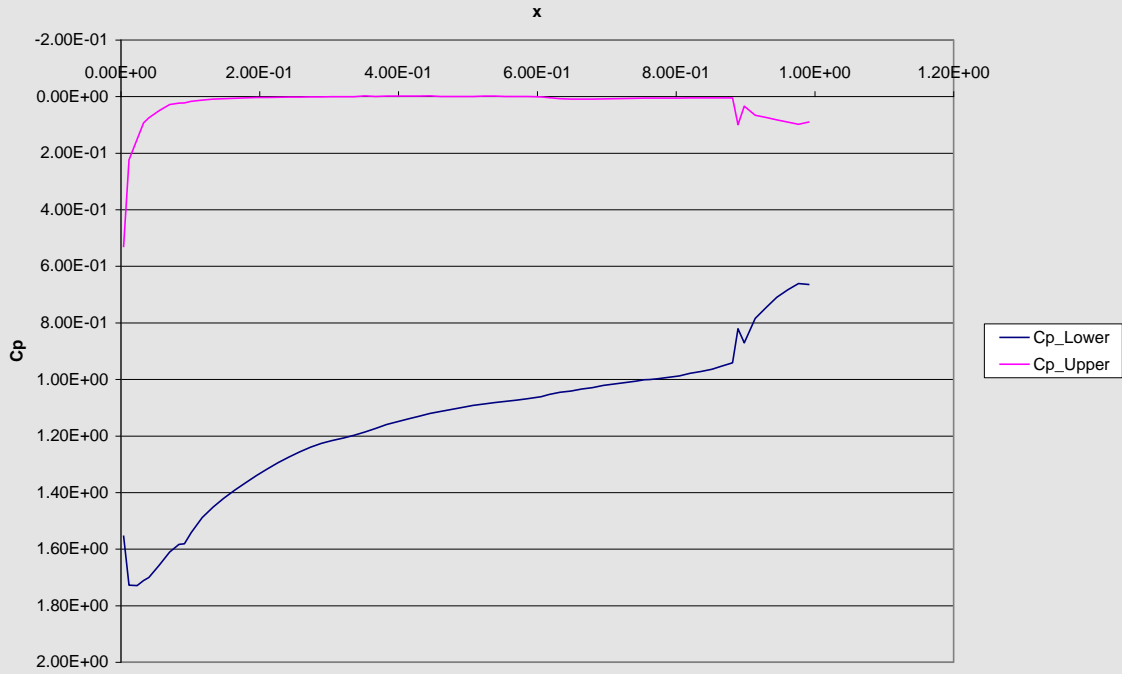
Cp Distribution M1.1a8



Cp Distribution M1.1a10



Cp Distribution M25.0a45



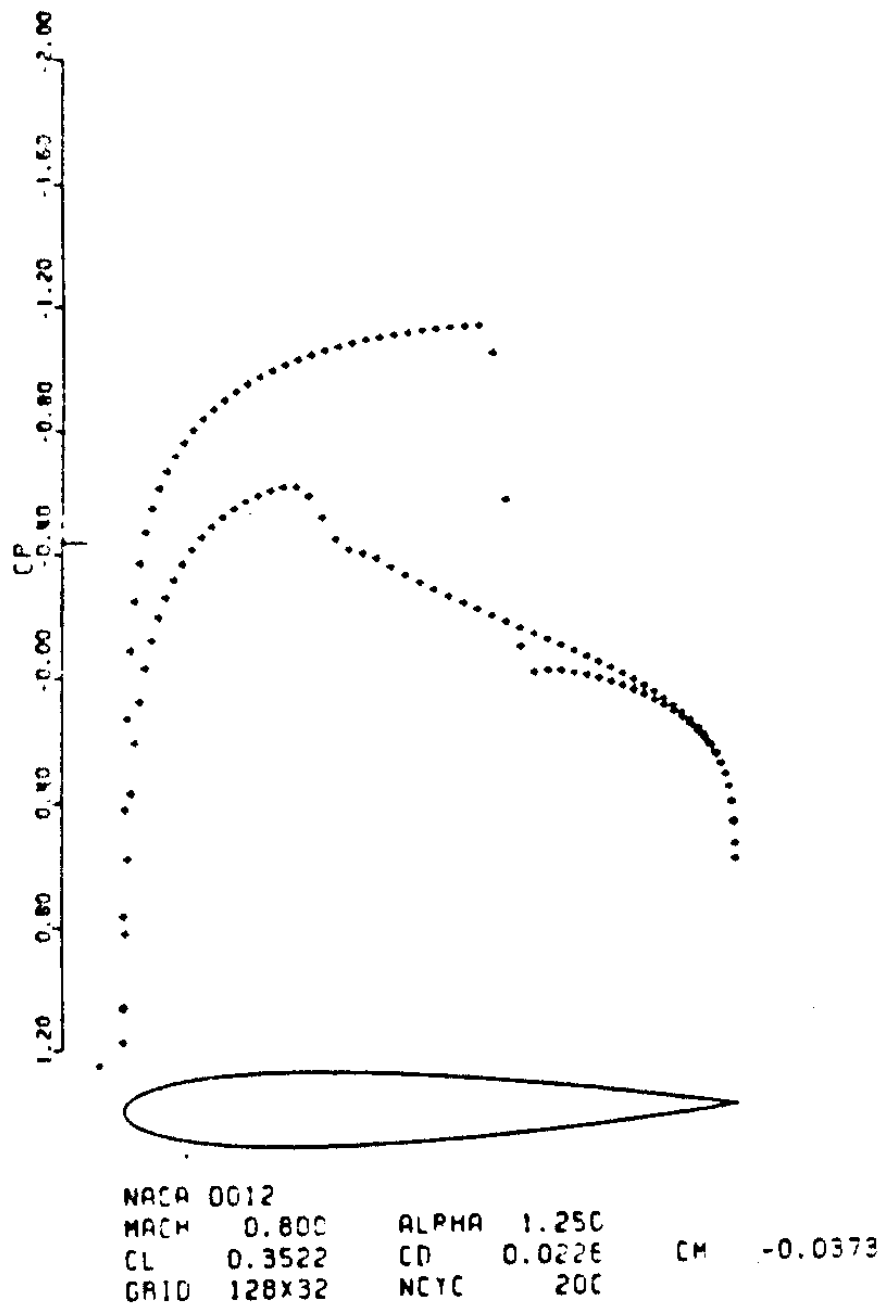


Figure 10

Supercritical Lifting Case

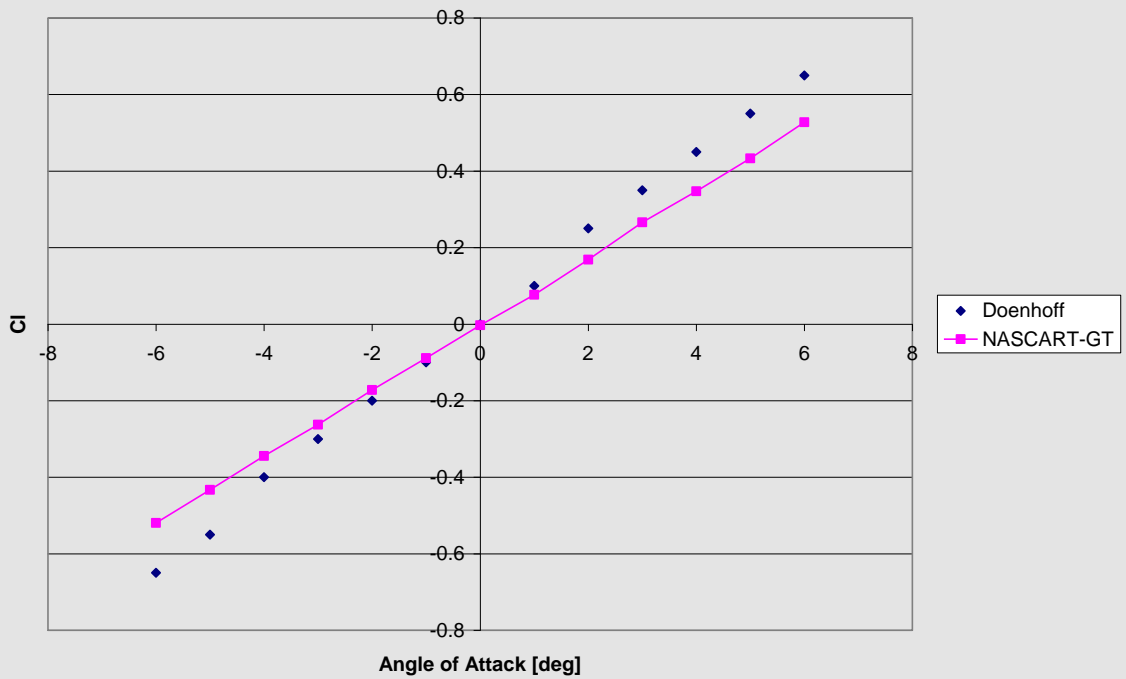
Pressure Distribution plot by Doenhoff at  $M_{\infty}=0.8$   $\alpha=1.25$

Cp Distribution M0.8a1.25



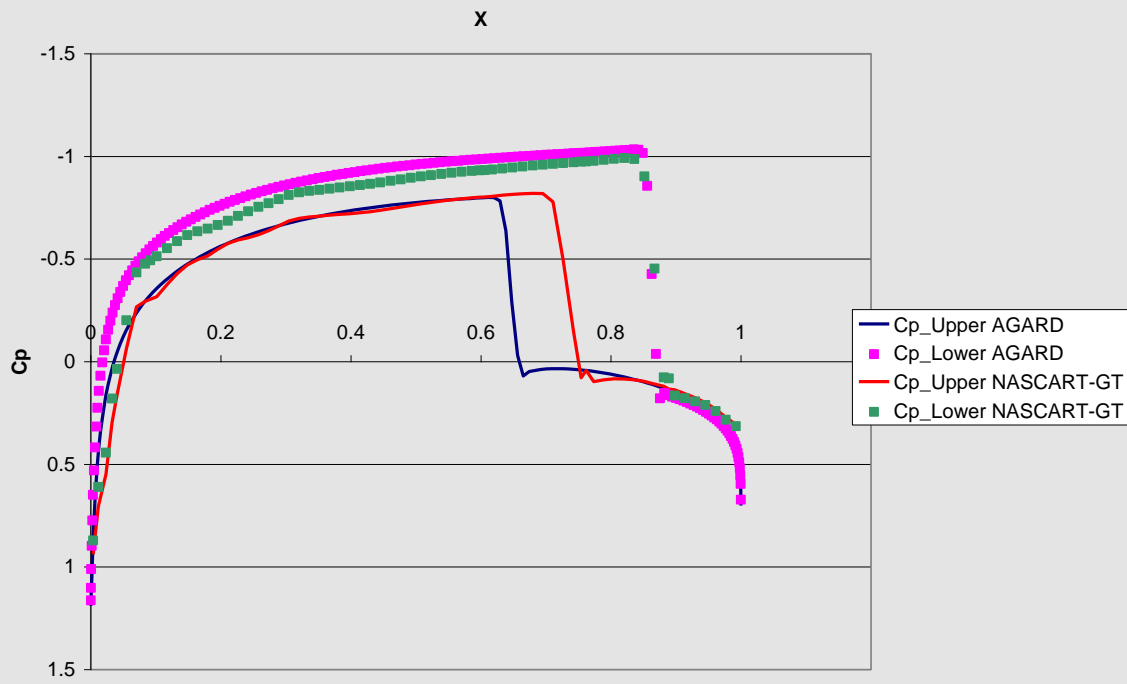
Pressure Distribution Plot by NASCART-GT at  $M_\infty=0.8$   $\alpha=1.25$

Cl Comparison



Lift Coefficient Comparison Doenhoff & NASCART-GT at  $M_\infty=0.3$ ,  $-6 \leq \alpha \leq 6$

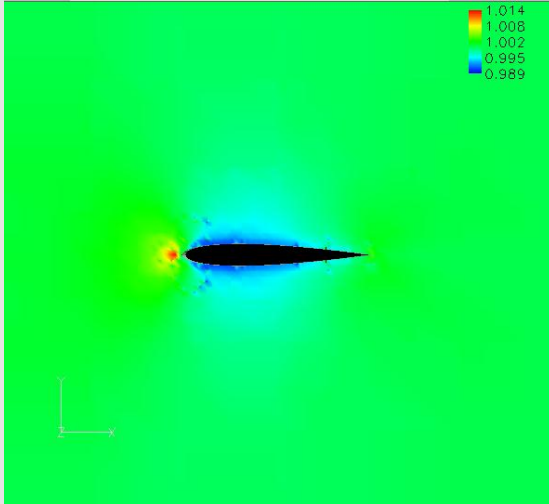
Cp Distribution M0.85a1 AGARD & NASCART



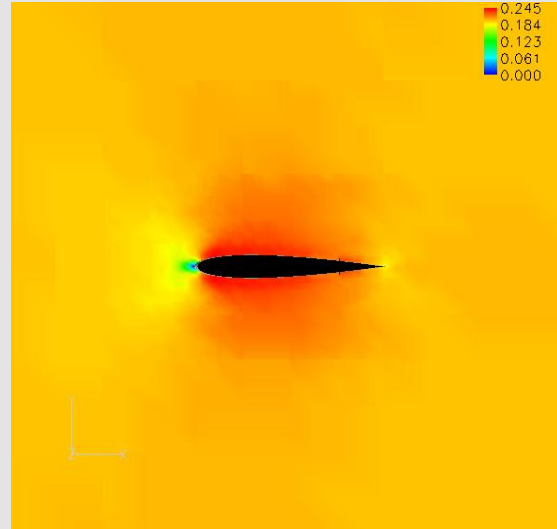
Pressure Coefficients for NASCART-GT and AGARD  $M_\infty=0.85$ ,  $\alpha=1$

## Appendix B: Color Floods and Other Graphics NACA 0012

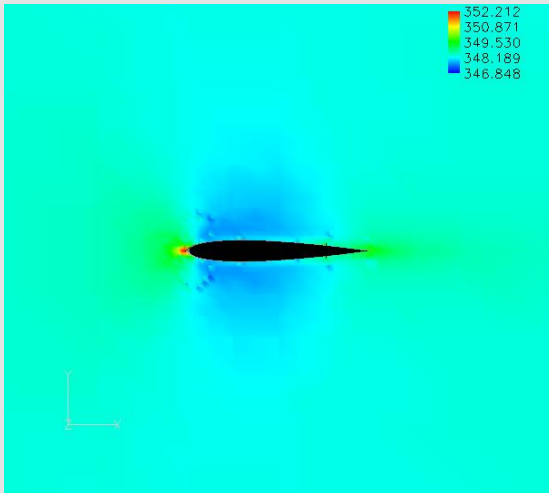
This appendix contains Fieldview color floods, scalar grids, scalar geometries, and other graphics for the NACA 0012. The low level oscillations are visible in the flows where  $M_\infty \leq 0.4$ .



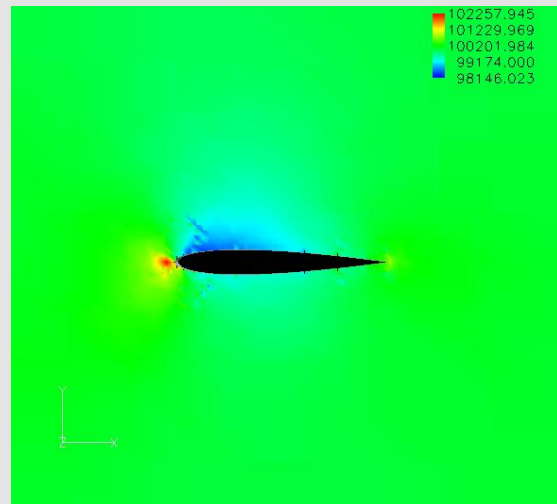
$M_\infty=0.2 \alpha=0$  Pressure  
Oscillations are noticeable around the low pressure areas



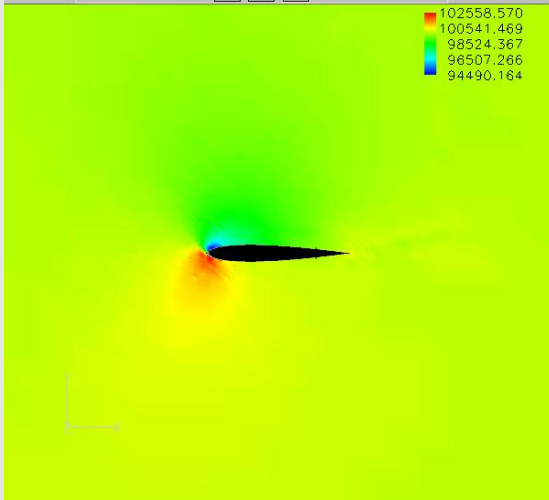
$M_\infty=0.2 \alpha=0$  Mach number



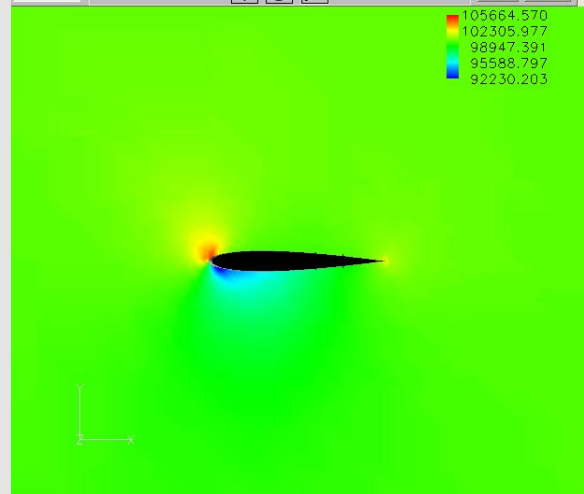
$M_\infty=0.2 \alpha=0$  Temperature



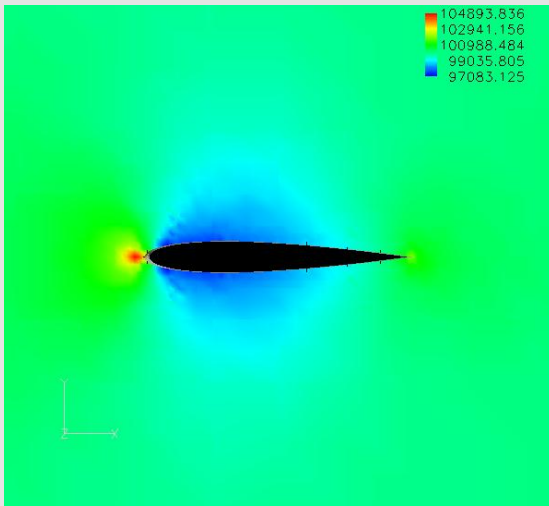
$M_\infty=0.2 \alpha=2$  Pressure  
Notice the increase in surface pressure on the lower surface



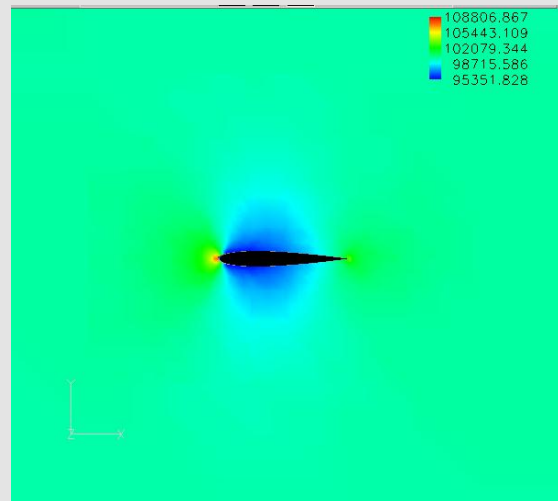
$M_\infty=0.2$   $\alpha=10$  Pressure  
 There is an increased area of high pressure on the tip of the airfoil



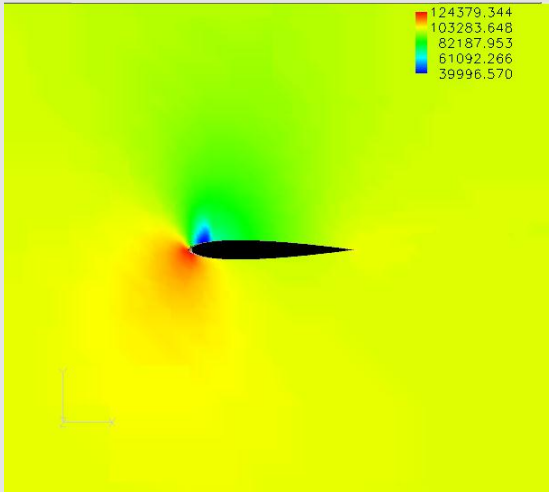
$M_\infty=0.3$   $\alpha=-6$  Pressure  
 This airfoil is a negative  $\alpha$ ; therefore the pressure values are reversed compared to an airfoil at positive  $\alpha$



$M_\infty=0.3$   $\alpha=10$  Pressure  
 The oscillations lessened drastically due to a slight increase in  $M_\infty$

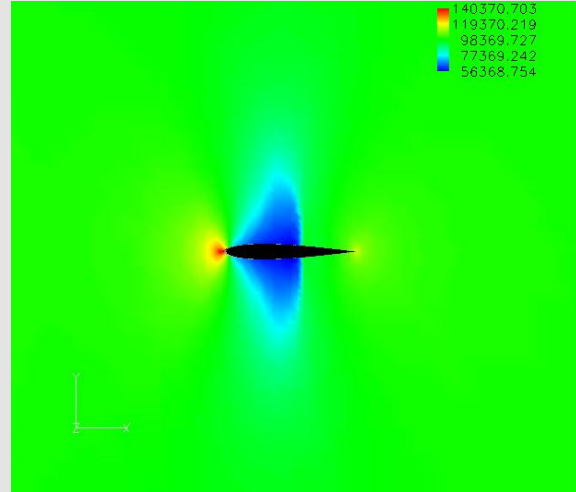


$M_\infty=0.4$   $\alpha=0$  Pressure  
 The flow oscillations are not even visible at  $M_\infty=0.4$



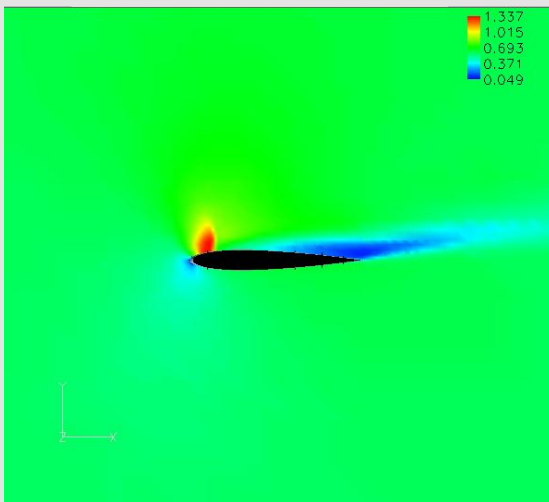
$M_\infty=0.6 \alpha=8$  Pressure

The small blue area is a low pressure region known as a suction peak. There is a larger area of low pressure, the green area that covers the bulk of the airfoils upper surface



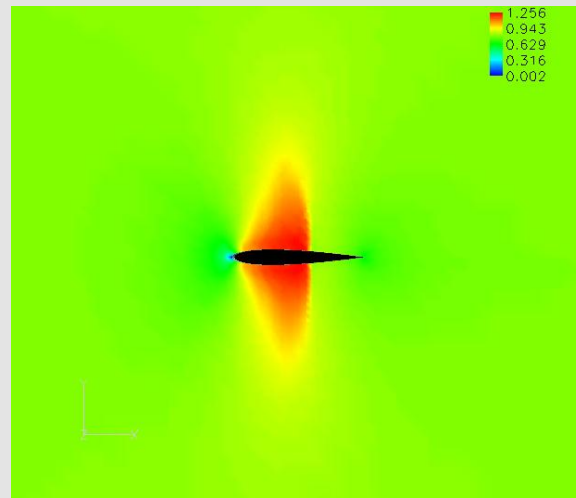
$M_\infty=0.8 \alpha=0$  Pressure

$M_\infty=0.8$  is the start of the transonic test cases. The suction peaks are increasing in size as  $M_\infty$  increases



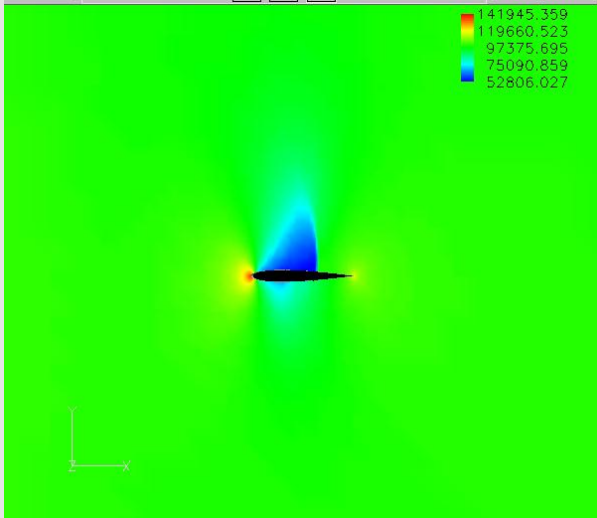
$M_\infty=0.6 \alpha=10$  Mach number

There are areas of low Mach numbers on the tip of the airfoil and from the middle to past the trailing edge

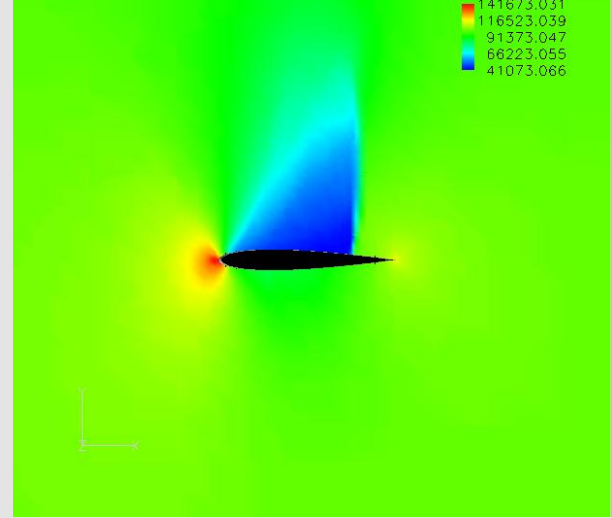


$M_\infty=0.8 \alpha=0$  Mach number

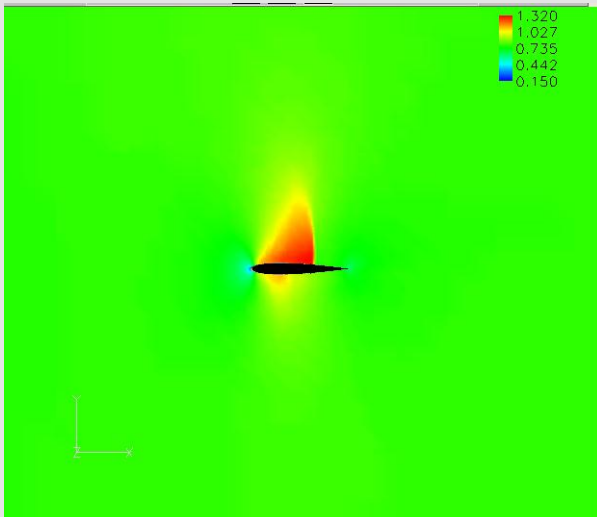
This  $M_\infty$  plot shows that in the areas of low pressure the flow actually reaches supersonic speeds. Also at the tip of the airfoil the  $M_\infty$  is low because of the stagnation point. The stag point is like the flow hitting a brick wall it comes almost to a stop



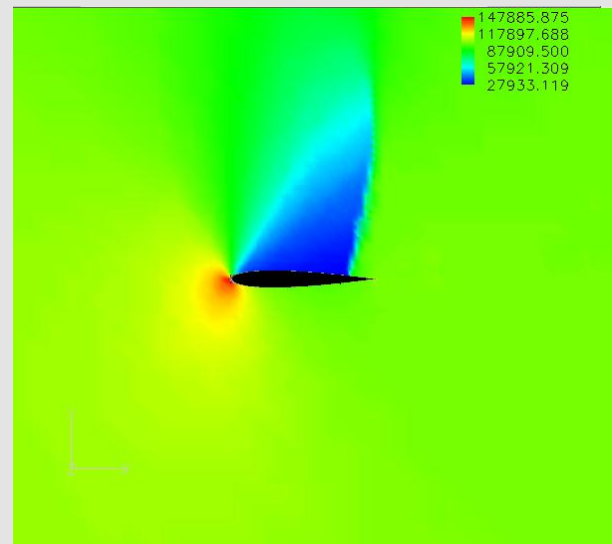
$M_\infty=0.8$   $\alpha=1.25$  Pressure  
 The increase in  $\alpha$  of less than two degrees significantly reduces the low pressure area on the lower surface



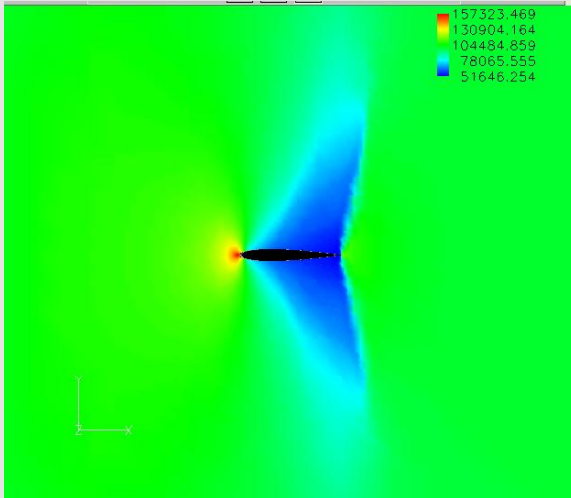
$M_\infty=0.8$   $\alpha=4$  Pressure  
 At  $\alpha=4$  there is no low pressure area on the lower surface



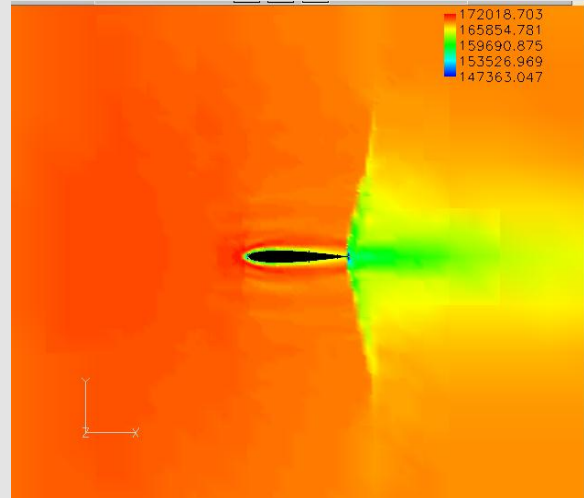
$M_\infty=0.8$   $\alpha=0$  Mach number  
 Mach number also reflects the decrease in low pressure areas



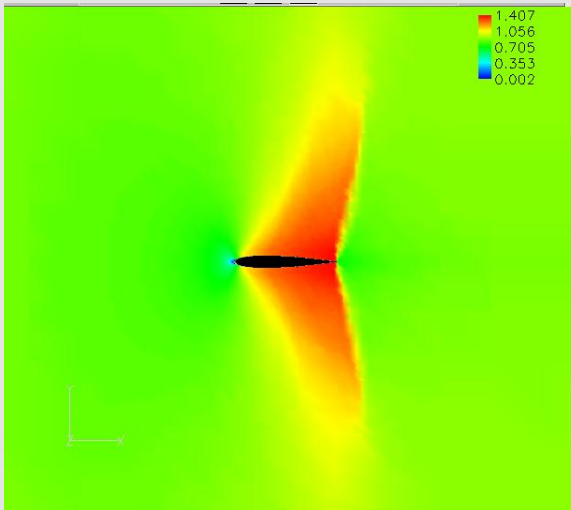
$M_\infty=0.8$   $\alpha=10$  Pressure  
 The suction peak at high  $\alpha$  extends almost to the trailing edge of the airfoil



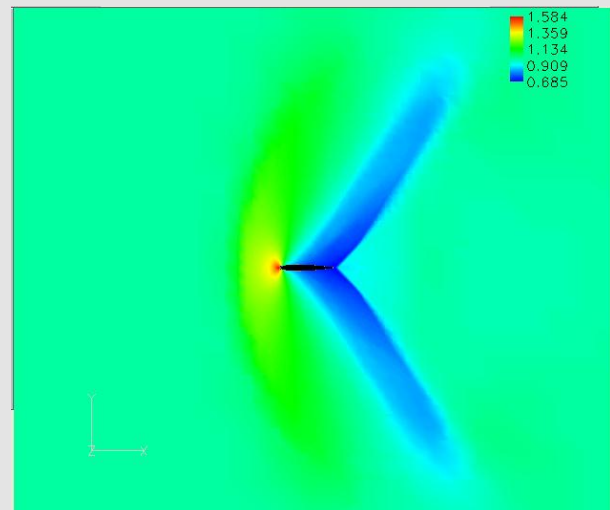
$M_\infty=0.9 \alpha=0$  Pressure  
The suction peaks extends almost past the trailing edge at high transonic cases



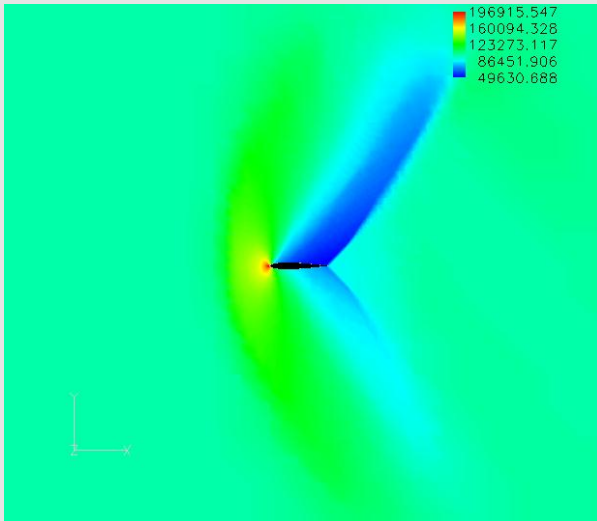
$M_\infty=0.9 \alpha=0$  Stagnation Pressure  
Stag pressure shows boundaries for pressure gradients



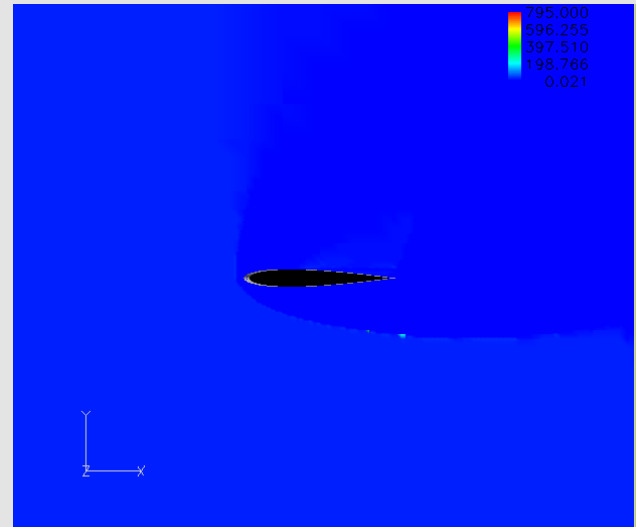
$M_\infty=0.9 \alpha=0$  Mach number  
The low pressure regions induce a supersonic flow



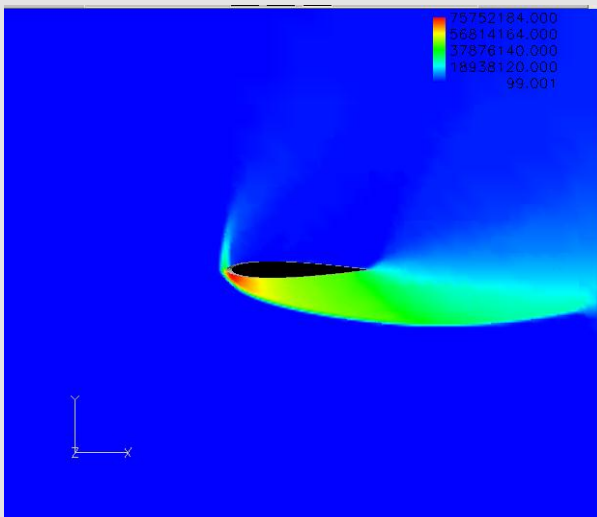
$M_\infty=1.1 \alpha=0$  Pressure  
The elongated suction peak areas and the high pressure areas in front of the airfoil are effects of a supersonic shockwave



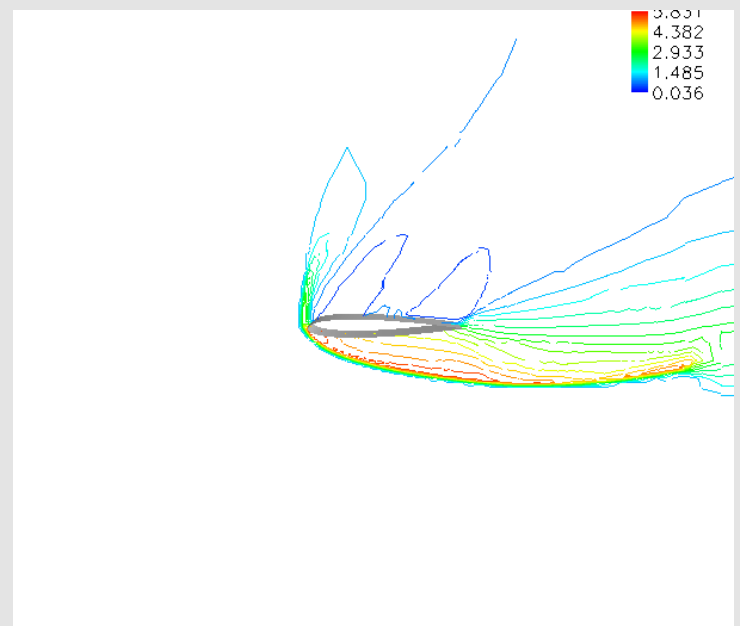
$M_\infty=1.1 \alpha=6$  Pressure  
 The low pressure area is still present to some extent at  $\alpha=6$  on the lower surface in supersonic flows



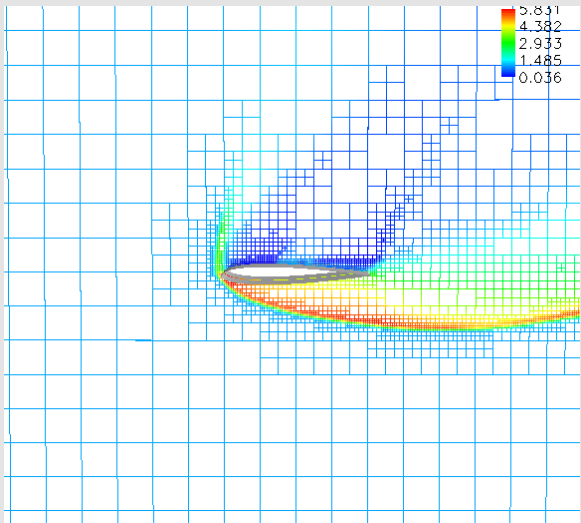
$M_\infty=25.0 \alpha=45$  Mach number  
 At high Mach numbers the flow becomes compressed, therefore there is no visible shockwave because the air is traveling at a uniform speed



$M_\infty=25.0 \alpha=45$  Pressure  
 This is an extreme case but lift is still being generated



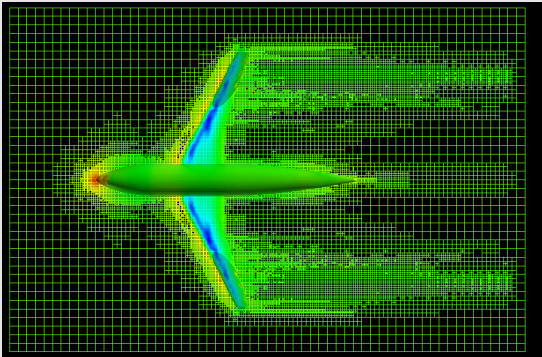
$M_\infty=25.0 \alpha=45$  Pressure  
 This is an example of a contour line plot which is just another way of showcasing results



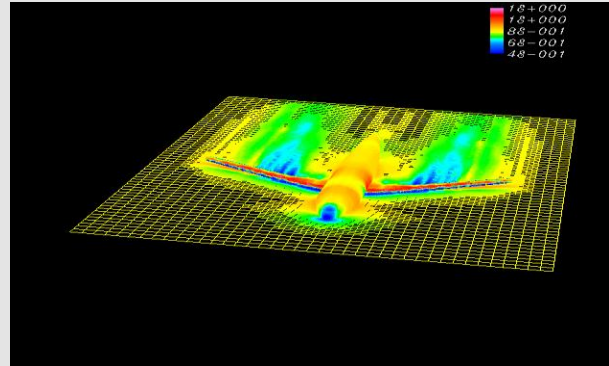
$M_\infty=25.0$   $\alpha=45$  Pressure  
This is an example of a scalar Cartesian grid

## Appendix C: Color Floods and Other Graphics DLR-F4 Wing Body Geometry

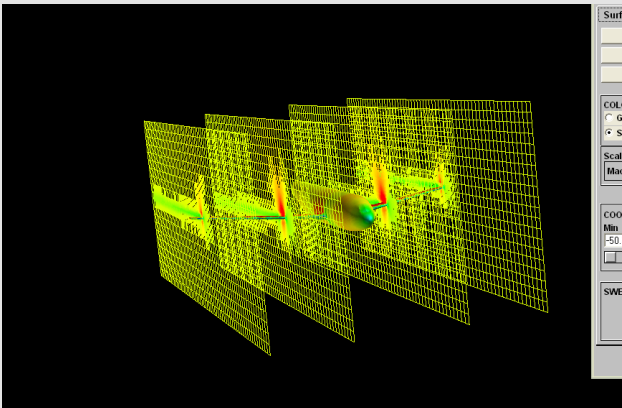
This appendix contains graphics from the DLR-F4 test cases ( $M_\infty=0.75$   $\alpha=0$ )



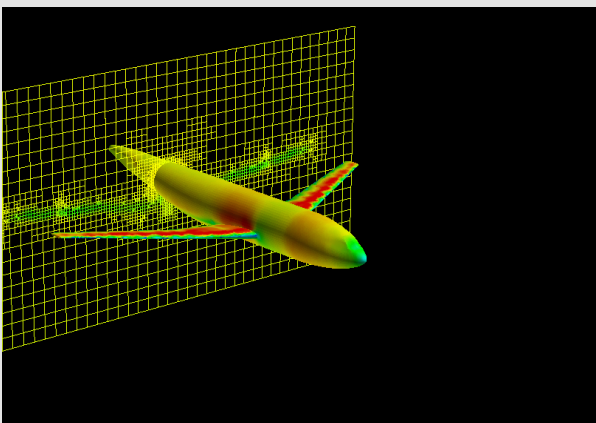
Scalar geometry and grid showing density



Mach number along the z plane



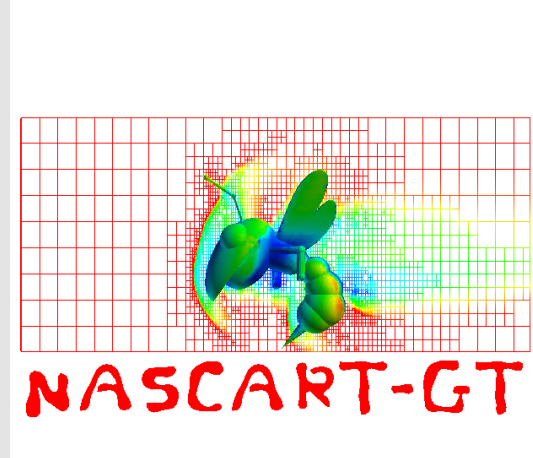
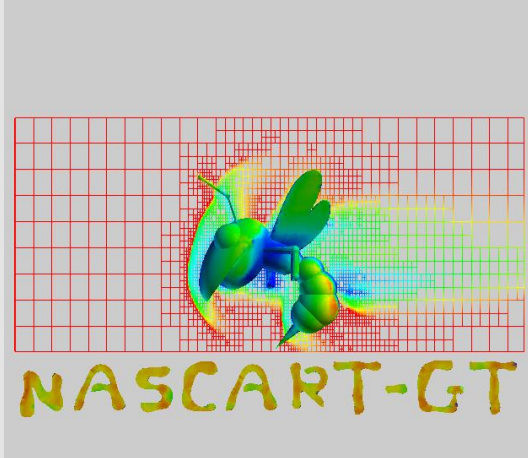
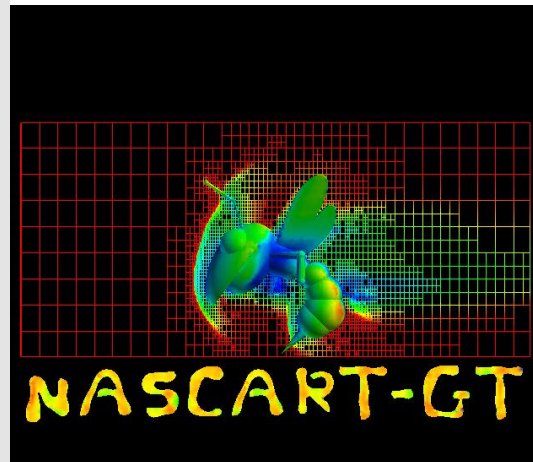
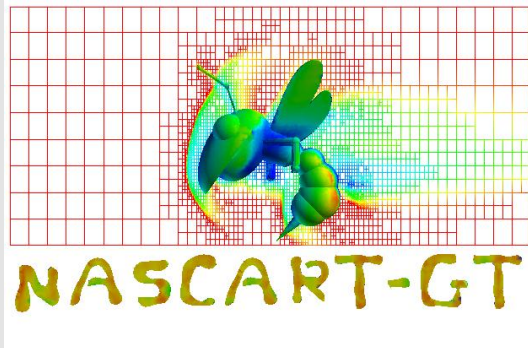
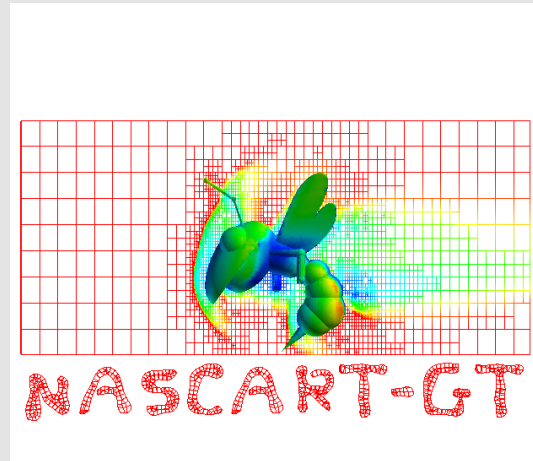
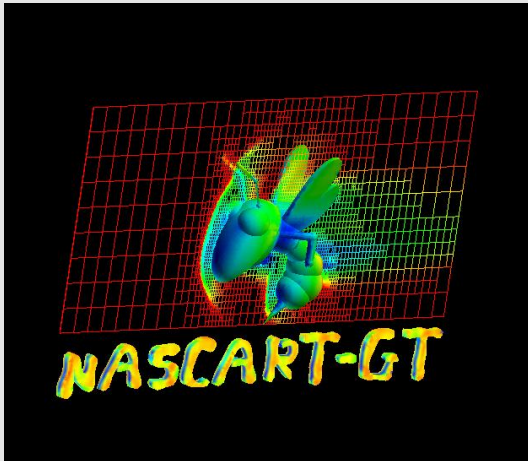
Scalar geometry and grids: Mach number

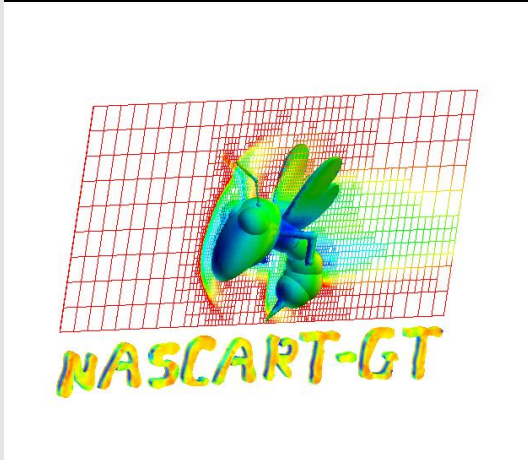
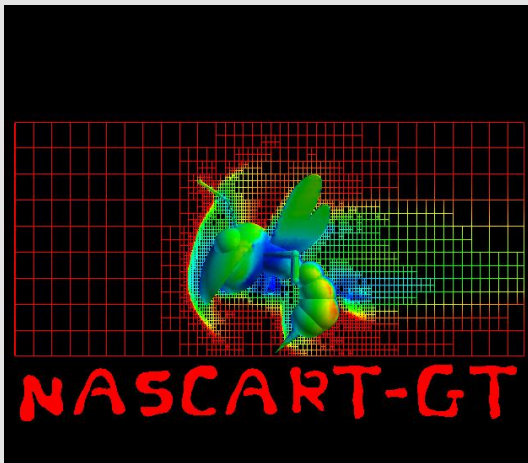


Plot showing Mach number wake that trails the wings along the x plane

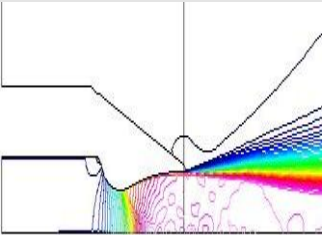
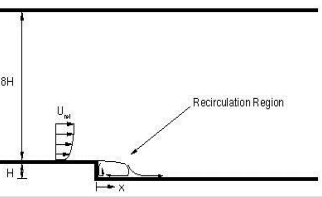
Appendix D: Buzz

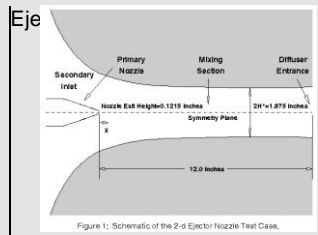
Contains graphics of buzz; finished logos:







<p>Fraser Subsonic Diffuser</p> 	<p>straight section of pipe followed by a 5 degree half-angle conical diffuser.</p>	<p>Axisymmetrical</p>	<p>1) Fraser, H.R., "The Turbulent Boundary Layer in a Conical Diffuser," <i>Journal of the Hydraulic Division</i>, Proceedings of the American Society of Civil Engineers, pp. 1684-1-17, June 1958.  2) Dudek, J.C., N.J. Georgiadis, and D.A. Yoder, "Calculation of Turbulent Subsonic Diffuser Flows Using the NPARC Navier-Stokes Code," AIAA Paper 96-0497, January 1996.</p>	<p>Turbulent</p>	<p>Under Headings of "Comparison Data" and "Computational Studies"</p>	<p>Under Headings of "Comparison Data" and "Computational Studies"</p>	<p>Turbulent</p>	<p><a href="http://www.grc.nasa.gov/WWW/wind/valid/fraser/fraser01/fraser01.htm">http://www.grc.nasa.gov/WWW/wind/valid/fraser/fraser01/fraser01.htm</a></p>
<p>Geometry</p>	<p>Geometry Description</p>	<p>2-D, 3-D, or Axisymmetric Flow</p>	<p>Experimental Data Reference</p>	<p>Boundary Layer: Laminar or Turbulent Flow</p>	<p>List of Experimental Data Available</p>	<p>Computed Results References</p>	<p>Computed Results: Laminar or Turbulent Flow</p>	
	<p>The geometry is the axisymmetric, converging-diverging nozzle profiles as defined by Eggers.</p>	<p>Axisymmetric</p>	<p>Eggers, J.M. "Velocity Profiles and Eddy Viscosity Distributions Downstream of a Mach 2.22 Nozzle Exhausting to Quiescent Air," NASA TN D-3601, September 1966.</p>	<p>Laminar</p>	<p>Appendix B ('Tabulation of Velocity Profiles') of Eggers report.</p>	<p>Under Comparison Data and Computational Studies</p>	<p>Laminar</p>	<p><a href="http://www.grc.nasa.gov/WWW/wind/valid/axinoz/">http://www.grc.nasa.gov/WWW/wind/valid/axinoz/</a></p>
<p>Driver-Seegmiller Incompressible Backward Facing Step</p> 	<p>Backward Facing Step</p>	<p>2-D</p>	<p>John W. Slater of NASA's Glenn Research Center</p>	<p>Turbulent</p>	<p>1) <a href="http://www.grc.nasa.gov/WWW/wind/valid/backstep/backstep01/backstep01.html">http://www.grc.nasa.gov/WWW/wind/valid/backstep/backstep01/backstep01.html</a>  2) <a href="http://www.grc.nasa.gov/WWW/wind/valid/backstep/backstep02/backstep02.html">http://www.grc.nasa.gov/WWW/wind/valid/backstep/backstep02/backstep02.html</a></p>	<p>Under Computational Studies</p>	<p>Turbulent</p>	<p><a href="http://www.grc.nasa.gov/WWW/wind/valid/backstep/backstep/">http://www.grc.nasa.gov/WWW/wind/valid/backstep/backstep/</a></p>



Mixing section is formed by contoured upper and lower walls, widths of both the primary nozzle discharge slot and the mixing section were 8.00 inches

2-D

Reference Data is found on the web site

Turbulent

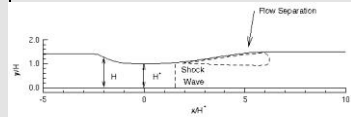
Data tables, Downloads, Grids, Other Files (accessible form web page)

Download tar File, Grids, Input Parameters and Files, Computation, Comparisons of the Results

Turbulent

<http://www.grc.nasa.gov/WWW/wind/valid/eject/eject.html>

Sajben Diffuser



The throat is located at  $x = 0$  inches and has a height  $h_{thr}$  of 0.14435 feet (44 millimeters or 1.7322 inches)

2-D

Six References Listed on Web Site

Turbulent

Multiple Studies and Files (accessible from web page)

Under Comparison Data and Computational Studies

Turbulent

<http://www.grc.nasa.gov/WWW/wind/valid/transdif/transdif.htm>

**Geometry**

**Geometry Description**

**2-D, 3-D, or Axisymmetric Flow**

**Experimental Data Reference**

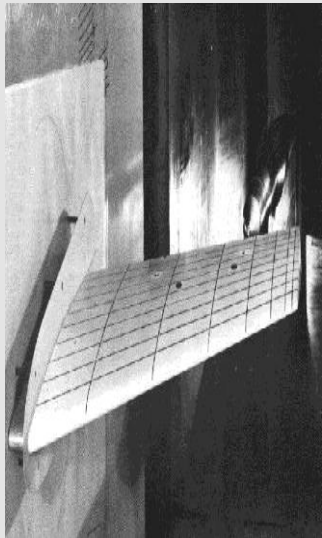
**Boundary Layer: Laminar or Turbulent Flow**

**List of Experimental Data Available**

**Computed Results References**

**Computed Results: Laminar or Turbulent Flow**

ONERA M6 Wing



Swept, semi-span wing with no twist

3-D

1) Schmitt, V. and F. Charpin, "Pressure Distributions on the ONERA-M6-Wing at Transonic Mach Numbers," *Experimental Data Base for Computer Program Assessment*. Report of the Fluid Dynamics Panel Working Group 04, AGARD AR 138, May 1979.  
 2) Mani, M., J.A. Ladd, A.B. Cain, and R.H. Bush, "An Assessment of One- and Two-Equation Turbulence Models for Internal and External Flows", AIAA 97-2010, June 1997.

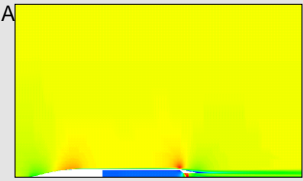
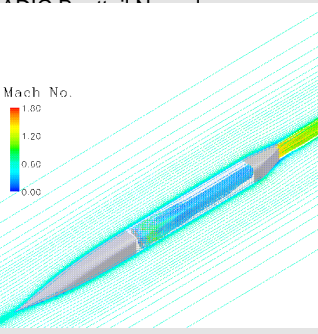
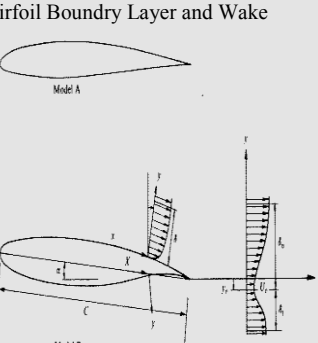
Turbulent

Comparison Data, Computational Studies and Other Files (accessible form web page)

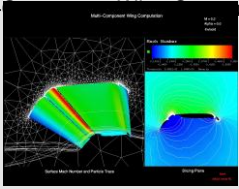
Under Comparison Data and Computational Studies

Turbulent

<http://www.grc.nasa.gov/WWW/wind/valid/m6wing/m6>

		2-D/Axisymmetric	NASA D-1.22-L boattail/nozzle documented in NASA TP 1766	Turbulent	Computational Studies (accessible form web page)	Under Computational Studies	Turbulent	<a href="http://www.grc.nasa.gov/WWW/wind/valid/madicoz/m">http://www.grc.nasa.gov/WWW/wind/valid/madicoz/m</a>
		3-D	Putnam, L.E., Mercer, C.E., "Pitot-Pressure Measurement in Flow Fields Behind a Rectangular Nozzle With Exhaust Jet for Free-Stream Mach Numbers of 0.00, 0.60, and 1.20," NASA TM 88990, November 1986.	Turbulent	Computational Studies (accessible form web page)	Under Computational Studies	Turbulent	<a href="http://www.grc.nasa.gov/WWW/wind/valid/madicoz/m">http://www.grc.nasa.gov/WWW/wind/valid/madicoz/m</a>
<p style="text-align: center;"><b>Geometry</b></p>	<p style="text-align: center;"><b>Geometry Description</b></p>	<p style="text-align: center;"><b>2-D, 3-D, or Axisymmetric Flow</b></p>	<p style="text-align: center;"><b>Experimental Data Reference(s)</b></p>	<p style="text-align: center;"><b>Boundry Layer: Laminar or Turbulent Flow</b></p>	<p style="text-align: center;"><b>List of Experimental Data Available</b></p>	<p style="text-align: center;"><b>Computed Results References</b></p>	<p style="text-align: center;"><b>Computed Results: Laminar or Turbulent Flow</b></p>	
<p>Airfoil Boundry Layer and Wake</p> 	<p>Chord of both airfoils: C = 24 in. 610 mm.</p>	2-D	NAKAYAMA, A. (1985). Characteristics of the flow around conventional and supercritical airfoils. <i>J. Fluid Mech.</i> 160, 155	Turbulent	Data Available on Web Page, however inaccesable without correct ID and Password	Data Available on Web Page, however inaccesable without correct ID and Password	Turbulent	<a href="http://cfd.me.umist.ac.uk/cgi-bin/cfd/db/prpage.cgi?11&amp;EXP&amp;database/cases/case11/Case">http://cfd.me.umist.ac.uk/cgi-bin/cfd/db/prpage.cgi?11&amp;EXP&amp;database/cases/case11/Case</a>

Multi-Resolution Simulation



A wing section including flaps

3-D

NASA Official: Walt Brooks

Turbulent

Downloadable data available on web page.

Downloadable data available on web page.

Turbulent

<http://www.nas.nasa.gov/Research/Datasets/Barth/index.shtml>

**Geometry**

**Geometry Description**

**2-D, 3-D, or Axisymmetric Flow**

**Experimental Data Reference(s)**

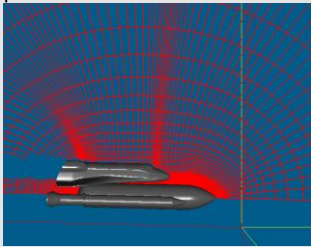
**Boundary Layer: Laminar or Turbulent Flow**

**List of Experimental Data Available**

**Computed Results References**

**Computed Results: Laminar or Turbulent Flow**

Space Shuttle Launch Vehicle



A model of the space shuttle, external fuel tank and solid rocket boosters

3-D

1) P.G. Buning, I.T. Chiu, F.W. Martin, Jr., R.L. Meakin, S. Obayashi, Y.M. Rizk, J.L. Steger, and M. Yarrow, "Flowfield Simulation of the Space Shuttle Vehicle in Ascent," Fourth International Conference on Supercomputing, Vol II, Supercomputer Applications, Kartashev & Kartashev, eds., 1989, pp. 20-28.  
 2) F.W. Martin, Jr. and J.P. Slotnick, "Flow Computations for the Space Shuttle in Ascent Mode Using Thin-Layer Navier-Stokes Equations," Applied Computational Aerodynamics, Progress in Astronautics and Aeronautics, Vol. 125, P.A. Henne, ed., American Institute of Aeronautics and Astronautics, Washington, D.C., 1990, pp. 863-886.

Turbulent

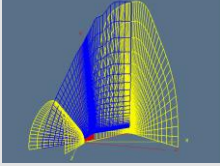
Downloadable data available on web page. (grid, solution, tar archive)

Download Solution

Turbulent

<http://www.nas.nasa.gov/Research/Datasets/Buning/index.shtml>

Delta Wing at 40 degrees angle of attack



Represents flow past delta wing aircraft at moderately high angle of attack.

3-D

J.A. Ekaterinaris and L.B. Schiff, "Vortical Flows over Delta Wings and Numerical Prediction of Vortex Breakdown," AIAA Paper 90-0102, AIAA Aerospace Sciences Conference, Reno, NV, January 1990.

Turbulent

Downloadable data available on web page. (grid, solution, gzip tar archive)

Download Solution

Turbulent

<http://www.nas.nasa.gov/Research/Datasets/Ekaterinaris/index>

**Geometry**

**Geometry Description**

**2-D, 3-D, or Axisymmetric Flow**

**Experimental Data Reference**

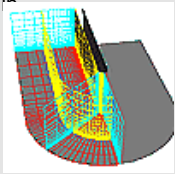
**Boundary Layer: Laminar or Turbulent Flow**

**List of Experimental Data Available**

**Computed Results References**

**Computed Results: Laminar or Turbulent Flow**

Blunt Fin



Airflow over flat plate with a blunt fin rising from the plate

3-D

C.M. Hung and P.G. Buning, "Simulation of Blunt-Fin Induced Shock Wave and Turbulent Boundary Layer Separation," AIAA Paper 84-0457, AIAA Aerospace Sciences Conference, Reno, NV, January 1984.

Turbulent

Downloadable data available on web page. (grid, solution, compressed tar archive)

Download Solution

Turbulent

<http://www.nas.nasa.gov/Research/Datasets/Hung/index.shtml>

Tapered Cylinder Unsteady Flow



Tapered Cylinder

3-D

[The paper "Numerical Simulation of Flow Past a Tapered Cylinder" by Dennis Jespersen and Creon Levit describes this work.](#)

Turbulent

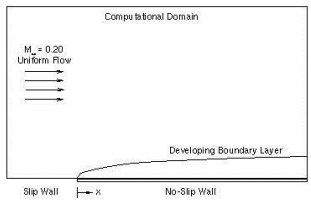
Downloadable data available on web page. (grid and tar files)

Download tar files

Turbulent

<http://www.nas.nasa.gov/Research/Datasets/Jespersen/index>

Flat Plate



Flat Plate

2-D

Experiment conducted by Scott Lawrence, 1995

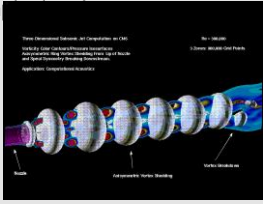
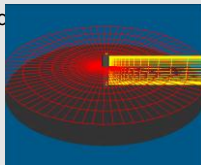
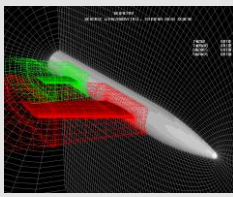
Turbulent

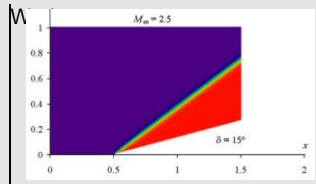
Downloadable data available on web page. (grid, solution, compressed tar archive)

Download Solution

Turbulent

<http://www.nas.nasa.gov/Research/Datasets/Lawrence/index>

	Impinging Jet	3-D	<a href="#">Dr. T. Pulliam, Ph.D., May, 1995</a>	Turbulent	Downloadable data available on web page. (grid, solution, compressed tar archive)	Download tar files	Turbulent	<a href="http://www.nas.nasa.gov/Research/Datasets/Pulliam/index.sh">http://www.nas.nasa.gov/Research/Datasets/Pulliam/index.sh</a>
<b>Geometry</b>	<b>Geometry Description</b>	<b>2-D, 3-D, or Axisymmetric Flow</b>	<b>Experimental Data Reference</b>	<b>Boundary Layer: Laminar or Turbulent Flow</b>	<b>List of Experimental Data Available</b>	<b>Computed Results References</b>	<b>Computed Results: Laminar or Turbulent Flow</b>	
	Incompress. Liquid oxygen flow across a flat plate with a cylindrical post rising perpendicular from the plate	3-D	S. E. Rogers, D. Kwak, U. Kau, "A Numerical Study of Three-Dimensional Incompressible Flow Around Multiple Posts," AIAA Paper 86-0353, AIAA Aerospace Sciences Conference, Reno, Nevada, 1986.	Turbulent	Downloadable data available on web page. (grid, solution, compressed tar archive)	Download Solution	Turbulent	<a href="http://www.nas.nasa.gov/Research/Datasets/Rogers/index.sh">http://www.nas.nasa.gov/Research/Datasets/Rogers/index.sh</a>
	Tutorial Geometry	3-D	1) J.A. Benek, P.G. Buning, and J.L. Steger, "A 3-D Chimera Grid Embedding Technique," AIAA-85-1523-CP, AIAA 7th Computational Fluid Dynamics Conference, Cincinnati, OH, July 15-17, 1985. 2) J.A. Benek, J.L. Steger, F.C. Dougherty, and P.G. Buning, "Chimera: A Grid-Embedding Technique," AEDC-TR-85-64, Arnold Engineering Development Center, Arnold AFS, TN, April 1986.	Turbulent	Downloadable data available on web page. (plot, etc.)	Download Plot	Turbulent	<a href="http://www.nas.nasa.gov/Research/Datasets/Benek/index.sh">http://www.nas.nasa.gov/Research/Datasets/Benek/index.sh</a>



A wedge with a half angle of 15°

2-D

1) John, J.E.A., *Gas Dynamics*, Second Edition, Prentice Hall, New Jersey, 1984.

Turbulent

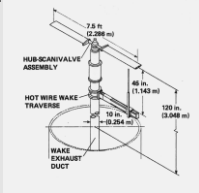
Data Available on Web Page

Graphs and Charts available on web page

Turbulent

<http://www.caselab.okstate.edu/research/verification/compr2d>

Hovering Rotor



rotor model for this test employed two cantilever-mounted, manually adjustable blades with half degree precone. Rotor is 7.5 ft across

3-D

F.X. Caradonna and C. Tung, "Experimental and Analytical Studies of a Model Helicopter Rotor in Hover," *NASA Technical Memorandum 81232*, NASA, 1981.

Turbulent

Data Available on web page

Found in Data Section

Turbulent

<http://www.caselab.okstate.edu/research/experiment/rotor.htm>

Geometry

Geometry Description

2-D, 3-D, or Axisymmetric Flow

Experimental Data Reference

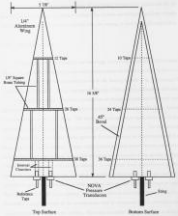
Boundary Layer: Laminar or Turbulent Flow

List of Experimental Data Available

Computed Results References

Computed Results: Laminar or Turbulent Flow

80° Delta Wing



slender delta wing with 80° leading edge sweep, a root chord of 16 5/8 inches, a total wing span of 5 7/8 inches measured at the base of the delta wing, and a thickness of 1/4 inch

3-D

Arena, A.S., "An Experimental and Computational Investigation of Slender Wings Undergoing Wing Rock," *Ph.D. Dissertation*, Department of Aerospace and Mechanical Engineering, Notre Dame, April 1992.

Laminar

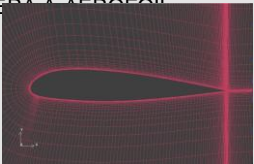
Charts and Numerical data available on web site

Available on web page

Laminar

<http://www.caselab.okstate.edu/research/experiment/delta80>

ONE-A-AREFOCUS



2-D

University of Glasgow: Dept. of Aerospace Engineering

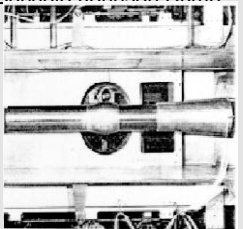
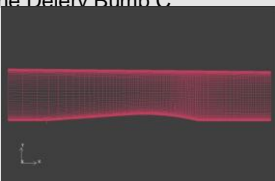
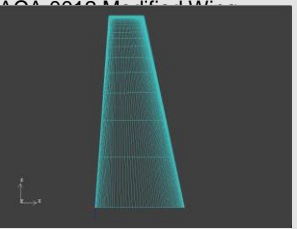
Laminar

Charts and Graphical Data available on web page

Available on web page

Laminar

<http://www.aero.gla.ac.uk/Research/CFD/projects/cfdval/reso>

<p>The Bachalo-Johnson Bump</p> 	<p>Designed to investigate the interaction between the shock wave and the turbulent boundary layer</p>	<p>2-D</p>	<p>University of Glasgow: Dept. of Areospace Engineering</p>	<p>Turbulent</p>	<p>Charts and Graphical Data available on web page</p>	<p>Available on web page</p>	<p>Turbulent</p>	<p><a href="http://www.aero.gla.ac.uk/Research/CFD/projects/cfdval/reso">http://www.aero.gla.ac.uk/Research/CFD/projects/cfdval/reso</a></p>
<p>The Delery Bump.C</p> 	<p>Designed to invetigate the effects of adverse pressure gradients and shock waves on the separation of the viscous boundry layer.</p>	<p>2-D</p>	<p>University of Glasgow: Dept. of Areospace Engineering</p>	<p>Turbulent</p>	<p>Charts and Graphical Data available on web page</p>	<p>Available on web page</p>	<p>Turbulent</p>	<p><a href="http://www.aero.gla.ac.uk/Research/CFD/projects/cfdval/reso">http://www.aero.gla.ac.uk/Research/CFD/projects/cfdval/reso</a></p>
<p>Cor</p> 	<p>This case was developed specifically with validation</p>	<p>3-D</p>	<p>University of Glasgow: Dept. of Areospace Engineering</p>	<p>Turbulent</p>	<p>Charts and Graphical Data available on web page</p>	<p>Available on web page</p>	<p>Turbulent</p>	<p><a href="http://www.aero.gla.ac.uk/Research/CFD/projects/cfdval/reso">http://www.aero.gla.ac.uk/Research/CFD/projects/cfdval/reso</a></p>
<p><b>Geometry</b></p>	<p><b>Geometry Description</b></p>	<p><b>2-D, 3-D, or Axisymmetric Flow</b></p>	<p><b>Experimental Data Reference</b></p>	<p><b>Boundry Layer: Laminar or Turbulent Flow</b></p>	<p><b>List of Experimental Data Available</b></p>	<p><b>Computed Results References</b></p>	<p><b>Computed Results: Laminar or Turbulent Flow</b></p>	
<p>NACA 0012 M. f. LW</p> 	<p>Wing comprizes a root profile based on the NACA 0012 aerofoil and includes taper in the wing form</p>	<p>3-D</p>	<p>University of Glasgow: Dept. of Areospace Engineering</p>	<p>Turbulent</p>	<p>Charts and Graphical Data available on web page</p>	<p>Available on web page</p>	<p>Turbulent</p>	<p><a href="http://www.aero.gla.ac.uk/Research/CFD/projects/cfdval/reso">http://www.aero.gla.ac.uk/Research/CFD/projects/cfdval/reso</a></p>